# ALTERED GLUCOSE METABOLISM IN CANCER METASTASIS AND DRUG RESISTANCE

---

**A Dissertation**

**Presented to**

**the Faculty of the Department of Biology & Biochemistry**

**University of Houston**

—

**In Partial Fulfillment**

**of the Requirements for the Degree**

**Doctor of Philosophy**

—

**By**

**Jinyu Chen**

**August 2013**

**ALTERED GLUCOSE METABOLISM IN CANCER METASTASIS AND DRUG RESISTANCE**

**Jinyu Chen**

**APPROVED:**

**Dr. Zhang Weihua, Chairman**

**Dr. Margret Warner**

**Dr. Seema Khurana**

**Dr. Dina Chelouche Lev**

**Dr. Boyi Gan**

**Dr. Dan Wells** Dean, College of Natural Sciences and Mathematics

***For Katelyn***

# ACKNOWLEDGEMENTS

I would like to express my deep gratitude to Dr. Zhang Weihua, my advisor, for his patient guidance, enthusiastic encouragement, and useful critiques during the planning and development of my research work. His willingness to give his time so generously has been very much appreciated. I would also like to express my very great appreciation to my committee members Dr. Margret Warner, Dr. Seema Khurana, Dr. Dina Chelouche Lev, and Dr. Boyi Gan, for their valuable and constructive suggestions in keeping my progress on schedule. My grateful thanks are also extended to my lab members for their generous help and assistant during experiments. Last, but certainly not least, I would like to acknowledge the support provided by my family during my most stressful time of life so far, and my little daughter whose smiles have given me strength to stay strong.

# ALTERED GLUCOSE METABOLISM IN CANCER METASTASIS AND DRUG RESISTANCE

---

**An Abstract of a Dissertation**

**Presented to**

**the Faculty of the Department of Biology & Biochemistry**

**University of Houston**

—

**In Partial Fulfillment**

**of the Requirements for the Degree**

**Doctor of Philosophy**

—

**By**

**Jinyu Chen**

**August 2013**

# ABSTRACT

Glucose, one of the most important energy sources for living organisms, is first broken down through glycolysis then either undergoes oxidative phosphorylation in the mitochondrion or fermentation in the cytosol. Abnormal glucose metabolism was first discovered by Dr. Otto Warburg, i.e. cancer cells carry out irreversible fermentation of glucose in the presence of oxygen, which is also termed aerobic glycolysis. My studies focus on understanding altered glucose metabolism in cancer metastasis and drug resistance. We found that breast cancer brain metastasized cells developed enhanced oxidation of certain amino acids and gluconeogenic activity for survival and proliferation when glucose level is limited. We also found that drug-resistant colon cancer cells exhibited up-regulated aerobic glycolysis to meet the need of a higher amount of intracellular ATP to cope with chemotherapeutic stress. These results suggest alterations in glucose metabolism play critical roles in the development of cancer brain metastasis and drug resistance. The molecular mechanisms identified by this study may serve as potential therapeutic targets for cancer treatment.

# TABLE OF CONTENTS

# CHAPTER 1 INTRODUCTION

## 1.1 Cancer Biology

Based on the ability to invade, tumor is divided into two categories, benign tumor and malignant tumor (Cancer) (Weinberg 2007). Benign tumors respect the boundary created by the basement membrane, i.e. they do not invade and can be removed by surgery. By contrast, malignant tumors invade into underlying tissue and disseminate to distant organs through metastasis. Cancer is a disease that has been present throughout human history. Recorded as “there is no treatment” in an ancient Egyptian textbook on trauma surgery, cancer is still one of the leading causes of death of human beings, second in the United States where about half of all men and 1/3 of all women will develop cancer during their lifetime (Murphy 2000).

Multicellular organisms are made of trillions of cells that are strictly programmed to grow, proliferate, differentiate, and die. Fine and complex cellular mechanisms control how cells behave: how they divide when needed, switch to different metabolic pathways when energy need and substrate availability altered, die when damaged. Cancer starts with some cells growing out of control in the body, dividing regardless of anti-proliferative signals, bypassing programmed cell death. To date, we know that cancer is not a single disease but a complex and heterogeneous disease with over 200 different types. Within the same type of primary tumor or metastatic lesion, there are subpopulations of cancer cells with

distinct phenotypes and genotypes. For example, pathologists routinely examine sections of different sites of a same tumor and report the highest grade only (Fisher, Pusztai et al. 2013).

## 1.2 Metabolism and Cancer

Although cancers are very complex disease, they still shared common hallmark characteristics. By 2000, “The Hallmarks of Cancer” has been defined as: self-sufficiency in growth signals, insensitivity to growth-inhibitory signals; evasion of apoptosis, limitless replicative potential, sustained angiogenesis, tissue invasion and metastasis. A decade later, the “reprogrammed energy metabolism” was added as another hallmark of cancer (Hanahan and Weinberg 2011).

Altered glucose metabolism in cancer was discovered by Otto Warburg in 1920s.It is the first metabolic phenomenon of cancer brought to our attention. To date, it is known that in addition to “the Warburg effect”, cancer cells alter cellular metabolism in multiple ways, such as utilization of glutamine and other amino acids, and fatty acids. Cancer cells tend to ferment glucose and produce large amounts of lactate even in the presence of oxygen. They also tend to have enhanced *de novo* fatty acid synthesis while normal cells usually uptake fatty acid from the blood (Pandey, Liu et al. 2012); Interestingly, cancer cells are very sensitive to glutamine deprivation and will stop proliferating if glutamine is

removed from the cell culture media. This need for glutamine is termed “glutamine addition” in cancer cells (Erickson and Cerione 2010).

It is speculated that these metabolic alterations are adjustments made to assist proliferation of cancer cells; however the driving forces for altered metabolism in cancer cells remain largely undefined. The focus of my study is a better understanding on altered glucose metabolism in cancer cells, especially on its particular roles in the development of cancer metastasis and drug resistance, which may provide us with more therapeutic targets for cancer treatment.

## 1.3 Glucose Biochemistry and Physiology

### 1.3.1 Glucose fates in the cell

Glucose is the primary energy substrate for mammalian cells. Dietary glucose is taken up by intestinal cells and transported into the blood and enters cells through glucose transporters. To utilize glucose, a 10-step metabolic pathway, namely glycolysis, converts glucose to pyruvate in the cytosol. During this process, a 6-carbon glucose molecule is broken down to 2 molecules of 3-carbon pyruvate with a gain of 2 molecules of ATP. There are 2 fates of pyruvate inside a cell following glycolysis. One is to be oxidized via the oxidative phosphorylation (OXPHOS) in the mitochondria, and the other is to be converted to lactic acid in the cytosol (fermentation). In normal cells, in presence of a sufficient level of oxygen, pyruvate is transported into the mitochondria and

completely oxidized to carbon dioxide through OXPHOS. Under hypoxic conditions, pyruvate is converted to lactate, in a process called fermentation.

OXPHOS oxidizes glucose completely, while fermentation utilizes glucose far less efficiently but produces ATP 100 times faster than the OXPHOS (Vander Heiden, Cantley et al. 2009). In differentiated cells, oxygen is the determinant of whether a cell catabolizes glucose mainly via OXPHOS or fermentation since oxygen is an essential component of OXPHOS. However, proliferating cells and cancer cells tend to convert majority amount of pyruvate to lactate regardless the presence of oxygen, which is also termed “aerobic glycolysis” (the Warburg effect) and we will discuss cancerous aerobic glycolysis in cancer cells in details later.

In addition to its role in generating ATP, glucose also provides substrates for the pentose phosphate pathway (PPP) to produce ribose, the building block for nucleotide synthesis. PPP is critical for proliferating cells because nucleotides are needed for DNA replication and NADPH is needed for maintaining cellular redox balance. PPP is a branch pathway of glycolysis in which glucose-6-phophate (G6P) serves as the substrate. Intermediates of glycolysis, fructose-6-phosphate and glyceraldehyde-3-phosphate can be shuttled into PPP via gluconeogenesis (Cantor and Sabatini 2012).

Glycolysis is also connected with the synthesis of certain amino acids. 3-phosphoglycerate flows into serine biosynthesis pathway by providing backbone

for multiple nonessential amino acids (Cantor and Sabatini 2012). Pyruvate can be converted into alanine through transamination.

Citrate can be shunted out of mitochondria and feed into *de novo* fatty acid synthesis (Jones and Thompson 2009). Mitochondria-derived citrate can be converted to acetyl-CoA and oxaloacetate (OAA) after transport into the cytosol. OAA then can be either used to produce α-ketoglutarate and NADPH or converted to aspartate through transamination (DeBerardinis, Lum et al. 2008).

### 1.3.2 Glucose fates in the body

#### *Glucose absorption, distribution and regulation*

As one of the major nutrients in blood, glucose can be ingested directly from diet. The normal range of blood glucose concentration is 4.16-6.1mM (Hill, J. 2004); interstitial tissue contains a comparatively lower glucose concentration, usually less than 3mM (Pittas, Hariharan et al. 2005). Glucose in the interstitial tissue in the brain is very low with an average of 0.47mM (Hill, J. 2004).

Glucose level in the body is controlled in a strict manner to maintain glucose homeostasis. When blood glucose level is high, insulin stimulates glucose uptake into muscle and fat. Instead of accumulating too many separate glucose molecule, organs, typically the liver, tend to store glucose in the form of glycogen. The formation of glycogen by polymerizing G1P through glycogen synthase is called glycogenesis. When blood glucose decreases, there are 3

sources of glucose in the body: intestinal absorption, glycogenolysis which is the breakdown of glycogen to release glucose, and gluconeogenesis which is the synthesis of glucose from intermediate metabolites of glycolysis (Hill, J. 2004).

Gluconeogenesis, which takes place in the liver and kidney, is the metabolic pathway through which of glucose is generated from other substrates including gluconeogenic amino acids which are released from proteolysis, glycerol from lipolysis and lactate (Previs and Brunengraber 1998).

Gluconeogenesis is involved in the Cori cycle, which is an important mechanism for maintenance of glucose homeostasis. The Cori cycle, also known as lactic acid cycle, refers to the process through which muscle cells produce lactate from glucose through fermentation, such as during exercise. Lactate can be reconverted back to glucose via a similar but reverse pathway to glycolysis, gluconeogenesis, in the liver cells (Fig 1.1).

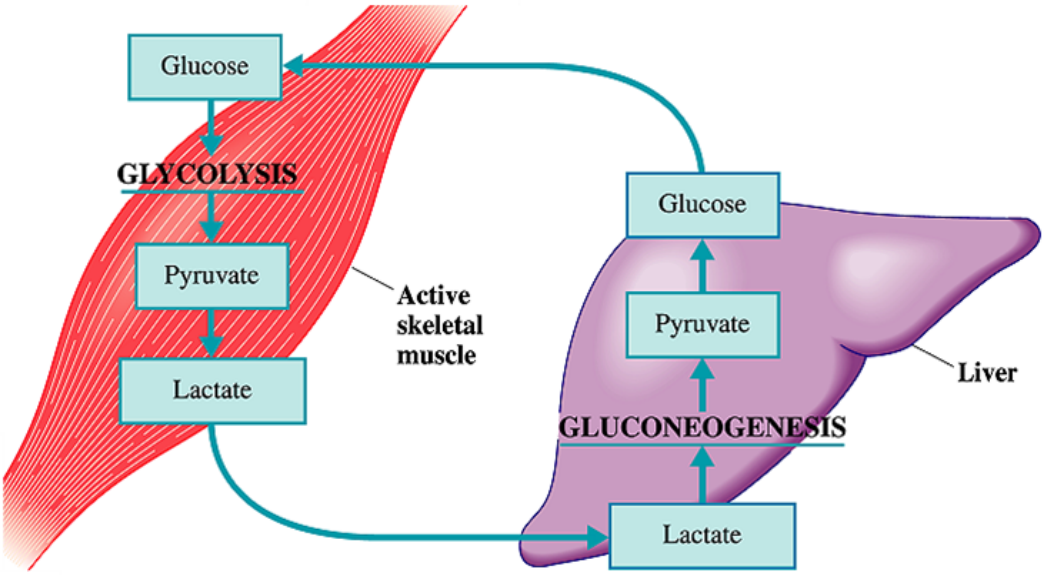


**Figure1.1 The Cori cycle**

## 1.4 Altered Glucose Metabolism in Cancer

### 1.4.1 Discovering the Warburg effect

In 1920s, Dr. Otto Warburg isolated different tumor tissues from patients and cultured thin slices of these tissues (<400 μm) *in vitro*, and he found that cancer cells used a high amount of glucose and produced large amount of lactate even in the presence of oxygen (Warburg, 1924). This altered glucose metabolism in cancer cells is termed “aerobic glycolysis” or “the Warburg effect”. Though cancer is a complex disease with over 200 different types, altered glucose metabolism is one of the most common phenotypes among different types of cancer (Cantor and Sabatini 2012).

### 1.4.2 Mechanisms regulating glucose metabolism in cancer cells

#### *Signaling pathways*

Up-regulation of glycolytic enzymes is common among different types of cancer (Moreno-Sanchez, Rodriguez-Enriquez et al. 2009). Although the fundamental driving force of aerobic glycolysis in cancer cells remains undefined, researchers have shown that altered metabolism is regulated by oncogenes and tumor suppressors (Figure1.4.2a). For example, the PI3K/AKT/mTOR pathway is one of the most common constitutively activated pathways in human cancers. PI3K/AKT is downstream of most growth factors and its activation enhances glucose uptake and glycolysis through increasing glucose transporters and

hexokinase (Kohn, Summers et al. 1996, Elstrom, Bauer et al. 2004, Buzzai, Bauer et al. 2005). Through AKT mediated signaling, PFK1 activity is enhanced in a PFK2 dependent manner (Kohn, Summers et al. 1996, Deprez, Vertommen et al. 1997, Shinano, Osaki et al. 2001, Rathmell, Fox et al. 2003). In addition, *de novo* fatty acid synthesis can also be stimulated by AKT (Berwick, Hers et al. 2002). Mammalian target of rapamycin complex 1(mTORC1) is a well characterized downstream regulator of AKT that inhibits two inhibitory proteins of mTORC1. Active mTORC1 can alter metabolisms by stimulating protein synthesis, hypoxia induced factor 1α (HIF-1α), and c-Myc (Laplante and Sabatini 2012). HIF-1α and c-Myc are regulators of glucose metabolism, which will be discussed in more details later.

P53 is a transcription factor that is considered as a tumor suppressor owing to its function in enhancing DNA repair, initiating cell cycle arrest and apoptosis during tumorigenesis (Vousden and Ryan 2009). P53 is coded by the *TP53* gene that is often mutated in most human cancers (Cantor and Sabatini 2012). P53 has been intensively studied for its tumor suppressive function, but recently its role in regulating glucose metabolism in cancer has also been revealed. P53 was found to transcriptionally induce TIGAR, TP53-induced glycolysis and apoptosis regulator, which negatively regulates PFK1 (Bensaad, Tsuruta et al. 2006). P53 also suppresses expression of several glucose transporters (Schwartzenberg-Bar-Yoseph, Armoni et al. 2004). P53 is further found to bind directly to glucose-6-phosphate dehydrogenase (G6PDH), a rate-

limiting enzyme in pentose phosphate pathway, which indicated its potential role in inhibition of ribose and nucleotide production (Jiang, Du et al. 2011).

Mammalian cells respond to oxygen deprivation, hypoxia, by enhancing hypoxia inducible factor (HIF) signaling to maintain ATP via glycolysis. HIF activity relies on the stability of HIF-1α that is primarily regulated in an oxygen-dependent manner. HIF-1α was first identified by Semenza and Wang, and later was recognized as a key responding protein to cellular hypoxic stress (Semenza and Wang 1992). In normal cells, HIF-1α is constitutively expressed and degraded in the presence of oxygen. In the presence of oxygen, hydroxylases including prolyl hydroxylase domain enzymes (PHD) and HIF asparaginyl hydroxylase factor inhibiting HIF (FIH) are activated and hydroxylate proline residudes in the oxygen-dependent degradation domain (ODD) of HIF-1α, which attracts VHL protein complex to bind to the ODD domain. Binding of VHL to HIF-1α results in repression of HIF-1α transcriptional activity and HIF-1α ubiquitination for proteasomal degradation. During oxygen deprivation, PHD and FIH are inactive and unable to hydroxylate HIF-1α, which leads to up-regulation of HIF-1α. Up-regulated HIF-1α is then transported into the nucleus and binds to HIF1β to form heterodimer to activate transcription of downstream genes.

Studies have shown that HIF-1α is overexpressed in various types of tumors and correlates with poor diagnosis and tumor growth (Zhong, De Marzo et al. 1999, Talks, Turley et al. 2000). Oncogenic pathways including MAPK pathway and PI3K pathway can regulate HIF-1α, downstream of which involves

regulation of various aspects of cancer biology including cell survival and proliferation, glucose metabolism, pH regulation, and cell migration (Patiar and Harris 2006).

Many of the HIF-1α target genes are glycolytic enzymes, which include GLUT1, GLUT3, HK1, HK2, AMF/GPI, ENO1, GLUT1, GAPDH, LDHA, PFKBF3, PFKL, PGK1, PKM, and TPI (Semenza 2003). Up-regulation of these glycolytic genes speeds up glucose uptake, glycolysis and rate of ATP production. HIF-1α is almost undetectable in normal cells under normoxia, while it is common to observe constitutively accumulated HIF-1α in cancer cells regardless the levels of oxygen. Similar to the constitutive up-regulation of HIF-1α, cancer cells also present constantly enhanced aerobic glycolysis.

Like HIF-1α, c-Myc is also a transcriptional factor that is believed to regulate 15% of all genes (Dang, O'Donnell et al. 2006), and thus is essential for cell proliferation and growth. C-Myc is considered to have an oncogenic effect since in many cancers c-Myc is mutated and constitutively active. (Dominguez-Sola, Ying et al. 2007). Overexpression of c-Myc results in DNA damage and checkpoint activation (Kim, Zeller et al. 2004, Dominguez-Sola, Ying et al. 2007). It is also shown that c-Myc is a regulator of glycolysis since overexpressed c-Myc is shown to up-regulate glycolytic enzymes independent of hypoxia (Kim, Zeller et al. 2004). Studies have revealed that C-Myc can upregulate/activate a set of glycolytic genes including ENO1, HK2, LDHA, GAPD, PFKM, TPI1, GPI, and

PGK1, among which HK2, LDHA, and ENO1 directly interact with c-Myc (Kim and Dang 2006).

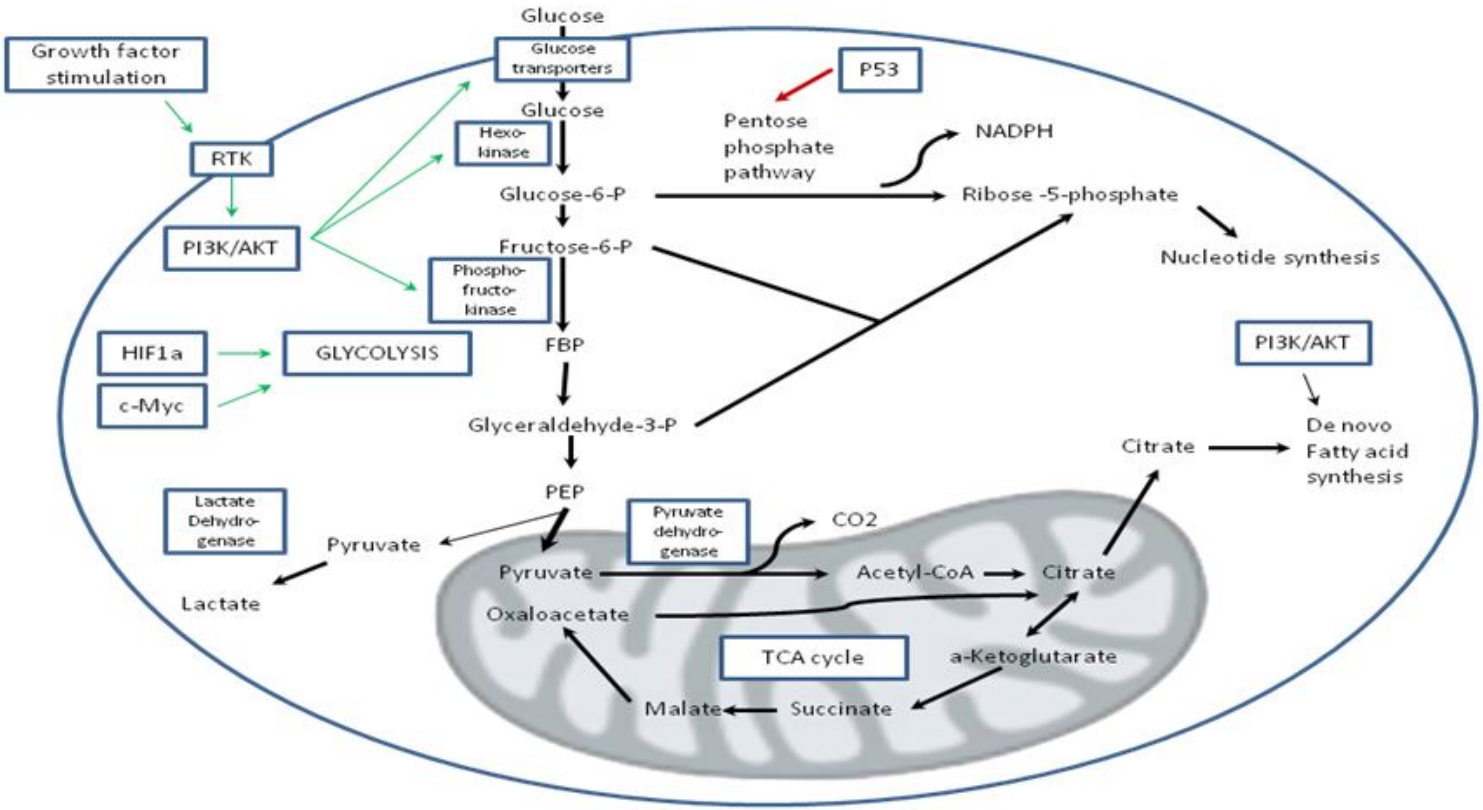


**Figure 1.4.2a Glucose metabolism is regulated by different signaling pathways.**

**(Matthew G, Vander Heiden, Science, 2009)**

***Mitochondria pyruvate carrier***

Pyruvate lies in the center of hub of cellular metabolism; it is the 3 carbon product of 10-step glycolysis in the cytosol. There are different fates of pyruvate: it can flow into different metabolic pathways such as the TCA cycle in the mitochondria, gluconeogenesis, alanine synthesis through transamination, and fatty acid synthesis. Identifying of mitochondria pyruvate carrier (MPC) might give us insight on how pyruvate is controlled when transported into mitochondria. MPC1 and MPC2 are identified as mitochondria pyruvate carrier required for pyruvate transport in yeast, drosophila and human, and blocking MPC resulted in accumulation of glycolytic intermediates and decrease in TCA cycle intermediates (Bricker, Taylor et al. 2012). Mutated MPC1 is found in children suffering from lactic acidosis and hyperpyruvatemia, while pyruvate dehydrogenase level is found normal in these patients (Bricker, Taylor et al. 2012). Since cancer is a metabolic disease, MPC might exert a significant impact on the altered metabolism found in cancer. A recent finding revealed that insulin sensitizer thiazolidinedione specifically inhibits MPC through PPARγ. (Divakaruni, Wiley et al. 2013). Although so far very limited work in done on MPC and metabolism in cancer, possible implications of MPC on cancer metabolism is exciting since pyruvate metabolism related enzymes such as pyruvate dehydrogenase, pyruvate kinase, and lactate dehydrogenase are altered in cancer cells (Schell, Rutter, 2013). More research is required to determine MPC in various types of cancer and its relationship with altered metabolism in cancer

cells. It's worth noting that possibly defected MPC which prevents pyruvate from entering mitochondria may well explain the Warburg effect.

### *ATP and altered glucose metabolism*

Adenosine triphosphate (ATP), the biological currency inside a cell, transports chemical energies among different energy consuming events. As mentioned above, ATP is generated through glycolysis and OXPHOS. Warburg proposed that the preference of cancer cells for aerobic glycolysis might be due to mitochondria deficiency in producing ATP. Now we know that mitochondria are functional in many types of cancer cells and cancer conduct aerobic glycolysis and OXPHOS together to generate needed ATP (Table 1) (Moreno-Sanchez, Rodriguez-Enriquez et al. 2009).

**Table 1 Energy metabolism in malignant tumor cells**

| Tumor | Organism | Prevailing energy pathway | % ATP contribution |
|---|---|---|---|
| Glioma C6 | Rat | OxPhos | 80 |
| Oligodendroglioma, meningioma, medulloblastoma | Human | Glycolysis | 60 |
| Glioblastoma multiforme, Astrocytoma C6 | Human, Rat | Glycolysis and OxPhos | 50 |
| Transformed brain | Hamster | OxPhos | 71 |
| Colon sarcoma | Human | OxPhos | 70 |
| Novikoff hepatoma | Rat | Glycolysis | 75 |
| Ehrlich Lettré, Ehrlich, Walker-256, Morris 3683 and Dunings LC18 hepatomas; ascites mouse cancer; sarcoma 27 | Rat, mouse | Glycolysis and OxPhos | 50 |
| Reuber H-35, Morris (7793,7795, 7800, 5123), and AS-30D hepatomas | Rat | OxPhos | 97 |
| Lung carcinoma | Human | OxPhos | 95 |
| Breast cancer | Human | OxPhos | 95 |
| MCF7 breast carcinoma | Human | OxPhos | 80 |
| Melanoma | Human | OxPhos | 97 |
| HeLa cervix, ovarian and uterus carcinomas | Human | OxPhos | 90 |

(Moreno-Sanchez, Rodriguez-Enriquez et al. 2009)

One of the sensors of intracellular ATP level is AMP-activated protein kinase (AMPK) that is composed of α, β, and ϒ subunits (Stapleton, Mitchelhill et al. 1996). AMPK can sense AMP: ATP ratio changes in the cell and be activated by increasing intracellular AMP level (Fisslthaler and Fleming 2009). Upon stimulation, AMPK increases intracellular ATP production by inhibiting anabolic pathways and enhancing catabolic pathways such as glucose uptake, mitochondrial biogenesis, and fatty acid oxidation (Winder 2001, Zadra, Priolo et al. 2010).

Intracellular ATP level has been a parameter measured along with cell viability, chemo-sensitivity test of drugs in cancer studies (Nogaki and Ichihashi 1988, Verrax, Dejeans et al. 2011, Ota, Geschwind et al. 2013, Tang, Wang et al. 2013). Intracellular ATP level is associated with cell death. For example, DNA damaging anticancer agents led to ATP depletion before causing necrosis in cancer cells (Martin, Bertino et al. 2000); glucose starvation causes a drop of intracellular ATP level before necrosis in rat cardiac myocytes (Tatsumi, Shiraishi et al. 2003).

A recent finding on the intracellular ATP level and cancer cells focused on an enzyme, ER UDPase (ENTPD5), which promotes glycosylation of proteins in ER. It was found that ENTPD5 promoted rapid ATP consumption, and this enzyme is also found mediate the increase of glycolysis. Although there is no solid evidence linking decrease intracellular ATP pool and increase of glycolytic activity, these studies of ENTPD5 in intracellular ATP level and glycolysis

indicate intracellular ATP plays an important role in aerobic glycolysis. (Read, Hansen et al. 2009, Zadran, Amighi et al. 2012).

### 1.4.3 Interactions of altered glucose metabolism and other metabolic pathways

Of all the amino acids, glutamine is the one with the highest blood concentration and, besides glucose, is recognized as one of the major energy sources for cancer cell proliferation. Because glucose can only provide carbon, oxygen, and hydrogen, but not nitrogen, it is not by itself enough to maintain proliferating cells. As one of the non-essential amino acid (NEAA), glutamine plays an important role in cancer metabolism. Many cancers with high glycolytic rate cannot survive without exogenous glutamine, which is termed “glutamine addiction” (Wise and Thompson 2010).

Another characteristic of tumor metabolism is the enhanced *de novo* fatty acid synthesis. While normal differentiated cells prefer to uptake exogenous lipids, *de novo* fatty acid is important for lipid synthesis and protein modification required for cancer cells which are highly proliferative (Hatzivassiliou, Zhao et al. 2005, Menendez and Lupu 2007, Fritz and Fajas 2010). Key enzymes in *de novo* fatty acid synthesis have been found to be up-regulated in many types of cancer (Menendez and Lupu 2007, Tennant, Duran et al. 2010). One of the substrates of fatty acid synthesis, citrate, is derived from TCA cycle and transported out of

mitochondria. Glucose and glutamine are the main source for carbon flux into the TCA cycle; high rates of glycolysis and glutamine oxidation are permissive for *de novo* fatty acid synthesis. Oncoprotein and tumor suppressor signaling pathways regulating glycolysis also regulate *de novo* fatty acid synthesis, such as PI3K, P53 and Myc (Zhang and Du 2012).

Altered glucose metabolism not only can produce ATP needed in the rapid proliferating cancer cells, but also provides macromolecular building blocks for production of lipid, nucleotide, protein, and maintenance of redox balance.

## 1.5 Project Summary and Significance

### 1.5.1 Project 1. Altered glucose metabolism in breast cancer brain metastasized cells.

More than 90% of cancer are highly glycolytic, which is not often observed in benign tumors.. When we tried to find out correlations between aerobic glycolysis and tumor invasiveness, to our surprise, we found that the survival and growth of a breast cancer brain metastasized cell line was less glycolytic than its parental cell line.

Further studies showed that these brain metastasized cells were able to survive and proliferate in the absence of glucose. Enhanced oxidative catabolism of branched chain amino acid and increased gluconeogenesis contributed to this glucose-independent survival and proliferation. Cancer cells isolated from human

breast cancer brain metastasis also exhibited similar phenotypes. Brain metastases of human breast cancers were also found to express high levels of rate-limiting gluconeogenic enzymes that include fructose-1, 6-bisphosphatases (FBP), and Phosphoenolpyruvate carboxykinase (PEPCK). Metabolomic flux analysis supported the gluconeogenic nature of the brain metastatic cells. Glycogen levels were also up-regulated in the brain metastases.

Our findings identified a novel metabolic program that accompanies brain metastasis and suggest that targeting the pathways of amino acid oxidation and gluconeogenesis may provide strategies for the treatment of breast cancer brain metastasis.

### 1.5.2 Project 2. Altered glucose metabolism in the development of cross drug resistance of colon cancer cells.

Irreversible aerobic glycolysis and constitutively active HIF-1α, regulator of glycolysis, drew our attention to intracellular ATP pool. Increasing intracellular ATP in cancer cells down-regulated glycolysis and HIF-1α, and surprisingly, resulted in drug resistance of colon cancer cells. More detailed studies of intracellular ATP and drug resistance were carried out on well characterized drug-resistant colon cancer models. We found that drug-resistant cells produce more ATP through aerobic glycolysis but not OXPHOS, yet they still demonstrated enhanced aerobic glycolysis and HIF-1α signaling. Increasing

intracellular ATP in drug-sensitive cells made them more drug-resistant, while depletion of intracellular ATP sensitized drug-resistant cells to chemotherapeutic treatment.

Based on our findings, we proposed the concept of “ATP debt” which drives metabolic alterations in development of drug resistance in cancer cells. The extra amount of intracellular ATP in drug-resistant cancer cells is considered as an “ATP debt” that needs to be paid for gaining drug resistance. During the development of drug resistance, cancer cells shift to elevated aerobic glycolysis to reduce the “ATP debt” so as to survive under therapeutic stress.

# CHAPTER 2 MATERIALS AND METHODS

## 2.1 Materials

Minimal essential medium containing 5mmol/L glucose, customized glucose/glutamine/glutamate/BCAA free minimal essential medium, vitamins, nonessential amino acids, penicillin-streptomycin, sodium pyruvate, L-glutamine, and TRIzol reagent, First-Step RT-PCR Kit were purchased from Life Technologies (Carlsbad, CA). Oxaliplatin and 5-FU were purchased from the MD Anderson Cancer Center pharmacy (Houston, TX). Glucose, glutamine, 13C-glutamine, alpha-ketoglutarate, valine, leucine, isoleucine, epigallocatechin gallate (EGCG), alpha-ketoglutaric acid sodium, fatal calf serum, rabbit polyclonal antibodies against beta actin, GLUD1, GLUD2, BCKDK, FBP1, FBP2, PEPCK1, and PEPCK2, ATP-based CellTiter-Glo Luminescent Cell Viability kit were purchased from Promega. Fetal bovine serum, Tris-HCl, KCl, $MgCl_2$, $(NH_4)_2SO_4$, dithiothreitol, fructose 6-phosphate, NADH, aldolase, triosephosphate isomerase and α-glycerophosphate dehydrogenase, glutaraldehyde, paraformaldehyde, ATP bioluminescent assay kit, glutamate, malate, L succinate, and ADP were purchased from Sigma-Aldrich (St. Louis, MO). Universal control shRNA, shRNA-FBP2, shRNA-BCKDH-E1 were from Sigma-Aldrich (Table 2). 14C-leucine and hydroxide haymine were purchased from Thermal Fisher Scientific (Waltham, MA). FBP2 expression plasmid was purchased from Addgene. Glucose membrane, lactate membrane, and reaction buffer powders for measurement of glycolytic activity were purchase from YSI Life Science

(Yellow Springs, Ohio). Antibody against PARP was purchased from Cell Signaling Technology (Danvers, MA). HIF-1α antibody was purchased from BD Transduction Laboratories. Glut-1 antibody was purchased from Abcam. B-actin, p21, and hexokinaseII antibodies were purchased from Santa Cruz Biotechnology. VEGFA antibody was purchased from R&D System. PCR Master Mix was purchased from Roche. Chloroform solution of phosphatidylcholine, cholesterol, and 1, 2 dioleoyl-3-trimethyl-ammonium-propane were purchased from Avanti Polar Lipids (Alabaster, Alabama). Cell extraction buffer was purchased from Biorad.

**Table 2 Target sequences of shRNAs are listed in the following table.**

| Gene name | target region | target sequence |
|---|---|---|
| FBP2 | exon 5 | GATCCGCAAACAGTGTGCT |
| FBP2 | 3'-UTR | GCCACAGGCGATTCTATGG and CTGCTTACGACAGGTTTGG |
| BCKDH-E1 | exon 5 | GGAACGCCACTTCGTCACT |

## 2.2 Cell Lines and Cell Culture

### 2.2.1 Cell lines

Human colon cancer cell lines HT29 and HCT116, human breast cancer cell line MDA-MB-231, and human breast cancer brain metastasized MDA-MB-361 were purchased from ATCC (American Type Culture collection). MDA-MB-231Br3 cell line is established by in vivo selection as described in Kim, Huang et al (2004).

### 2.2.2 Cell culture

Colon cancer cell lines were cultured in minimal essential medium containing 5mmol/L glucose and supplemented with vitamins, nonessential amino acids, penicillin-streptomycin, sodium pyruvate, L-glutamine, and 10% of fetal bovine serum. Oxaliplatin resistant cells were cultured with addition 2 μmol/L of Oxaliplatin unless otherwise indicated.

MDA-MB-231, MDA-MB231Br3, and MDA-MB-361 cells were maintained in low glucose Dulbecco's Modified Eagle Medium (DMEM) containing 5mmol/L glucose and supplemented with penicillin-streptomycin, sodium pyruvate, and 10% of fetal bovine serum unless otherwise indicated. Special cell culture mediums containing containing no glucose/glutamine, with or without BCAAs were customized by Invitrogen (CA, USA). To make a complete special medium, dialyzed Fetal bovin serum using a dialysis bag with permeability of 2K (Thermo

Scientific, Rockford, IL) was add as 5% (v/v) to no glucose Dulbecco's Modified Eagle Medium. A final concentration of 100 units/mL of penicillin and 100µg/mL of streptomycin were also supplemented to the special medium. Other components including glucose, glutamine, and 14C-glutamine were added when needed in different experiments.

## 2.3 Development of Drug-resistant Model

Human colon cancer HT29 and HCT116 cells were exposed to an initial oxaliplatin concentration of 0.1 µmol/L and survived cells were cultured till confluence of 80% for 3 passages (~6 weeks). Survived cells were then exposed to 0.5µmol/L of oxaliplatin for 3 passages (~8 weeks). Cells survived the second dosage were finally exposed to clinically relevant plasma concentration, 2 µmol/L of oxaliplatin for 3 passages (~10 weeks). The surviving cells were named HT29-OxR and HCT116-OxR. Cell viability was measured by a Vi-cell XR cell viability analyzer (Beckman Coulter). In vitro experiments were carried out at confluence of 70% and at least 3 independent experiments were performed. All cell lines are identified by short repeats sequencing and 100% matched to the ATCC database.

## 2.4 Metabolic Measurement

### 2.4.1 Measure glycolytic activity

Cells were seeded in 6-well plates at $0.5X10^6$ to $1X10^6$ density and allowed overnight attachment. The next day fresh medium were changed at 200 uL approximately 3 hours prior to the assay. Cell culture medium were collected every 3 hours for 9 hours. Glucose and lactate concentration were measured by a Dual-Channel Biochemistry Analyzer-2700D (YSI Life Sciences). Average glucose consumption and lactate production were calculated at each time point from triplicate samples and normalized by cell number. Cell numbers were obtained using a Beckman Counter cell viability analyzer.

### 2.4.2 Measurement of BCAA oxidation

Cells were cultured in T-75 flask until >50% confluency. Prior to the experiment, a 4.2 cm diameter filter paper soaked with 1 mL of hydroxide of hyamine was inserted into the ventilation cap of the flask. 8 hours after changing to 14C-Leucine (final concentration: 2 μM) containing medium, $^{14}CO_2$ absorbed in the filter paper was analyzed in liquid using a liquid scintillation analyzer.

### 2.4.3 Amino acid profiling in cell culture medium

Amino acids profiling was carried out via HPLC measurement of amino acids in cell culture medium. The levels of amino acids, glutatmine, glutamate, valine, leucine, and isoleucine were measured by HPLC at the co-facility of Medical Genetics Laboratories of Baylor College of Medicine, Houston, TX.

### 2.4.4 Mitochondria isolation and substrate ATP production

Mitochondria of different cell lines were isolated following standard protocol of Mitochondria Isolation Kit from Thermo Scientific (Rockford, IL). Isolated mitochondria were kept on ice and immediately proceed to measure activity via substrate ATP production. ATP production was measured by ATP Bioluminescent Assay Kit from Sigma (FL, AA) with minor modification. Briefly, ATP assay mix was prepared with 40 μL of ATP assay mix and 2mL of dilution buffer in advanced and stored at -80°C. White 96-well plate was used for reaction with total 100uL assay mix each well. 41 μL mitochondria (0.2-1.0 μg) were added into the well with 4 μL of electron transport substrate which can either be 500 mM glutamate plus 500 mM malate, or 500mM succinate. 5 μL ADP (100 μM) was added and served as time 0. After 30-45 seconds' incubation, 50uL of assay reaction mixture was added. After 2 minutes from time 0, kinetic measurement was carried out for 10 minutes with 1 minute's interval at a sensitivity level of 100. A 0 to 0.25 nM ATP standard curve was generated by a standard solution of 10uM ATP. Bioluminescence measurement was carried out as triplicate using

BioTek Instruments FLx-800 Fluorescent Microplate Reader equipped with KC4 BioTek software. ATP produced by mitochondria was normalized by protein concentration of mitochondria samples, thus was expressed as “nmol ATP/min/mg protein”.

### 2.4.5 In-plate measurement of mitochondrial oxygen consumption

Cells were seeded in a 24-well plate according to different growth rate the day before analysis. On day two cells were changed to unruffled seahorse assay medium 30 minutes prior to the assay. Then OCR and ECAR were measured every 10 minutes for 2 hours. Average was calculated from quadruplicate samples and normalized by viable cells measured by Vi-cell XR analyzer (Beckman Counter). OXR and ECAR were measured using Seahorse XF 24 analyzer (Seahorse Bioscience).

### 2.4.6 Measurement of cellular ATP, ADP, and AMP

To measure relative intracellular ATP amount, cells were first seeded in 24 wells with 20,000 cells each well. After overnight attachment, single-one-step reagent provided by the ATP-based CellTiter-Glo Luminescent Cell Viability Kit (Promega) was added into each well with equal volume. After 15 minutes rocking at room temperature, cellular ATP level was measured by a luminescent plate reader. The same layout of 24-well plate was prepared for cell counting to

normalize ATP content. The absolute amount of cellular ATP, ADP and AMP was measured by the high-performance liquid chromatography coupled mass spectrum (HPLC-MS) with standard protocol. Exponential growing cells were first trypsinized and harvest in microcentrifuge tubes and washed with 4.2% glycerol once. Cell pellets were immediately incubated on ice in 100% ethanol and then resuspended in 100mL of distill water and proceeded to ultrasound fractionation. Cellular ATP, ADP, and AMP were then released to the supernatant. The fractionated mix was then centrifuged at 15,000rpm for 5 minutes. Supernatants were then injected into HPLC-MS for measurement for ATP, ADP, and AMP content which were later normalized with cell number.

### 2.4.7 Spectrophotometric assay for phosphofructose kinase activity

Phosphofructose kinase (PFK) activity was measured by monitoring NADH oxidation during enzymatic reaction. Reaction assay mixture contained 5 mM dithiothreitol, 10 mM $(NH_4)_2SO_4$, 5 mM $MgCl_2$, 50 mM KCl, 50 mM Tris-HCl (pH=8.0). Coupling enzymes in this assay were 30 unit/mL aldolase, 30 unit/mL triosephosphate isomerase, and 10 unit/mL α-glycerophosphate dehydrogenase. Whole cell lysate with 50 μg/mL of total protein was first added into the assay mix with coupling enzyme and incubated at 37°C for 10 minutes. Reaction started when fructose 6-phosphate and NADH with a total final concentration of 10mM and 0.28mM were added into the mix. NADH oxidation was measured by decreased absorbance at 340 nm in microplate reader at 37°C. Wells containing

no protein lysate served as control to measure non-specific NADH oxidation. Triplicate reactions were carried out.

### 2.4.8 13C-glutamine labeling and total cell metabolite extraction

MDA-MB-231 and MDA-MB-231Br3 cells were cultured in 6-well plates in glucose-free medium for 12 hours, and then the medium was refreshed to 13C-glutamine containing glucose-free/containing medium for an additional 6 hours. Eighty% methanol (in water) was prepared and incubated on dry ice prior to metabolite extraction. Cells were washed by PBS then dry ice cold 80% methanol (250 μL/well) was added directly into the well and quenched all metabolic activity in the cells. Cell culture plates were immediately transferred to -80°C freezer for 10 minutes on dry ice. Experiment was carried on on dry ice only from here. Cell mixture in the wells were collected in 1.5mL eppendorf tube after incubation, and then centrifuged at 14,000 g/min for 5 minutes at 4°C. After supernatants were collected in new eppendorf tubes, additional 70 μL/tube of dry ice cold 80% methanol was added into previous tubes to resuspend cell fragments to dissolve the remaining metabolites and centrifuge at 14,000g/min for 5 minutes at 4°C. Supernatants were collected and combined with the previous supernatants. This recollecting step was repeated if necessary. After all supernatants collected together, tubes were put in a frozen vacuum to dry out overnight. Powder-like dry metabolites were stored at -80°C until analysis.

### 2.4.9 Targeted mass spectrometry (LC/MS/MS)

Dried metabolite pellets were re-suspended using 20 μL LC/MS grade water for mass spectrometry. 10 μL were injected and analyzed using a 5500 QTRAP hybrid triple quadrupole mass spectrometer (AB/SCIEX) coupled to a Prominence UFLC HPLC system (Shimadzu) via selected reaction monitoring (SRM) of a total of 254 endogenous water-soluble metabolites for steady-state analyses of samples. Some metabolites were targeted in both positive and negative ion mode for a total of 285 SRM transitions using positive/negative polarity switching. ESI voltage was +4900V in positive ion mode and –4500V in negative ion mode. The dwell time was 3 ms per SRM transition and the total cycle time was 1.67 seconds. Approximately 10-13 data points were acquired per detected metabolite. Samples were delivered to the MS via hydrophilic interaction chromatography (HILIC) using a 4.6 mm i.d x 10 cm Amide Xbridge column (Waters) at 350 μL/min. Gradients were run starting from 85% buffer B (HPLC grade acetonitrile) to 42% B from 0-5 minutes; 42% B to 0% B from 5-16 minutes; 0% B was held from 16-24 minutes; 0% B to 85% B from 24-25 minutes; 85% B was held for 7 minutes to re-equilibrate the column. Buffer A was comprised of 20 mM ammonium hydroxide/20 mM ammonium acetate (pH=9.0) in 95:5 water:acetonitrile. Peak areas from the total ion current for each metabolite SRM transition were integrated using MultiQuant v2.0 software (AB/SCIEX). For $^{13}C$ labeled experiments, SRMs were created for expected $^{13}C$ incorporation of U-$^{13}C$ glutamine in various forms for targeted LC/MS/MS.

Unsupervised hierarchical clustering was performed using Ward's method (Ward, 1963) in the R statistical computing package (www.r-project.org/).

### 2.4.10 $^{14}$C-Leucine oxidation assay for BCAA oxidation

To determine the activity of BCAA oxidation, $^{14}$C-leucine was added into the cell culture medium at a concentration of 2.0 μM. To absorb $CO_2$, a filter paper pad of 4.2 cm diameter soaked with 1ml hydroxide of haymine was inserted into the ventilation cap of the T-75 cell culture flask. After 8 hr of culturing, the filter paper pads were removed and inserted into scintillation counter vials containing 4 ml scintillation liquid. The radioactivity of $^{14}$C was measured by a Liquid Scintillation Analyzer, Tri-Carb 2810TR (PerkinElmer). Triplicates of sample of each experimental group were measured.

## 2.4 Cell viability assay

### 2.4.1 MTT assay and 50IC value determination

Cell growth inhibition assay was carried out in 96 wells by MTT assay. 1,500-3,000 cells were first seeded in a 96-well plate. In the same day of seeding, working solution containing oxaliplatin or 5-FU with 2X of the final concentration were added to the cell suspension. After 72 h, 50 μL of MTT reagent was added into each well for an additional 4 hours. Supernatant was then removed and 200

μL of dimethyl sulfoxide (DMSO) was added into each well to dissolve the formazan precipitates in the cells. Reading of absorbance was then obtained by a MultiSkan plate reader (LabSystems) at 570 nm. Fractional survival was plotted against logarithm of drug dose. IC50 Values were calculated by Prisms software (GraphPad Software).

### 2.4.2 Cell viability measured by hemocytometer

Cell viability was measured by hemocytometer. Briefly, cell culture medium was first collected and centrifuge at 3000 rpm for 3 minutes. The attached cells were trypsinized and collected into the same tube. The tubes were centrifuge at 3000 rpm for 3 minutes. After the supernatant was removed, cell pellet was resuspended in 500 μL phosphate buffered saline (PBS). 10 μL of cell sample was mixed with 10 μL of trypan blue solution then 10 μl of mixture was loaded into each side of hemocytometer. Non-stained live cells and blue dead cells were counted on each side and calculated as viability in %.

## 2.6 Protein Analysis

### 2.6.1 Western blot

Whole cell lysate were collected from cell culture at 70%-80% confluence. Lysis buffer was prepared in advance containing Cell extraction buffer (Biorad),

proteinase inhibitor(biorad), and PMSF(biorad) and kept on ice. Cells were washed by PBS and calculated amount of lysis buffer was added directly to the cells. Cells were then scrapped down and collected in a microcentrifuge tube and incubate on ice. Cell lysis were vortexed 3 times every 10 minutes and then centrifuged at 15,000 rpm at 4°C for 10 minutes. Supernatant containing lysised protein was collected and protein concentration was measured. Different protein samples were normalized to same concentration then added equal amount of 1Xsample buffer containing requested β-Mercaptoethanol. Mixed protein samples were boiled in dry bath for 5 minute at 100°C, centrifuged then ready to run on a SDS-PAGE gel. SDS-PAGE gel is composed of upper stacking gel and lower separation gel. The separation gel was prepared according to standard protocol using Gel buffer, proto gel buffer purchased from National Dianostic plus water, APS, and TEMED. Separation gel was left to air dry with sealing layer of isopropano on the top. After separation gel was solidified, isopropano was removed and stacking gel was added on the top with gel comb. Stacking gel was prepared according to standard protocol using stacking buffer, proto gel buffer purchased from National Dianostic plus water, APS and TMEMD. After stacking gel was solidified, comb was removed and the gel was place in gel-running cassette (Biorad) with requested amount of gel-running buffer. Approximately 10 μg of each sample was loaded into each well. 100Vott power was put on the cassette until the sample ran to the bottom of the gel. Gel with proteins was later transferred to PVDF membrane (Biorad) in a gel transfer cassette (Biorad).

Membrane with transferred protein was incubate with 5% milk for blocking then incubate with primary antibody diluted in 5% milk with 1:1000 dilution over night at 4°C on a shaker. The next day, membrane was first washed in 1XTBST (TBS buffer containing 0.5% Tween-20) for 10 minutes for 3 times. Secondary antibody diluted 1:3000 in 5% milk was then added and incubated with the membrane for 1 hour at room temperature. Membrane was washed in 1XTBST 3 times with fresh TBST every 10 minutes and then incubated in ECL solution for 2 minutes. A cassette was used to expose the membrane to a x-ray film in dark room. Exposed film was then visualized and washed in the machine.

### 2.6.2 Production of antibodies against BCKDH-E1 and pSer-BCKDH-E1

Peptide sequence CYRIGHHSTSDDSS for BCKDH-E1 and CYRIGHHpSTSDDSS for pSer-BCKDH-E1 was used to produce polyclonal antibodies in rabbit by Genscript USA Inc (Piscataway, NJ). Recombinant BCKDH-E1 and pSer-BCKDH-E1 was purchased from Globozymes(Carlsbad, CA) to test specificity of the antibodies (Figure 2.6.2).

**A**

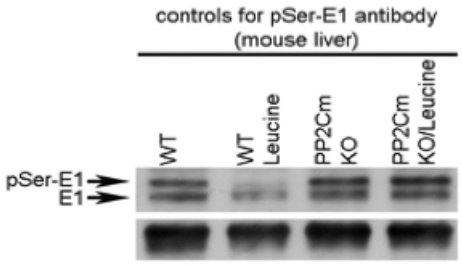


**B**

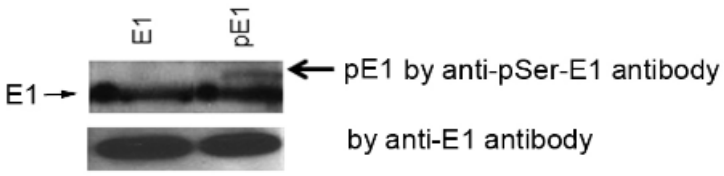


(E1 and in vitro phosphorylated E1)

**C**

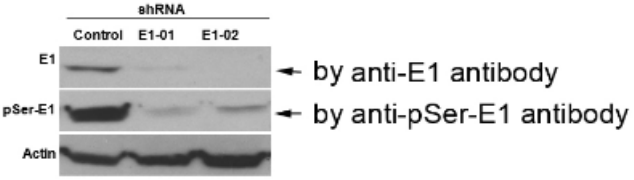


(cell extracts from MDA-MB-231 cells)

**D**

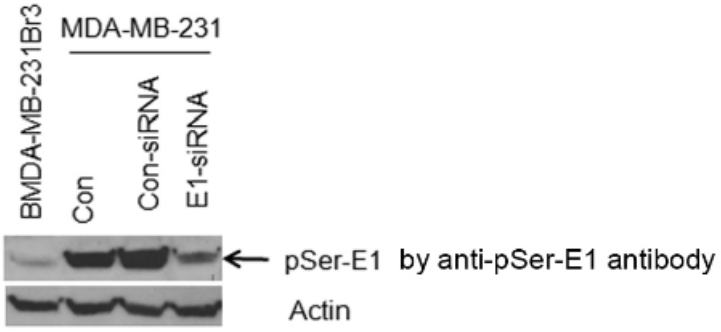

**Figure 2.6.2 Characterization of antibodies against BCKDH-E1 and BCKDH-pSer-E1.** A, Western blot analysis of liver extracts from wild type mouse, wild type mouse with rich leucine diet, PP2Cm knock-out mouse and PP2Cm knock-out mouse with rich leucine diet, using anti-p-Ser-E1 antibody. Leucine-rich diet down-regulated pSer-E1 level in the liver extracts of wild-type mouse, which is not seen in the PP2Cm knock-out mice liver extracts. (PP2Cm, protein phosphotase known to dephospholates pSer-E1) (Lu, Sun et al. 2009). B, Recombinant E1 is expressed and phosphorylated in vitro. Anti-E1 and anti-pSer-E1 antibodies were used to detect total E1 and pSer-E1. C, Western blot analysis of BCKDH-E1 and BCKDH-pSer-E1 in cell extracts of MDA-MB-231 cells with control vector, 2 shRNA targeting BCKDH-E1. Both BCKDH -E1 and BCKDH-pSer-E1 were shown down regulated via shRNA knock-down. D, Western blot analysis of p-Ser-E1 in MDA-MB-231 and MDA-MB-231Br3 cells. MDA-MB-231 cells were transfected with control vector and E1-shRNA.

### 2.6.3 Quantitative real-time PCR for VEGF-A

*VEGF-A* gene expression in parental and drug-resistant cell lines were analyzed by quantitative PCR using Taqman primers specific for *VEGF-A* gene. Actin is also amplified as internal control. When cells grew to ~70% confluence, total RNA was extracted using TRIsol reagent following its protocol. Reserse transcription PCR was carried out by First-Step RT-PCR kit, and then realtime PCR was carried out on ABI-7500 platform(Applied Biosystem) using PCR master Mix.

## 2.7 Direct ATP Delivery via Liposomes

Components of making chloroform were prepared in advance as: phosphatidylcholine (0.26mmol), cholesterol (0.12mmol), 1, 2 dioleoyl-3-trimethyl-ammonium-propane (10.8 μmol). Equal amount of each component were mixed and dry to form a film under nitrogen. 5 mL HEPES buffer (pH=7.5**) with or without 600 mmol/L ATP was added directly into the film. The mixture was shaken at 40°C for 30 minutes to allow encapsulation of ATP, and then freeze and thaw between liquid nitrogen and 30°C water bath for 4 times. None capsulated ATP was separated by dialysis in HEPES buffer overnight at 4°C. For each liposome treatment, 10 μL of control liposome or ATP liposomes were added directly in cells culturing in 6-well plates with 700 μL of medium. Whole cell lysis was collected at desirable time points for analysis.

## 2.8 Tissue Samples and Clinical Specimen

### 2.8.1 Metastasis ability measurement

MDA-MB-231 and MDA-MB-231Br3 cells were culture in Dulbecco's Modified Eagle Medium (DMEM) supplemented with 10% Fetal bovin serum, 100 units/mL of penicillin and 100 μg/mL of streptomycin. At exponential growth phase, cells were harvested using 0.25% Trypsin-EDTA, washed and resuspended in Ca2+/Mg2+ free Hanks' balanced Salt Solution (HBSS) before injected into the fat pad of mammary gland of female nude mice. Each injection contained 5000 cells per 100 μL of solution, 5 of mice was injected with each of the cell type. Twelve weeks after injection, brains of injected mice was harvested, fixed in cold 4% paraformaldehyde, embedded in paraffin and sectioned for hematoxylin/eosin staining. Histological analysis was carried out to determine metastasis event.

### 2.8.2 Periodic acid-Schiff stain

Slides were first deparaffinized in Xylene, then rehydrated in serial graded ethanol from 95%-50%. After rehydration, samples were incubated with 0.5% periodic acid for 5 minutes followed by 10 minutes' wash in deionized water. Slides were then placed in a staining glass trade full of PAS solution and heated in microwave for ~15 seconds or until red color appeared. Samples were immediately put to wash under running tap water for 5 minutes to stop staining

process. An additional 20 seconds' counter stain in hematoxylin was applied followed by wash for 5 minutes in tap water. It's necessary to check under microscope to make sure nucleis were stained then slides were ready for dehydration in serial graded ethanol from 50%-95%. Finally slides will be totally dehydrated in Xylene then mounted using DePax mounting medium.

### 2.8.3 Immunohistochemistry on clinical specimen

All clinical specimens were obtained with approval of Institutional Review Board from Tissue Bank of MD Anderson Cancer Center (Houston, Texas). Paraffin embedded specimens were first deparaffinized in Xylene, and then dehydrated in a grade series of alcohol (in PBS). Heated citrate buffer was used to retrieve antigen on the specimens which were then incubated in 3% of hydrogen peroxide in methanol to block endogenous peroxidase activity. 5% donkey serum was then added as blocking solution for 1hour at room temperature. After blocking, primary antibody at the required diluted concentration was added to incubate with the specimen at 4°C overnight. Recommended dilution of FBP1 and FBP2 antibodies were 1:500 and 1:200 respectively; recommended dilution of PEPCK. The next day samples were washed in PBS for 3 times then incubated with secondary antibody, biotinylated goat anti rabbit, at 1:500 dilution for 1 hour at room temperature. After being washed in PBS for 3 times, an ABC staining kit was applied on the sample for chromogenesis, and then slides were briefly-

around 20 second-counterstained with hematoxylin. Slides were sealed in DePex mounting medium and ready for further analysis.

### 2.8.4 Transmission electron microscopy

Different cell lines were cultured in 6-well plates until 70% confluency and then fixed in 0.1M cocodlate buffer (pH=7.3) containing 3% glutaraldehyde and 2%paraformaldehyde. One hour after fixation, cells were submitted to high-resolution electron microscopy facility at MD Anderson Cancer Center where cells were observed under JEM-1010 transmission electron microscope (JEOL USA, Inc.) and images were taken by AMT Imaging System (Advanced Microscopy Techniques).

### Statistics

Student two-tailed *t*-test was used to compare the values (mean±SD) of control and experimental groups. $P < 0.05$ is considered as significant difference.

# CHAPTER 3 ALTERED GLUCOSE METABOLISM IN BREAST CANCER BRAIN METASTSIZED CELLS

## 3.1 Introduction of the Problem

Aerobic glycolysis is one of the most common characteristics shared in cancer (Vander Heiden, Cantley et al. 2009, Locasale and Cantley 2011). It's also one of the distinguishing characteristic between benign and malignant tumor, as cancer cells are always highly glycolytic compared to their non-glycolytic and non-malignant counterparts (Koppenol, Bounds et al. 2011, Ward and Thompson 2012). Altered glucose metabolism in malignant tumors is also one of the reasons for the development of life threatening symptom, cachexia.

To study the relationship between altered glucose metabolism and metastatic potential of cancer cells, we hypothesized that glycolytic activity shall positively correlate with the aggressiveness of cancer cells. To test this hypothesis, we measured the glycolytic activity of a panel of paired cancer cell lines. In each pair of these cell lines, one is a parental cell line and the other is isolated from metastases formed by the parental cells in nude mice, and thus the later one is considered to be more aggressive. These pairs of cells are listed in table 3.

**Table 3 Cancer cell pairs being tested for glycolytic activity**

| | |
|---|---|
| **PC3** | **Human prostate cancer cells** |
| **PC3 MM2** | **Prostate to bone met isolates** |
| **K1735-P** | **Mouse melanoma** |
| **K1735-M2** | **Mouse melanoma s.c. to lung met isolates** |
| **KM12C** | **Human lung Dukes B2** |
| **KM12SM** | **Human lung Dukes B2 Cecal met isolates** |
| **PC14** | **Human lung adenocarcinoma** |
| **PC14PE6** | **Human lung adenocarcinoma iv to pleural effusion met isolates** |
| **MDA MB 231** | **Human breast cancer** |
| **MDA MB 231Br3** | **Human breast cancer nude mice brain met isolates (3 round)** |

As shown in Figure 3.1a, among the 5 pairs of cell lines we tested, faster lactate production and glucose consumption was observed in 4 of the more malignant cancer cells than their parental counterparts (Figure 3.1a).

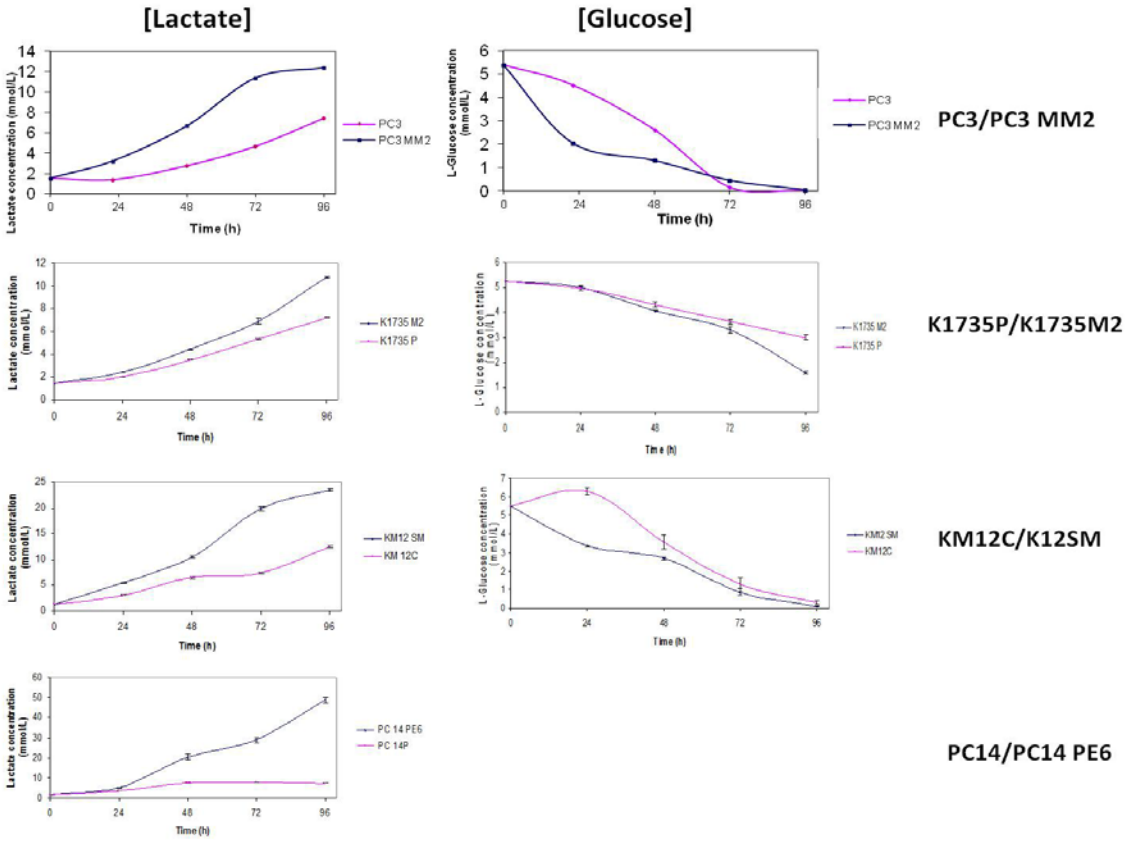


**Figure 3.1a Glucose and lactate concentration change in the cell culture medium in different pair of cancer cell lines.** All cells were culture in full DMEM low glucose medium and medium sample were collected every 24 hours. Measured glucose and lactate concentrations were normalized with cell number at each time point. Each point represent mean ± SD (n = 3).

However, when we tested MDA-MB-231 and MDA-MB-231Br3 cells, we found the brain metastasized MDA-MB-231Br3 cells are less glycolytic than MDA-MB-231 cells (Fig. 3.1b)

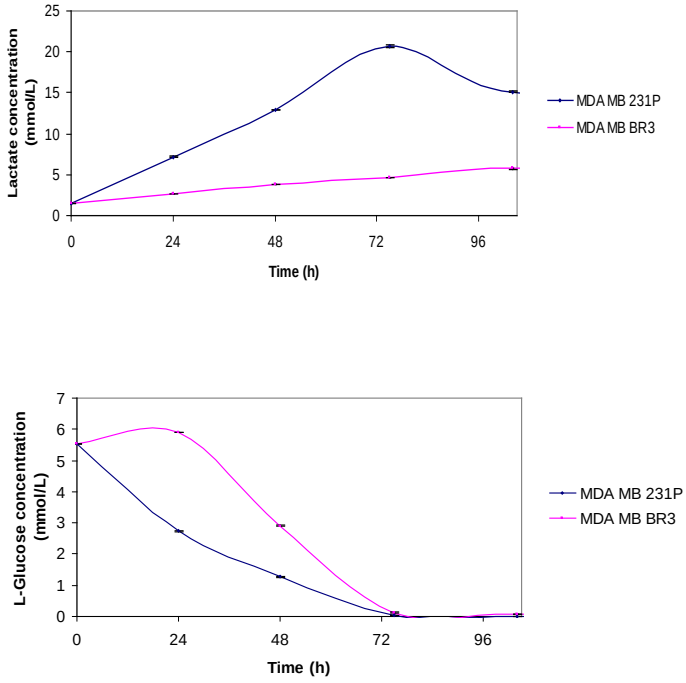


**Figure 3.1b MDA-MB-231P cells exhibited less glycolytic activity than MDA-MB-231Br3 cells.** Measured glucose and lactate concentrations were normalized with cell number at each time point. Each point represent mean ± SD (n = 3). Experimental result repeated more than 3 times.

Following the finding of less glycolytic phenotype of MDA-MB-231Br3 cells, we looked into the microenvironment of the brain which plays a key role in development of cancer after metastasis (Kim, Kim et al. 2011). Although the brain consumes large amount of glucose, free glucose is barely detected in the interstitial space of the brain (Fellows, Boutelle et al. 1992, Hu and Wilson 1997). The free glucose-restricted brain microenvironment seems to be one of the possible explanations for less glycolytic phenotype demonstrated in MDA-MB-231Br3 cells, yet MDA-MB-231Br3 cells are growing faster than MDA-MB-231 cells. We questioned what's the source of energy and biomass for MDA-MB-231Br3 cells which is fast growing yet less glucose dependent? In this chapter, we showed breast cancer brain metastasized cells are able to enhance oxidation of certain amino acids and gluconeogenic activity, and discuss how these enhanced pathways contribute to the survival and proliferation of breast cancer brain metastasized cells.

## 3.2 Result

### 3.2.1 MDA-MB-231Br3 cells proliferate in the absence of glucose

To compare the ability of metastasis to the brain between the MDA-MB-231Br3 cells and the parental MDA-MB-231 cells, we implanted 5,000 viable MDA-MB-231Br3 cells or MDA-MB-231 cells orthotopically into the mammary gland fat pad of immunodeficient (NU/NU) female mice (n=5 in each group). After

three months, the mice were sacrificed and the brains harvested for histological examination. Micro-metastases were observed in 3 of 5 the brains of MDA-MB-231Br3 cells injected mice (Figure 3.2.1 A) and in none of the mice injected with MDA-MB-231 cells.

We then questioned whether the survival of the metastatic cells could be due to altered metabolism. We first investigated the effects of cell-autonomous glucose metabolism. To test the role of glucose in the survival of the parental MDA-MB-231 and MDA-MB-231Br3 cells, we first determined the activity of aerobic glycolysis of these cells by measuring glucose consumption and lactate production by cells cultured in media containing 5mM glucose. As shown in Figure 3.2.1 B-C, the MDA-MB-231Br3 cells consumed less glucose and produced less lactate than the parental cells. To test the dependency of these cells on glucose for survival, we removed glucose from the cell culture medium. More than 95% of the parental MDA-MB-231 cells died within 72h of cell culture, whereas the brain metastatic MDA-MB-231Br3 cells remained viable and proliferative (Figure. 3.2.1 D-F). These data suggest that a significant metabolic shift from glucose-dependent to -independent viability occurred in the brain metastatic cells. To determine the cause of cell death of MDA-MB-231 cells cultured in glucose-free medium, we performed Western blot analyses on markers of apoptosis, caspase 3, and of autophagy, cleaved microtubule-associated protein 1A/1B-light chain 3 (LC3). As shown in Figure 3.2.1G, only the procaspase 3 (30kDa) but not the cleaved form of caspase 3 (20kDa) was

detected in MDA-MB-231 cells starved from glucose; however, a significant shift of LC3 from LC3I to LC3II occurred, indicating autophagy was associated with the death of these cells in the absence of glucose.

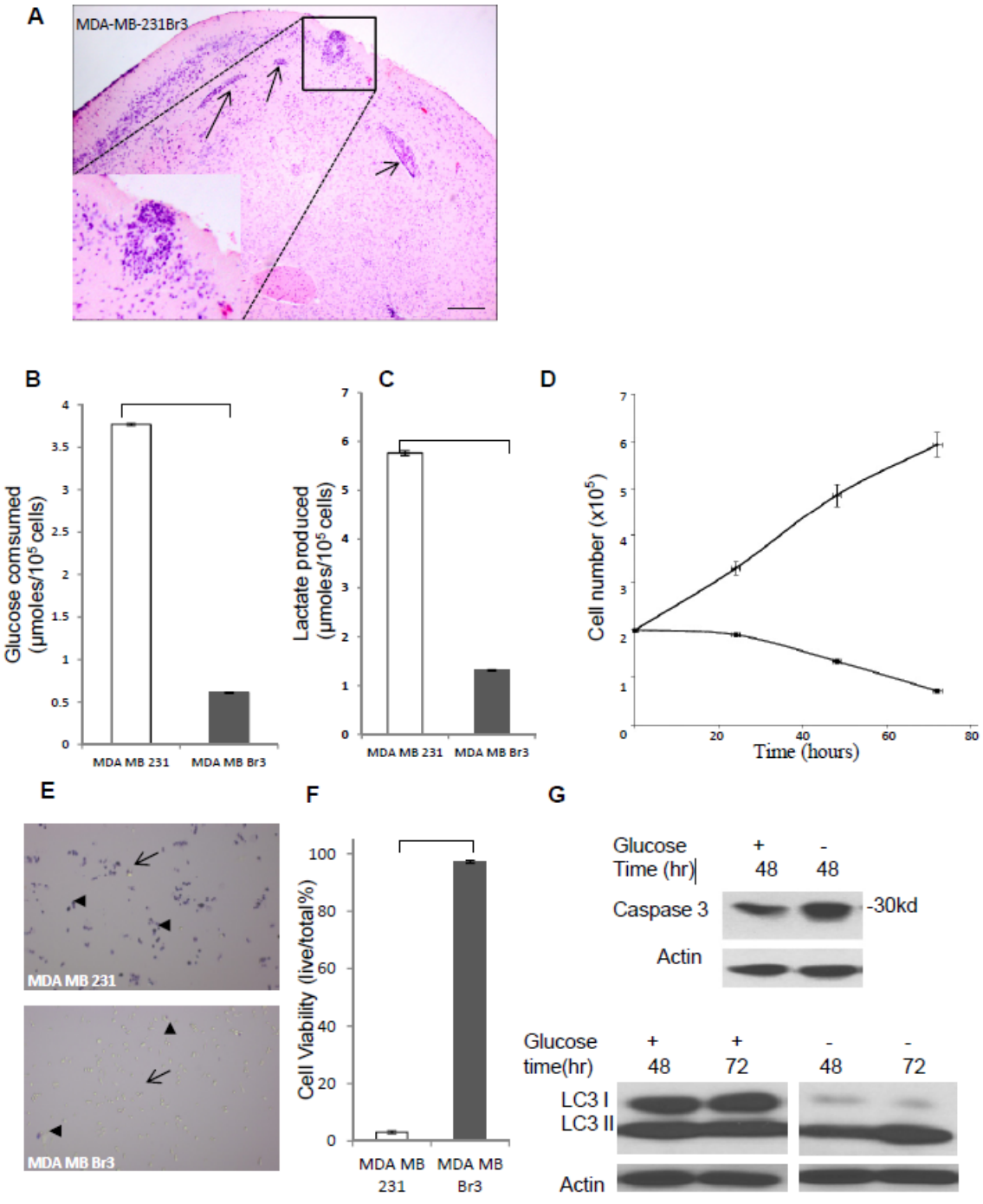
A
MDA-MB-231Br3
B
Glucose comsumed (µmoles/10⁵ cells)
MDA MB 231
MDA MB Br3
C
Lactate produced (µmoles/10⁵ cells)
MDA MB 231
MDA MB Br3
D
Cell number (x10⁵)
Time (hours)
E
MDA MB 231
MDA MB Br3
F
Cell Viability (live/total%)
MDA MB 231
MDA MB Br3
G
Glucose
Time (hr)
+
-
48
48
Caspase 3
-30kd
Actin
Glucose
time(hr)
+
+
-
-
48
72
48
72
LC3 I
LC3 II
Actin

**Figure 3.2.1 Characterization of MDA-MB-231Br3 cells.** (A)MDA-MB-231Br3 cells implanted into the mammary glands of female nude mice formed spontaneous micro-brain metastases (arrows). (B) and (C) MDA-MB-231Br3cells consume less glucose and produce less lactate than the MDA-MB-231cells during a period of 12 hr. Triplicates of samples were used in each group. (D) MDA-MB-231Br3 cells, but not MDA-MB-231 cells remained proliferative in the absence of glucose. (E) Removal of glucose from cell culture medium caused massive cell death in MDA-MB-231 cells but not the MDA-MB-231Br3 cells within 72 hr of cell culture. Trypan blue staining was used to identify dead cells (arrow heads). Live cells in MDA-MB-231 cells are indicated by arrows. (F) Quantification of results shown in F. Triplicates of samples were used in each group. (G) Western blot analyses of caspase 3 and LC3 of MDA-MB-231 cells cultured in the presence/absence of glucose. ($p<0.05$, t-test was used between the linked control groups and experimental groups).

### 3.2.2 Glutamine and BCAAs are critical for the glucose independent survival of MDA-MB-231Br3 cells

In addition to glucose, amino acids can also serve as energetic substrates. Considering the high levels of glutamine and BCAAs in the interstitial space of the brain (Yudkoff, Nissim et al. 1993, Yudkoff 1997), we hypothesized that the catabolism of these two classes of amino acids might play an important role in the survival of brain metastatic cells. Glutamine can be metabolized to glutamate by glutaminase, and glutamate can be further oxidized by glutamate dehydrogenases (GLUD1 and GLUD2) (Kovacevic and McGivan 1983) to the citric acid cycle intermediate α-ketoglutarate (α-KG). We therefore measured the extracellular levels of glutamine and glutamate of parental MDA-MB-231 and brain metastatic MDA-MB-231Br3 cells cultured for 24hr in glucose-free medium. We found that in the absence of glucose, the MDA-MB-231Br3 cells consumed more glutamine and produced more glutamate than the parental cells (Figure 3.2.2 A-B), indicating that the brain metastatic cells had an enhanced glutamine metabolism. Next, we determined the expression levels of GLUD1 and GLUD2 in the isolated pure mitochondria of both cell lines by Western blot analysis. As shown in Figure 3.2.2C, the MDA-MB-231Br3 cells expressed a higher amount of GLUD1 and GLUD2 than the MDA-MB-231 cells in the mitochondria.

The BCAAs (valine, leucine, and isoleucine) also exist in abundance in the brain. To examine their role in the survival of brain metastatic cancer cells, we

determined the changes of BCAAs in the glucose-free cell culture media of MDA-MB-231 and MDA-MB-231Br3 cells that had been cultured for 48 h. The levels of BCAAs increased in the medium of the parental MDA-MB-231 cells and decreased in the medium of the MDA-MB-231Br3 cells (Figure 3.2.2 D-F), suggesting that the brain metastatic cells, but not the parental cells, consumed BCAAs. To measure the BCAA-oxidizing abilities of these two cell types, we added $^{14}$C-Leucine to the culture media and measured $^{14}CO_2$ production after 8 h. As shown in Figure 2G, the brain metastatic cells exhibited significantly higher BCAA-oxidation rates than the parental cells. In the parental and brain metastatic cells, we measured the levels of the rate limiting enzymes of BCAA oxidation: the branched-chain ketoacid dehydrogenase E1 subunit (BCKDH-E1); the inactivated form of BCKDH-E1, pSer293-BCDKH-E1 (phosphorylated at serine 293 of the E1 subunit); and the BCKDH-inactivating kinase, the branched chain ketoacid dehydrogenase kinase (BDK) (Lu, Sun et al. 2009). The total amounts of BCKDH-E1 and BDK were found to be equal in these two types of cells, but the brain metastatic cells have a significantly lower level of pSer293-BCKDH-E1 (Figure 3.2.2H), indicating that the brain metastatic cells have higher BCAAs oxidation activity. To determine the relationship between pro-survival roles of BCAAs and glutamine, we performed cell death rescue experiments. The MDA-MB-231Br3 cells were first starved from glucose/BCAAs/glutamine for 6hr, and then supplemented with increasing amounts of glutamine (1-4mM) with/without BCAAs (800μM). Cell viabilities were measured at the 12hr after glutamine

addition. As shown in Figure 3.2.2I, BCAAs and glutamine synergistically increased the survival of MDA-MB-231Br3 cells. These data suggest that glutamine and BCAAs are required for the maximum survival of the brain metastatic cells in conditions of no glucose.

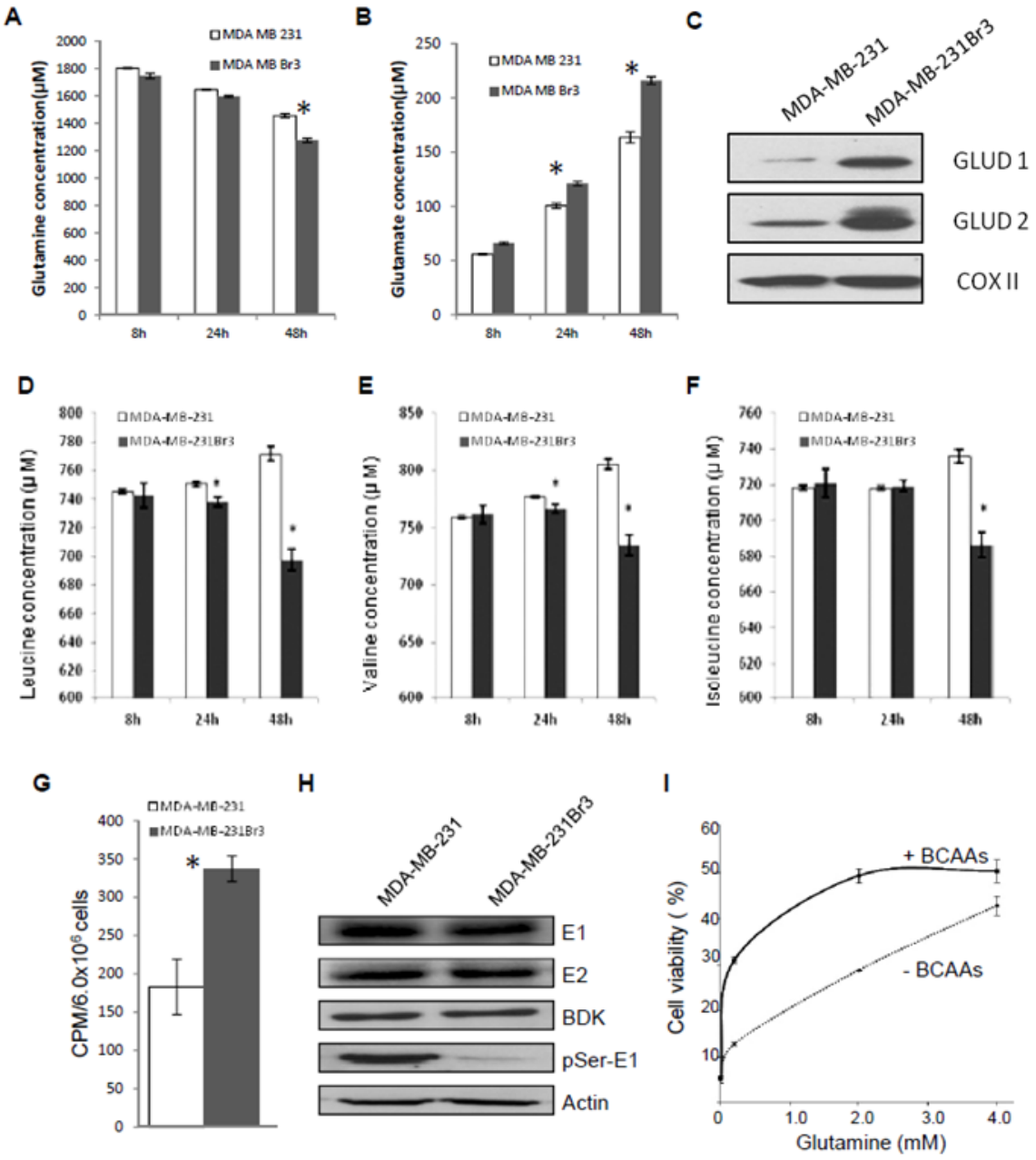
A
Glutamine concentration(μM)
MDA MB 231
MDA MB Br3
8h
24h
48h
B
Glutamate concentration(μM)
MDA MB 231
MDA MB Br3
C
MDA-MB-231
MDA-MB-231Br3
GLUD 1
GLUD 2
COX II
D
Leucine concentration (μM)
MDA-MB-231
MDA-MB-231Br3
E
Valine concentration (μM)
F
Isoleucine concentration (μM)
G
CPM/6.0x10^6 cells
H
E1
E2
BDK
pSer-E1
Actin
I
Cell viability ( %)
+ BCAAs
- BCAAs
Glutamine (mM)

**Figure 3.2.2 Roles of glutamine and BCAAs in the survival of MDA-MB-231Br3 cells. (**A) and (B) MDA-MB-231Br3 cells consumed a higher amount of glutamine and produced higher amount of glutamate than MDA-MB-231 cells after cultured in glucose-free medium for 48 h. Triplicates of samples were used at each time point. (C) MDA-MB-231Br3 cells contain a higher level of GLUD1 and GLUD2 than MDA-MB-231 cells. (D) to (F) The level of leucine, valine, and isoleucine decreased significantly in the medium of MDA-MB-231Br3 cells not in the MDA-MB-231 cells cultured in glucose-free condition. Triplicates of samples were used at each time point. ($p<0.05$, *t*-test was used between the asterisk marked groups). (G) MDA-MB-231Br3 cells produced a significantly higher level of $^{14}CO_2$ from $^{14}$C-leucine than MDA-MB-231 cells. (CPM, count per minute) ($p<0.05$, *t*-test). (H) Western blot analysis of BCKDH-E1 (E1), BCKDH-E2, BDK, pSer293-BCKDH-E1 (pE1) in MDA-MB-231 and MDA-MB-231Br3 cells. Actin was used as loading controls. (I) BCAA and glutamine are synergistically rescued MDA-MB-231Br3 cells from cell death caused by starvations of glucose/glutamine/BCAAs. Trypan blue uptake was used to identify dead cells and triplicates of samples were used in each group. ($p<0.05$, *t*-test was used between the asterisk marked control and experimental groups).

### 3.2.3 Rate limiting enzymes of gluconeogenesis are up-regulated in MDA-MB-231Br3 cells

Although the brain metastatic cells grow and survive in the absence of glucose, it remains unclear which carbon sources constitute the basic building blocks for proliferation, especially ribose production in the absence of glucose. One possibility is that the brain metastatic cancer cells have acquired the ability to carry out gluconeogenesis. There are two critical families of enzymes within the gluconeogenesis pathway: phosphoenylpyruvate carboxykinases (PEPCK1 and PEPCK2), which convert oxaloacetate to phosphoenylpyruvate (PEP); and fructose-1, 6-bisphosphatases (FBP1 and FBP2), which convert fructose-1,6-biphosphate to fructose-6-phosphate. We compared the expression levels of these two enzymes in the parental and brain metastatic cancer cells. As shown in Figure 3.2.3A, in MDA-MB-231Br3 cells, PEPCK2 expression was unchanged, FBP1 and PEPCK1 were significantly down-regulated, and FBP2 was significantly up-regulated, suggesting a shift favoring mitochondrial PEPCK2 for PEP production and FBP2 for fructose-6-phosphate production in the brain metastatic cells. We then tested the survival of MDA-MB-231Br3 cells after knockdown of FBP2 by shRNA targeting at the fifth exon of FBP2 gene. Knocking down FBP2 (Figure 3.2.3 B) resulted in a significant amount of cell death of the MDA-MB-231Br3 cells cultured in glucose-free medium, which was determined by trypan blue uptake and quantified by cell counting (Figure 3.2.3 C), suggesting that gluconeogenesis is critical for the survival of the brain metastatic

cells. To demonstrate that this phenotype was not due to an off-target effect of the shRNA, we expressed exogenous FBP2, that does not contain the 3'-UTR sequence in MDA-MB-231Br3 cells treated with shRNAs targeting the 3'-UTR of endogenous FBP2 (Figure 3.2.3D). It was found that knocking down FBP2 resulted in significant cell death of cells cultured in glucose-free medium, which was significantly rescued by expressing the exogenous FBP2 (Figure 3.2.3 E).

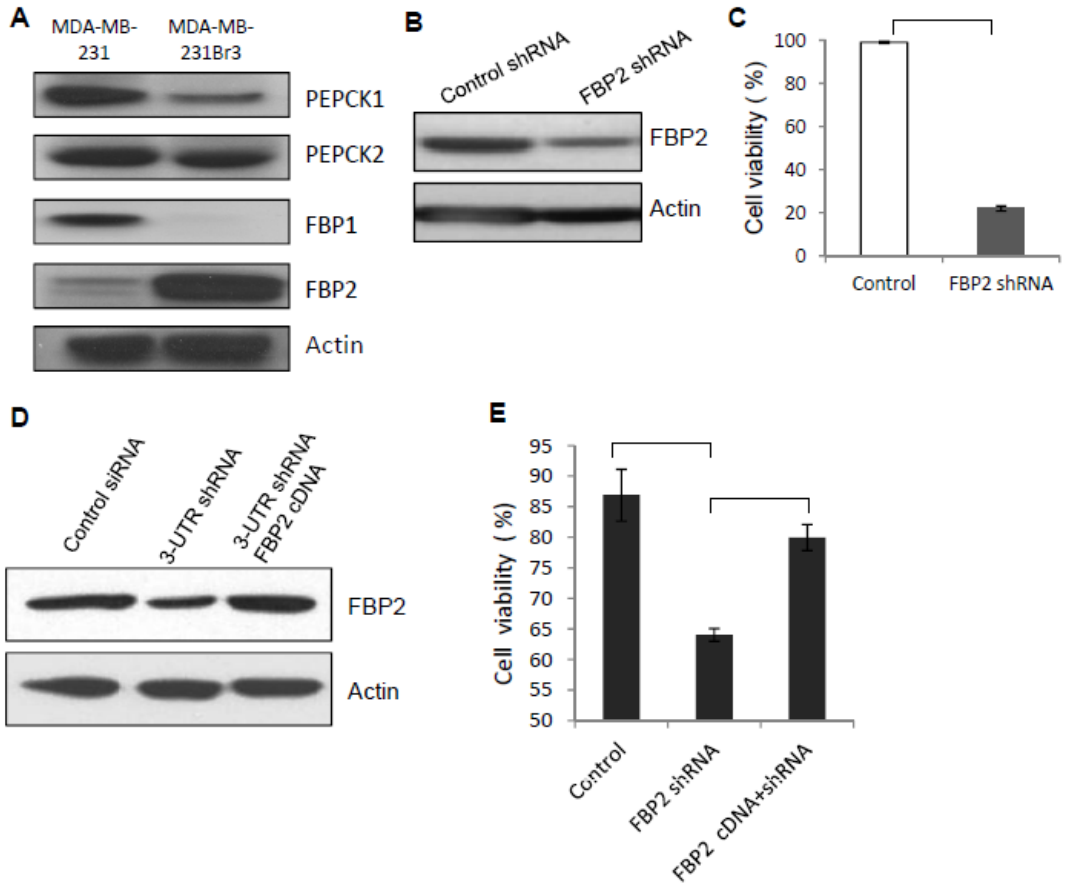


**Figure 3.2.3 Role of Gluconeogenic Enzymes in the Survival of Breast Cancer Brain Metastatic Cells.** (A) Western blot analyses of PEPCK1, PEPCK2, FBP1, FBP2 in MDA-MB-231 and MDA-MB-231Br3 cells. Actin was used as a loading control. (B) Western blot analysis of knocking down FBP2 by shRNA in MDA-MB-231Br3 cells. (C) Knocking down FBP2 by shRNA caused a significant amount of cell death in MDA-MB-231Br3 cells culture in glucose-free condition. (D) and (E) Knocking down FBP2-induced MDA-MB-231Br3 cell death was rescued by re-expression of exogenous FBP2. Trypan blue uptake was used to identify dead cells and triplicates of samples were used in each group. ($p<0.05$, *t*-test).

### 3.2.4 MDA-MB-361 cells exhibit glucose independent phenotypes similar to the MDA-MB-231Br3 cells

MDA-MB-231Br3 cells were derived by *in vivo* selection of brain metastases formed in the brain of nude mice. To determine whether breast cancers that metastasize to the brain in human patients can also acquire the ability to survive in low glucose, we examined MDA-MB-361 cells, a breast cancer cell line isolated from a brain metastasis of a patient (Zhang, Fidler et al. 1991). Like the MDA-MB-231Br3 cells, the MDA-MB-361 cells are completely viable and proliferative in glucose-free medium (Figure 3.2.4A). Similarly, the MDA-MB-361 cells have higher levels of total BCKDH-E1 and lower levels of pSer293-BCDKH-E1 as compared to the MDA-MB-231 cells; however, the BDK level is higher than that of the MDA-MB-231 parental cells (Figure 3.2.4B). In addition, the MDA-MB-361 cells have significantly higher levels of PEPCK1, PEPCK2, FBP1, FBP2, GLUD1, and GLUD2, indicating that they might have an even stronger gluconeogenic capacity than that of the MDA-MB-231Br3 cells (Figure 3.2.4B). These data suggest that the brain metastatic breast cancer cells derived by selection in mouse brain and the human brain adopted similar metabolic alterations, enhanced abilities of gluconeogenesis and BCAA oxidation.

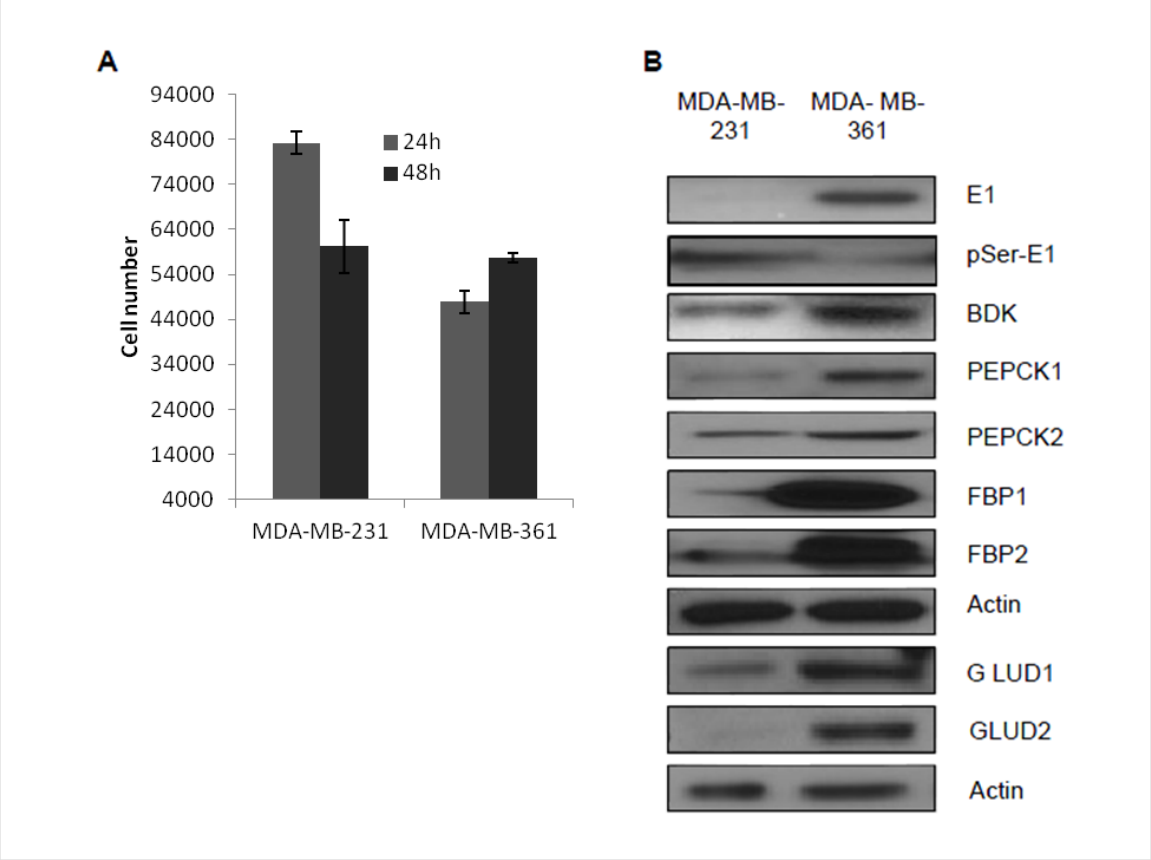


**Figure 3.2.4. Characterization of a Breast Cancer Brain Metastatic Cell Line, MDA-MB-361, Isolated from Human Tissues.** (A) Cell counts of MDA-MB-231P cells and MDA-MB-231Br3 cells culured in glucose-free medium. Triplicates of samples were used at each time point. (B) Western blot analysis of BCKDH-E1, pBCKDH-E1, BDK, PEPCK1, PEPCK2, FBP1 and FBP2, GLUD1, and GLUD2.

### 3.2.5 Metabolomics of brain-metastatic breast cancer cells upon glucose deprivation

To investigate the changes in metabolism that occur under glucose-free conditions, we carried out targeted mass spectrometry to measure the relative abundance of metabolites (Kelly, Breitkopf et al. 2011, Locasale, Melman et al. 2012, Yuan, Breitkopf et al. 2012) in brain metastatic cells cultured for 24 h in their native media containing either 5 mM glucose or 0 mM glucose. The metabolite profiles for each cell line under each condition were then analyzed using unsupervised hierarchical clustering. The data (Figure 3.2.5A) revealed distinct metabolic signatures that characterize the different glucose conditions. We isolated one such signature (Figure 3.2.5B) of metabolites whose levels decreased upon glucose withdrawal, which include many intermediates of glycolysis. The fold changes of some of these metabolites are presented in Figure 3.2.5C. Notably, glucose-1-phosphate (G1P) (Figure 3.2.5D) decreased significantly after glucose withdrawal, suggesting that sources other than glucose are feeding into glucose metabolism under these conditions. To determine whether these cells carry out gluconeogenesis using amino acid as substrates, we added $^{13}$C-glutamine into the cell culture media with/without glucose and measured the levels of $^{13}$C labeled TCA metabolites and fructose-6-phosphate (F6P) and glucose-6-phospate (G6P) after 6 h of cell culture. In response to glucose withdrawal, we found that the levels of fully labeled TCA metabolites, such as citrate, α-KG, succinate, fumarate, malate, and oxaloacetate, either

increased in the MDA-MB-231Br3 cells (Figure 3.2.5 E) or remained mostly unchanged in the MDA-MB-361 cells (Figure 3.2.5 F). These results indicate that glutamine-mediated anaplerosis contributes to a substantial amount of TCA cycle flux. More importantly, we observed significant labeling of glutamine-derived intermediates, including fructose-6-phosphate (Figure 3.2.5 G) and ribose-phosphate (Figure 3.2.5 H). The $^{13}$C-glutamine tracing data validate that the brain metastatic cells are gluconeogenic using amino acids as substrates. It is likely that other amino acids besides glutamine also contribute to the gluconeogenesis of these cells. Taken together, these data show that the MDA-MB-231Br3 and MDA-MB-361 cells undergo gluconeogenesis in the absence of external glucose.

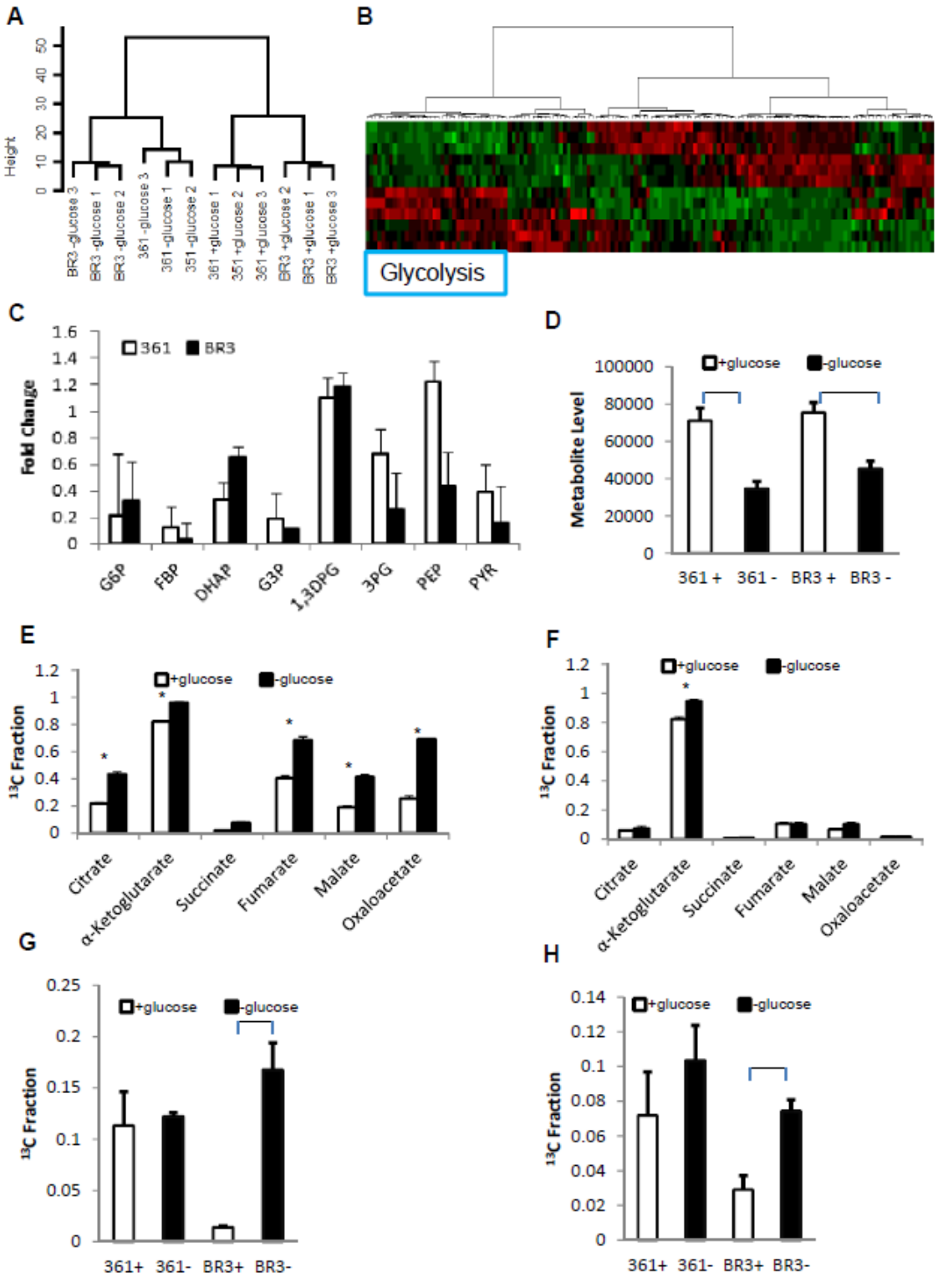
A
Height
0
10
20
30
40
50
BR3 -glucose 3
BR3 -glucose 1
BR3 -glucose 2
361 -glucose 3
361 -glucose 1
351 -glucose 2
361 +glucose 1
351 +glucose 2
361 +glucose 3
BR3 +glucose 2
BR3 +glucose 1
BR3 +glucose 3
B
Glycolysis
C
361
BR3
Fold Change
G6P
FBP
DHAP
G3P
1,3DPG
3PG
PEP
PYR
D
+glucose
-glucose
Metabolite Level
361 +
361 -
BR3 +
BR3 -
E
+glucose
-glucose
13C Fraction
Citrate
α-Ketoglutarate
Succinate
Fumarate
Malate
Oxaloacetate
F
+glucose
-glucose
13C Fraction
Citrate
α-Ketoglutarate
Succinate
Fumarate
Malate
Oxaloacetate
G
+glucose
-glucose
13C Fraction
361+
361-
BR3+
BR3-
H
+glucose
-glucose
13C Fraction
361+
361-
BR3+
BR3-

**Figure 3.2.5 Metabolic Profiling and Isotopic Tracing of Metabolites in Response to Glucose Withdrawal**. (A) Unsupervised hierarchical clustering across triplicate experiments (1-3) across three cell lines (MDAM231-BR3, MDAM 361) in the presence and absence of glucose. The resulting dendrogram is shown. The height denotes Euclidean distance. (B) Resulting heat map obtained from unsupervised hierarchical clustering. The red bar below denotes the signature that identifies metabolites that are decreased in each cell line in response to glucose withdrawal. (C) Changes of metabolites of glycolysis in MDA-MB-231Br3 and MDA-MB-361 cells in response to removal of glucose. (G6P, glucose-6-phosphate; FBP, fructose bisphosphate; DHAP, dihydroxyacetone phosphate; G3P, glycerol 3-phosphate; 1,3DPG, 1,3-diphospho-glycerate; 3PG, glycerate 3-phosphate; PEP, phosphoenolpyruvate; PYR, pyruvate). (D) Relative abundance of glucose-1-phosphate. Integrated ion current (metabolite level) for glucose-1-phospate is plotted for each cell line MDA-MB-361(361) and MDA-MB-231Br3 (BR3)) in the presence (glucose) and absence (no glucose) of glucose. (E) Glutamine tracing. The ratio of $^{13}C$ labeled to total metabolite pool ($^{13}C$ fraction) for citrate, α-ketoglutarate, succinate, fumarate, malate, and oxalocaccetate in MDA-MB-361 cells. (F) Same as in (E) but for MDA-MB-231Br3 cells. (G) Glutamine tracing. The ratio of $^{13}C$ labeled to total metabolite pool ($^{13}C$ fraction) for fructose-6-phosphate for each cell line MDA-MB-361(361) and MDA-MB-231Br3(BR3)) in the presence (glucose) and absence (no glucose) of glucose. (H) Glutamine tracing. The ratio of $^{13}C$ labeled to total metabolite pool ($^{13}C$ fraction) for ribose-phosphate for each cell line (MDA-MB-361(361) and MDA-MB-231Br3(BR3)) in the presence (glucose) and absence (no glucose) of glucose. All error bars are obtained from s.e.m (n=3).

### 3.2.6 Rate limiting enzymes of gluconeogenesis are highly expressed in human breast cancer brain metastasis

To further characterize the role of gluconeogenesis in breast cancer brain metastasis, we profiled the expression of the aforementioned rate limiting enzymes of gluconeogenesis in clinical specimens of breast cancer brain metastases (n=5) and their matched cancer tissues from the primary sites (n=2) by immunohistochemistry. As shown in Figure 3.2.6 A, the brain metastases were positive for both FBP1 and PEPCK2. The FBP2 or PEPCK1 positive cells were fractional and variable among the brain metastases. The matched cancer tissues from the primary sites were positive for FBP1, PEPCK1 and PEPCK2, but negative for FBP2; however the corresponding brain metastases exhibited positive FBP2 signals, suggesting an adaptation was made in the brain metastasis. The concurrent expression of FBP1 and PEPCK2 in the brain metastases supports the gluconeogenic phenotype of brain metastatic cancer cells.

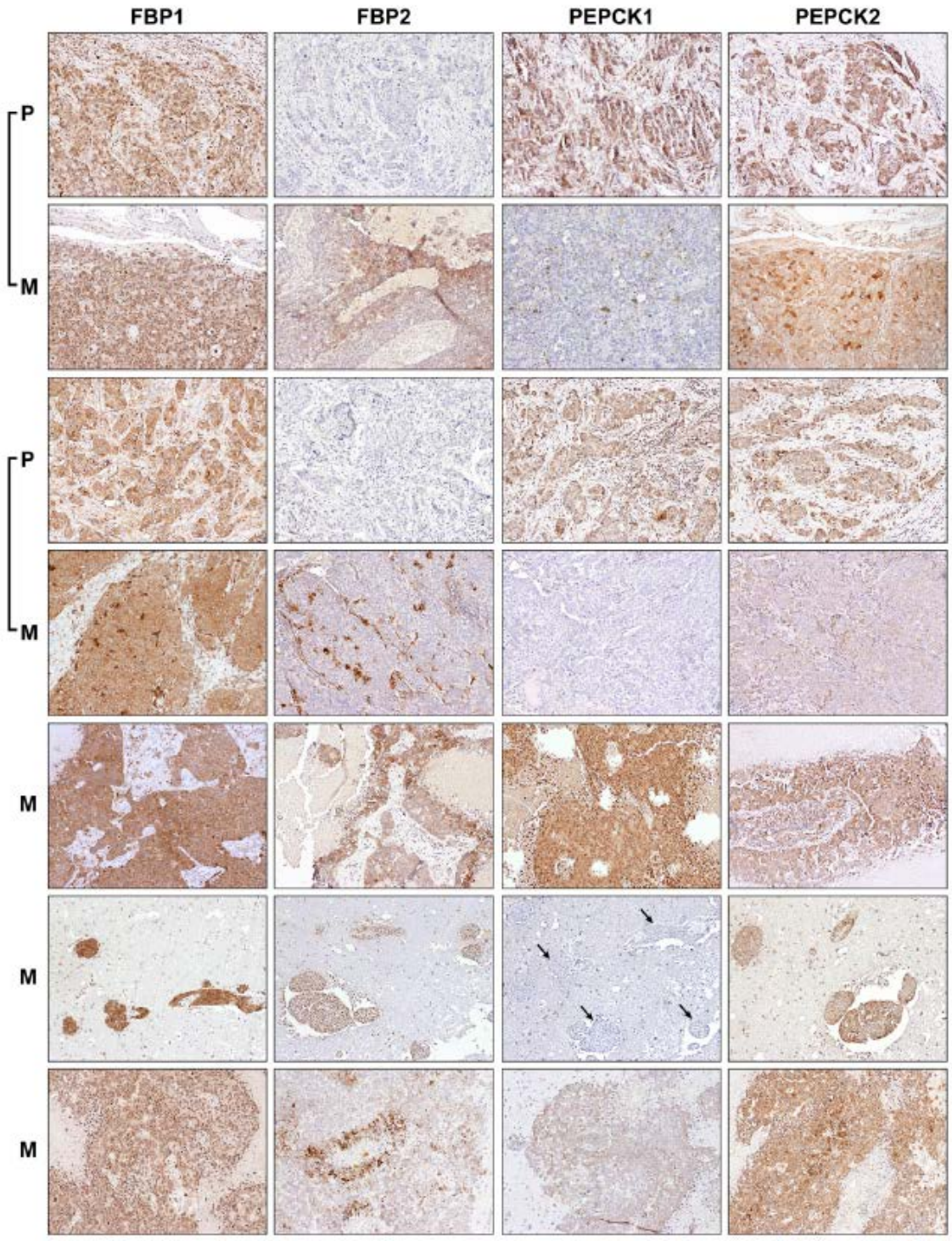
FBP1
FBP2
PEPCK1
PEPCK2
P
M
P
M
M
M
M

**Figure 3.2.6. Characterization of gluconeogenesis in breast cancer brain metastasis in clinical specimen**. Rate limiting enzymes of gluconeogenesis and glycogen in breast cancer brain metastases immunohistochemical stainings for FBP1, FBP2, PEPCK1, and PEPCK2 in human breast cancer brain metastases (M) and their matched primary tumors (P). Positive signals are in brown color (arrows indicate tumor metastases).

### 3.2.7 Breast cancer brain metastases contains higher levels of glycogen than cancer cells of primary sites

Considering the evidence for gluconeogenic activity in brain metastasis, we further tested whether the brain metastases can store glycogen. We used periodic acid-Schiff staining (PAS) to determine glycogen levels in the tissues of human breast cancer brain metastases (n=5), the mouse brain micrometastases (n=3) formed by MDA-MB-231Br3 cells, and primary breast cancer tissue samples (n=34) on a tissue microarray. We found that most of the cancer cells of MDA-MB-231Br3-metastases were PAS positive, and the human brain metastases contained a significantly higher amount ($P < 0.0001$) of PAS positive cancer cells than that of the primary cancers (Figure 3.2.7 A-G). These data indicate that the brain metastases produce and store glycogen.

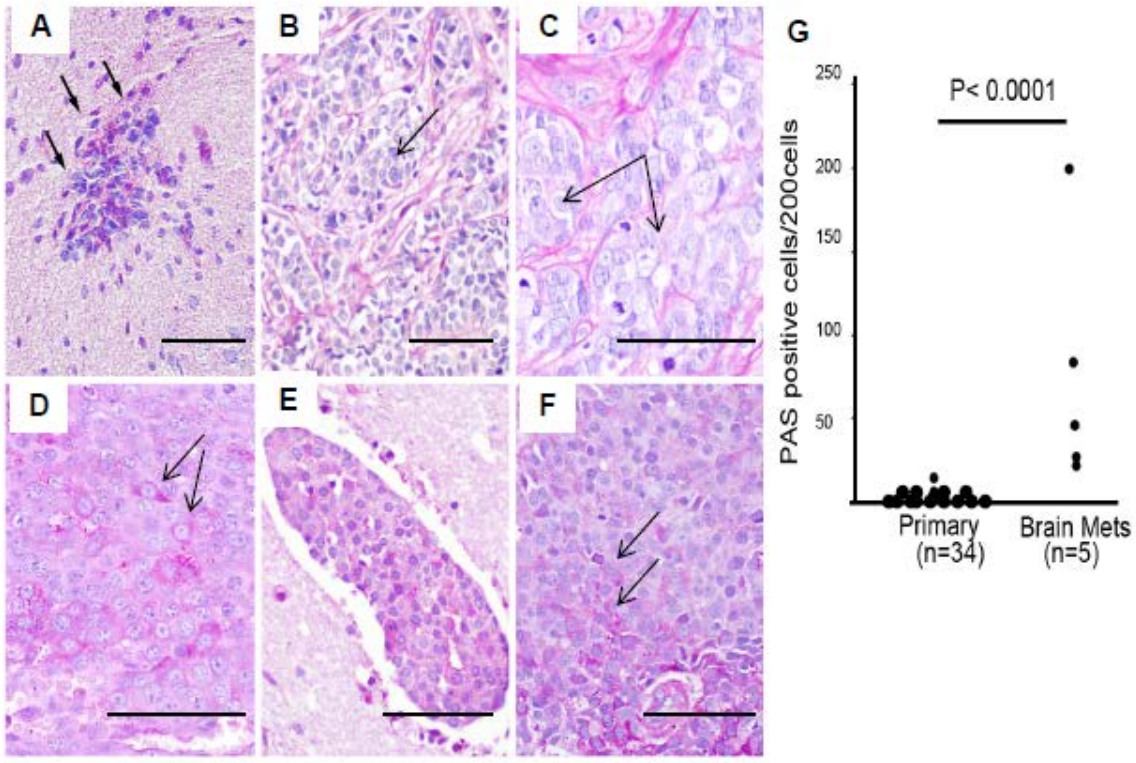


**Figure 3.2.7. Brain Metastatic Cells Contain High Levels of Glycogen**. (A) PAS staining for glycogen in the spontaneous brain metastases formed by MDA-MB-231Br3 cells (arrows, PAS signal is in pink color). (B) and (C) PAS staining of primary human breast cancers. Note the cancer cells are negative (arrows) and stromal cells are positive (pink color). (D) to (F) PAS staining in human breast cancer brain metastases (arrows, cancer cells with strong PAS signals). (G) Quantification of PAS positive cells of primary cancers (n=34) and brain metastases (n=5). (Two hundred cancer cells from each of three randomly selected areas were counted, and the numbers of PAS positive cells are plotted in a scatter chart. A chi-squared with two-tailed test was used to compare the two groups, which generated a P value < 0.0001.)

## 3.3 Discussion

Mutual adaptation between metastatic cancer cells and the microenvironment of a host organ have to be achieved for a successful establishment of cancer metastasis (Fidler 2003). Alterations at levels of gene expression and activities of signaling pathways in cells of both cancer metastasis and host organ have been well documented (Bos, Zhang et al. 2009, Chaffer and Weinberg 2011, Langley and Fidler 2011). Our data revealed that breast cancer brain metastatic cells can utilize gluconeogenesis and oxidation of branched chain amino acids for growth independent of glucose.

The brain interstitial space is a unique metabolic microenvironment. Because of the pre-metabolizing functions of astroglial cells that bridge blood vessels with neurons, the interstitial compartment of the brain is characterized with low levels of glucose (Fellows, Boutelle et al. 1992, Hu and Wilson 1997) and high levels of glutamate, as glutamate is major excitatory transmitter in the brain (Yudkoff, Nissim et al. 1993), and branched chain alpha-ketoacids (the first intermediate metabolite of BCAA oxidation)(Daikhin and Yudkoff 2000). Passing through the blood-brain-barrier, glucose is mainly taken up by astroglial cells and pre-processed in the astroglia for neuronal energy needs (Pellerin 2008), which results in an interstitial glucose level that is 10 times lower than the glucose level in the blood (Fellows, Boutelle et al. 1992, Hu and Wilson 1997). The elevated expression of mRNA of genes involved in glycolysis in brain metastatic cells (Chen, Hewel et al. 2007) might be a compensatory response to the low levels of

glucose in the interstitial space of the brain. The high rate of glutamate synthesis in the brain requires an amino group donor that is readily transaminated. At least two-thirds of the amino groups of brain glutamate are derived from BCAAs (Yudkoff, Nissim et al. 1993). The constant large scale uptake of BCAAs by the brain is sustained by large neutral amino acid transporters, which are highly expressed in the endothelial cells of brain vessels (del Amo, Urtti et al. 2008). Astroglial cells produce glutamine for neurons via transfer of an amino group from BCAA to glutamate, and the resulting branched chain α-ketoacid byproducts are released to the interstitial space, where they can be taken up by neurons for glutamine metabolism by deamination (Yudkoff, Nissim et al. 1993). The contribution of BCAAs to the survival of cancer brain metastasis is further supported by the fact that higher sensitivity was found by tracing $^{11}$C-BCAA for brain metastasis imaging than using the glucose analogue tracer $^{18}$FDG (Kirikae, Diksic et al. 1989, Ishiwata, Kubota et al. 1993, Ishiwata, Tsurumi et al. 1993), suggesting that brain metastatic cells take up a high amount of BCAAs. The shift from glucose metabolism to amino acid metabolism for survival exhibited by the brain metastatic cells provides further evidence that the organ microenvironment plays a critical role in the development of cancer metastasis.

Gluconeogenic activity is not normally presented in cells that are not originated from liver, kidney, intestine, or muscle (Previs, Brunengraber et al. 2009). The glycogenic feature of brain metastatic cells enables another pro-survival ability to these cells, glucose storage, which helps cancer cells to resist

external metabolic stresses. Gaining gluconeogenic/glycogenic ability and increasing amino acid oxidation provides brain metastatic cells with survival and proliferation power independent of external glucose. These studies suggest that targeting amino-acid-dependent gluconeogenesis may provide a novel approach to the treatment of fatal brain metastasis.

# CHAPTER 4 ALTERED GLUCOSE METABOLISM IN DEVELOPMENT OF CROSS DRUG RESISTANCE COLON CANCER CELLS

## 4.1 Introduction to the Problem

Since altered glucose metabolism in cancer cells was discovered by Dr. Otto Warburg in 1920s and studies have repeatedly confirmed that most cancers carry out aerobic glycolysis. One challenging question still remains to be answered is that what the driving force is for cancerous aerobic glycolysis. One popular hypothesis is the hypoxia-driven alteration in glucose metabolism, which argues that the hypoxia microenvironment inside solid tumors leads to constitutive activation of hypoxia inducible factor (HIF) that up-regulates glycolysis (Robey, Lien et al. 2005). In this case, HIF-1α functions as oxygen sensor and oxygen limitation takes the role of a possible driving force for aerobic glycolysis. This hypoxia-driven hypothesis is challenged by the fact that blood cancers are also glycolytic in an environment that is never hypoxic.

This hypoxia-driven mechanism is similar to how skeletal muscle cells carry out fermentation during exercise. However, the concept that muscle cells undergo fermentation during exercise, which has been long thought due to hypoxia condition, is being challenged. Studies have shown that during moderate-intense exercise, oxygen uptake is not limited to a level that would

affect oxidative phosphorylation in the cells (Bangsbo, Krustrup et al. 2000, Nyberg, Mortensen et al. 2010). Studies in cancer cells have also revealed that oxygen concentrations in the center of many solid tumors do not really reach the hypoxic threshold which would cause deficient OXPHOS in mitochondria (Moreno-Sanchez, Rodriguez-Enriquez et al. 2009). Moreover, proliferative T cells that are never hypoxic in the blood still carry out aerobic glycolysis during inflammation (Guindi 1999). Cancer cells exhibit constitutive aerobic glycolysis in the cell culture medium in which oxygen is abundant (Moreno-Sanchez, Rodriguez-Enriquez et al. 2007). Taken together, we argue that oxygen limitation/ hypoxia may not be the driving force for altered glucose metabolism in cancer cells.

We revisited the major biochemical events in skeleton muscle cells during exercise. It is actually known that a dramatic drop of intracellular ATP precedes the decrease of oxygen level (Gleim, 1993; Burton, 2004), which leads us to a hypothesis that insufficient intracellular ATP level may play a key role in driving aerobic glycolysis in cancer cells. To test this hypothesis, we first compared the levels of intracellular ATP of none cancer cells and their corresponding cancer cells. As shown in Figure 4.1a, cancer cells of tissues contain lower levels of intracellular ATP than their non-cancerous counterparts. These data raise some important questions: Since cancer cells have lower level of intracellular ATP, what would happen if we increase their intracellular ATP? Will it affect various

cancer phenotypes like aerobic glycolysis, constitutively active HIF1 signaling, and even drug resistance?

Naked ATP cannot be delivered into cells without altering the adenosine receptor mediated complex signaling (Khakh and North 2006). In this part of the study, we embedded ATP in liposomes and treated cells with liposomes, which we allowed us to transiently increase intracellular ATP level.

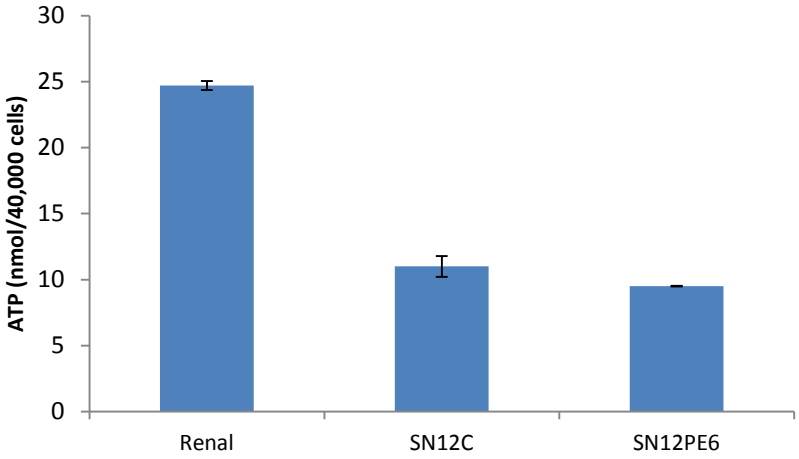
ATP (nmol/40,000 cells)
30
25
20
15
10
5
0
Renal
SN12C
SN12PE6

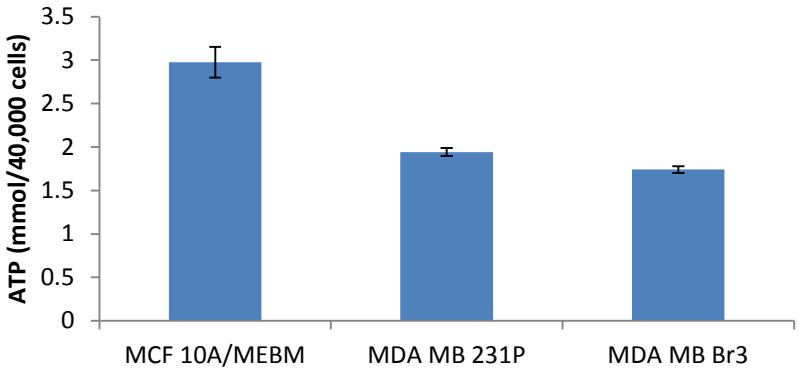
ATP (mmol/40,000 cells)
3.5
3
2.5
2
1.5
1
0.5
0
MCF 10A/MEBM
MDA MB 231P
MDA MB Br3

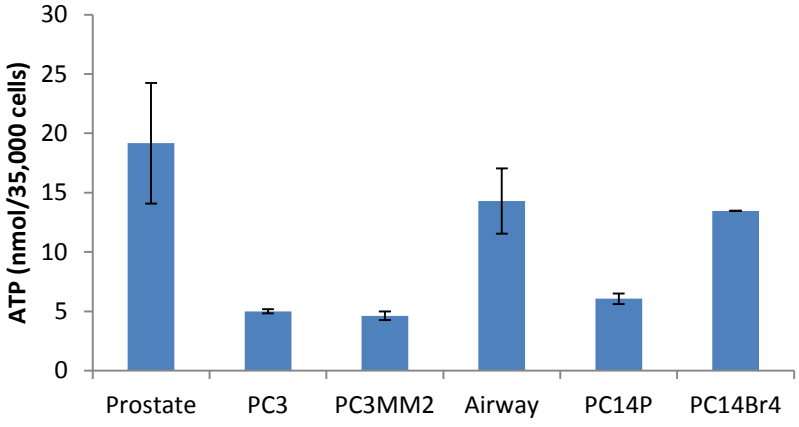
ATP (nmol/35,000 cells)
30
25
20
15
10
5
0
Prostate
PC3
PC3MM2
Airway
PC14P
PC14Br4

**Figure 4.1a Cancer cells contains less intracellular ATP than their non-cancerous counterpart.** Non-cancer cell lines: Renal (Renal epithelial cells), MCF 10A (mammary epithelial cells), Prostate (Prostate epithelial cells), Airway (small airway epithelial cells from human lung). Cancer cell lines: SN12 and SN12PE6 (Renal carcinoma), MDA-MB-231 and MDA-MB-231Br3 (human breast cancer), PC3 and PC3MM2 (human prostate cancer), PC14P and PC14Br4 (human lung adenocarcinoma)

As shown in figure 4.1b, after ATP liposome treatment, MDA-MB-231 cells consumed less glucose and produced less lactate, indicating a decreased glycolytic activity (Figure 4.1b A&B). Correspondingly, increasing intracellular ATP also results in decrease of hif-1α in MDA-MB-231 cells within 2 hours of treatment in MDA-MB-231 cells (Figure 4.1b C).

We also looked at the effect of increasing intracellular ATP on cancer cells' sensitivity to chemotherapeutic reagents. MDA-MB-231 cells were treated with Adriamycin in combination with either control liposomes or ATP liposomes; cell cycle analysis revealed that ATP-liposome prevented cells from Adriamycin-induced G2 phase arrest phenotype (Figure 4.1c). These data indicate that intracellular ATP level is also a key regulator of drug resistance of cancer cells. These data have been published as a Research Abstract (Chen, J et, al, 2011). All the preliminary data mentioned above indicate that intracellular ATP connects aerobic glycolysis, HIF-1α signaling, and drug-resistant phenotype of cancer cells, i.e. intracellular ATP sufficiency may play a fundamental role in cancerous glycolysis and drug resistance.

Acquired chemo-resistance is one of the major challenges in cancer treatment. Cancer cells develop drug resistance through mechanisms including increasing drug efflux, enhancing DNA damage repair and drug inactivation, enhancing anti-apoptotic gene expression (Wilson, Longley et al. 2006). Cancer cells resistant to one drug usually resistant to another drug, which refers to cross-resistance. Cross-resistant to different chemotherapeutic drug in cancer cells

implicated that there might be fundamental underlining principle of drug resistance.

Chemotherapeutic drugs target cell death to eliminate cancer and ATP depletion is associated with all types of programmed cell death including apoptosis, autophagy, and necrosis (Lemasters, Qian et al. 2002, Skulachev 2006, Vanlangenakker, Vanden Berghe et al. 2008). Altered glucose metabolism in caner which allows rapid ATP production in the cell have been shown to associate with tumor progression, metastasis, and relapse (Ferreira 2010, Kaelin and Thompson 2010, Hanahan and Weinberg 2011), yet its relationship with drug resistance development remains to be elucidated.

In this part of the study, using a colon cancer model, we carried out a set of experiments to investigate the role of intracellular ATP and the development of drug resistance in cancer cells. We found that intracellular ATP levels are a core determinant in the development of acquired cross-drug resistance of human colon cancer cells that harbor different genetic backgrounds. Drug-resistant cells were characterized by defective mitochondrial ATP production, elevated aerobic glycolysis, higher absolute levels of intracellular ATP, and enhanced HIF-1α–mediated signaling. Interestingly, direct delivery of ATP into crosschemoresistant cells destabilized HIF-1α and inhibited glycolysis. Thus, drug-resistant cells exhibit a greater "ATP debt" defined as the extra amount of ATP needed to maintain homeostasis of survival pathways under genotoxic stress. Direct delivery of ATP was sufficient to render drug-sensitive cells drug-resistant.

Conversely, depleting ATP by cell treatment with an inhibitor of glycolysis, 3-bromopyruvate, was sufficient to sensitize cells cross-resistant to multiple chemotherapeutic drugs. These data were published in 2012 in the Journal of Cancer Research (Zhou, Tozzi et al. 2012)

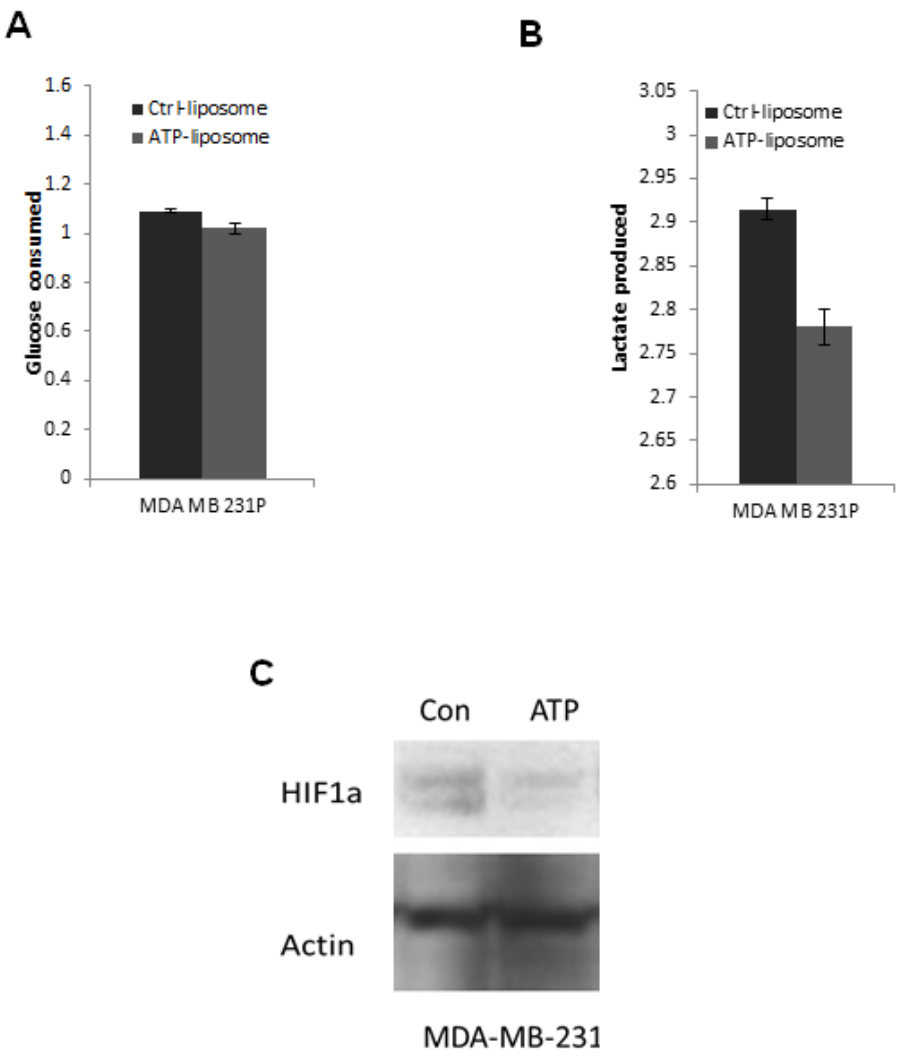


**Figure 4.1b Increase of intracellular ATP decreases glycolytic activity and down regulates hif1a in cancer cells.** (A) and (B) Lactate production and glucose consumption measured for MDA-MB-231 cells within 12 hours after delivery of liposomes. (C) Western blot analysis of hif1a after delivery of liposomes on MDA-MB-231 cells.

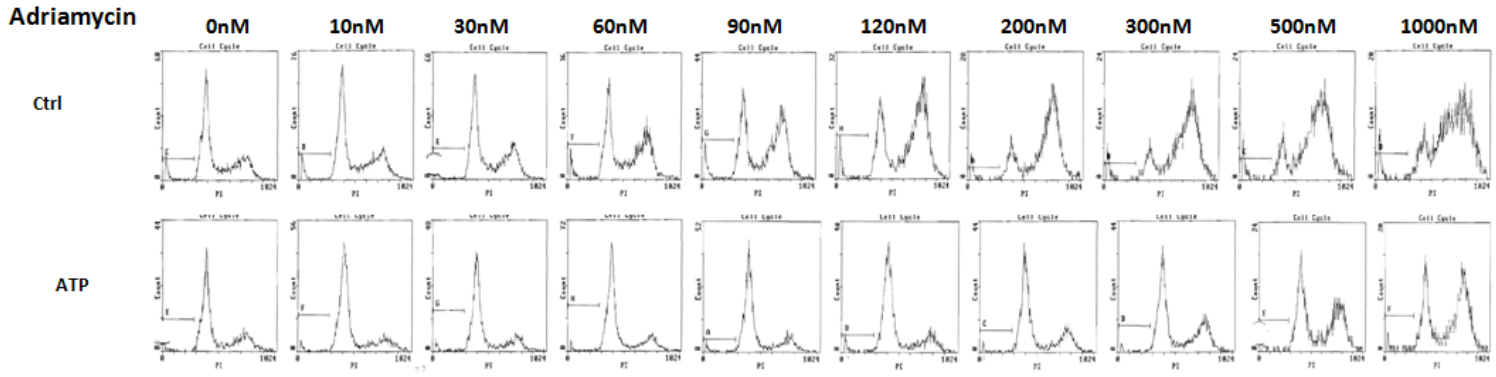




**Figure 4.1c Increase of intracellular ATP-altered drug response of MDA-MB-231 cells.** MDA-MB-231 cells were treated with elevated concentration of drugs with control/ATP liposomes. 24 hours after treatment, cells were fixed and stained with propidium iodide and analysis for cell cycle distribution.

## 4.2 Results

### 4.2.1 Characterization of chemoresistant phenotype of cross-resistant cell lines.

Cells stably resistant to oxaliplatin were developed by exposing parental HT29 and HCT116 cells to increasing doses of oxaliplatin over successive passages as described in the Experimental Procedures section (2.3). The surviving resistant cell lines were named HT29-OxR and HCT116-OxR. The proliferation rates of both HT29-OxR and HCT116-OxR cells were slower than those of their parental cells, HT29 and HCT116 (Figure. 4.2.1a A and Table 4), consistent with an up-regulation of cell cycle regulator p21 (Figure. 4.2.1a B). To confirm the chemoresistant phenotype after chronic oxaliplatin exposure, we compared the effect of oxaliplatin on HT29-OxR and HCT116-OxR cells to the effect on their parental cells by a 72-hr MTT assay (Figure. 4.2.1a C). As expected, HT29-OxR and HCT116-OxR cells were more resistant to the cytotoxic effects of oxaliplatin compared to parental, chemo-naïve cells.

**Table 4 Doubling time (Dt) of parental and resistant cells**

| Dt (hr) | HT29 | HCT116 |
|---|---|---|
| Parental | 18 | 15 |
| OxR cells | 31.7 | 22.5 |
| Fold change | 1.76 | 1.5 |

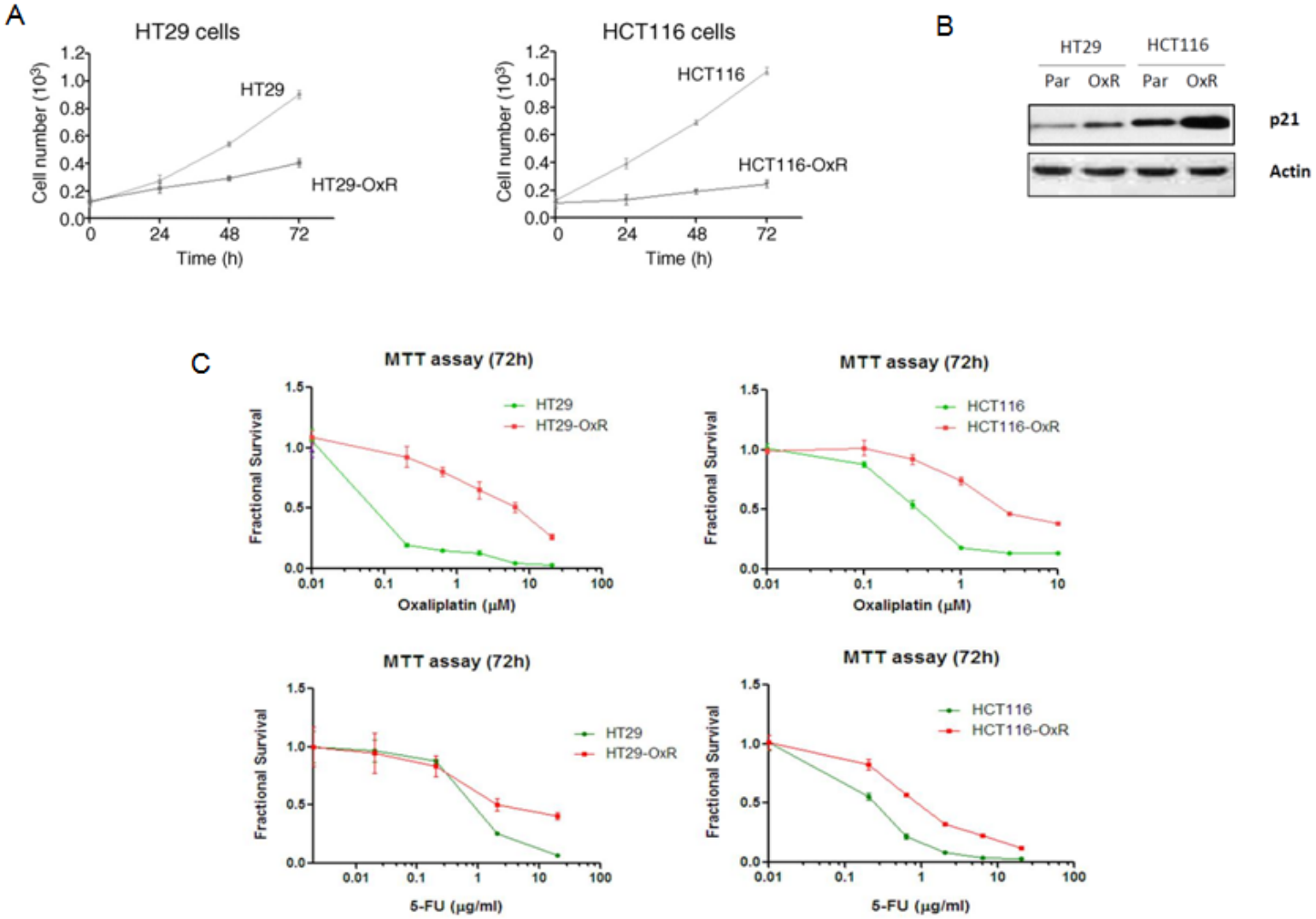
A
HT29 cells
Cell number (10³)
HT29
HT29-OxR
Time (h)
HCT116 cells
HCT116
HCT116-OxR
Time (h)
B
HT29
HCT116
Par
OxR
Par
OxR
p21
Actin
C
MTT assay (72h)
Fractional Survival
HT29
HT29-OxR
Oxaliplatin (μM)
MTT assay (72h)
HCT116
HCT116-OxR
Oxaliplatin (μM)
MTT assay (72h)
HT29
HT29-OxR
5-FU (μg/ml)
MTT assay (72h)
HCT116
HCT116-OxR
5-FU (μg/ml)

**Figure 4.2.1a Characterization of cross-chemoresistant cancer cell lines.** (A) Growth curve of parental and drug-resistant cell lines in 72 hours. Triplicate samples were measured at each time point. (B) Western blot analysis of P21 at whole cell level in parental and drug-resistant cell lines. Actin is used as loading control. (C) Survival inhibition curves from MTT assays showed a chemoresistant phenotype of HT29-OxR and HCT116-OxR cells to oxaliplatin (top) and 5-FU (bottom). All experiments were repeated at least three times. Representative data are shown.

To test the cross-chemoresistance of HT29-OxR and HCT116-OxR cells, we treated the resistant cells with 5-fluorouracil (5-FU), a drug with a different mechanism of action from that of oxaliplatin, and observed cross-resistance of both cell lines to 5-FU. The chemoresistant phenotype was also reflected by >130-fold and 30-fold increases in the $IC_{50}$ to oxaliplatin in the HT29-OxR and HCT116-OxR cells, respectively, and 3-fold and 5-fold increases in the $IC_{50}$ to 5-FU (Table 5). Furthermore, exposure of both parental and resistant cells to increasing concentrations of oxaliplatin (0.2, 2, and 20 μM) and 5-FU (0.2, 2, and 20 μg/ml) for 24 h induced a concentration-dependent apoptotic event in the parental cells, but not in the resistant cells, as reflected by measurement of annexin V-binding population by flow cytometry (Figure. 4.2.1b A&B) and detection of PARP, caspase 3 cleavage by Western blot (Figure. 4.2.1b C). Thus, the stably selected HT29-OxR and HCT116-OxR cells display a phenotype of cross-chemoresistance to both oxaliplatin and 5-FU.

**Table 5 $IC_{50}$ values for oxaliplatin and 5-FU in parental (Par) and oxaliplatin-resistant colon cancer cells**

| | HT29 | | | HCT116 | | |
|---|---|---|---|---|---|---|
| $IC_{50}$ | Par | OxR | O/P | Par | OxR | O/P |
| Oxal | 0.15 μmol/L | >20 μmol/L | >130 | 0.3 μmol/L | 9 μmol/L | 30 |
| 5-FU | 1 μg/mL | 3 μg/mL | 3 | 0.4 μg/mL | 2 μg/mL | 5 |

Abbreviation: O/P, ratio of OxR to parental cell values.

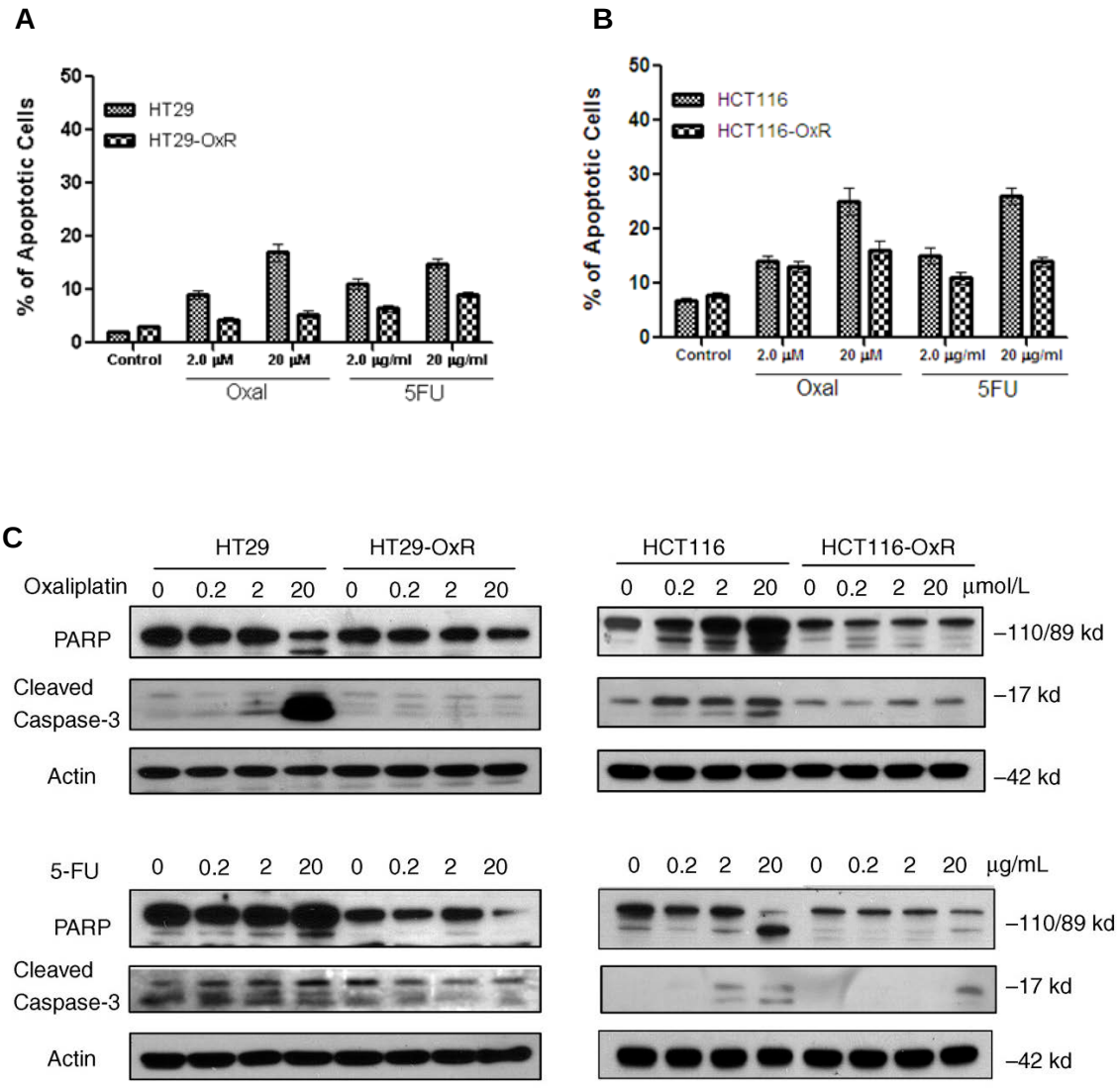
A
% of Apoptotic Cells
HT29
HT29-OxR
Control
2.0 μM
20 μM
2.0 μg/ml
20 μg/ml
Oxal
5FU
B
% of Apoptotic Cells
HCT116
HCT116-OxR
Control
2.0 μM
20 μM
2.0 μg/ml
20 μg/ml
Oxal
5FU
C
HT29
HT29-OxR
HCT116
HCT116-OxR
Oxaliplatin
0 0.2 2 20 0 0.2 2 20 μmol/L
PARP
Cleaved Caspase-3
Actin
–110/89 kd
–17 kd
–42 kd
5-FU
0 0.2 2 20 0 0.2 2 20 μg/mL

**Figure 4.2.1b Characterization of cross-chemoresistant cancer cell lines via apoptotic markers.** (A) and (B) Oxaliplatin and 5-FU treatment (48 h) induced concentration-dependent apoptosis in both parental cells but not in the OxR cells as shown by Annexin V-PI staining FACS analysis. Total percentage of early and late apoptotic cells were plotted in the bar graph. (C) HT29-OxR and HCT116-OxR showed decreased PARP cleavage (and thus decreased apoptosis) under 24 h treatment with oxaliplatin (top panels) and 5-FU (bottom panels). Actin served as a loading control. All experiments were repeated at least three times. Representative data are shown.

### 4.2.2 Metabolic alterations and mitochondrial defects of chemoresistant cells

We hypothesized that under chronic exposure to genotoxic stressors, such as oxaliplatin and 5-FU, the surviving resistant cells will need to alter their energy metabolism to adapt to the continuous stress. Thus, we examined the cellular ATP levels of HT29-OxR, HCT116-OxR, and their respective parental cell lines using an ATP-based luminescent assay. Both resistant cell lines showed a 2-fold increase in total cellular ATP levels compared to their parental cells (Fig. 4.2.2 A), indicating that a higher amount of ATP was produced in the resistant cells.

Cells produce ATP through two related mechanisms: glycolysis and mitochondrial oxidative phosphorylation. To determine which was involved in the chemoresistant cells, we measured the oxygen consumption rate using a Seahorse Bioenergizer (Seahorse Bioscience), which is often an indicator of mitochondrial oxidative phosphorylation activity (Qian and Van Houten 2010). Interestingly, the HT29-OxR and HCT116-OxR cells exhibited a significantly elevated cellular oxygen consumption rate, suggesting the OxR cells may produce more ATP through up-regulation of their mitochondrial oxidative phosphorylation (Figure. 4.2.2 B).

To further determine changes in mitochondria, we examined the ultra-structure of mitochondria by transmission electronic microscopy (TEM). As shown in Figure. 4.2.2 C, the TEM images showed two different patterns of alterations in the mitochondria of HT29-OxR and HCT116-OxR cells. The

morphology of mitochondria of HT29-OxR is similar to the mitochondria of its parental cells; however, the mitochondria of HCT116-OxR cells are more elongated than that of its parental cells. A more condensed mitochondrial form was observed as a common feature in both resistant cell lines.

The data demonstrating enhanced oxygen consumption and the increased density of mitochondria in the resistant cells suggest that the mitochondria of these cells are more active, possibly for the purpose of generating more ATP. To test this, we measured the ATP-producing capacity of mitochondria isolated from the parental and resistant cells using complex-I substrates glutamate and malate and complex-II substrate succinate. Surprisingly, the mitochondria of resistant cells actually were significantly less capable of producing ATP than were their parental cells (Figure. 4.2.2 D). In addition, the reserve mitochondrial oxidative phosphorylation capacity was significantly lower in the OxR cells after treatment with the uncoupler carbonilcyanide p-triflouromethoxyphenylhydrazone (FCCP), as measured by the Seahorse Bioenergizer, suggesting defective mitochondrial function (Figure. 4.2.2 E). Taken together, these data suggest that the resistant cells utilized an alternative energy-producing mechanism to maintain a higher ATP levels.

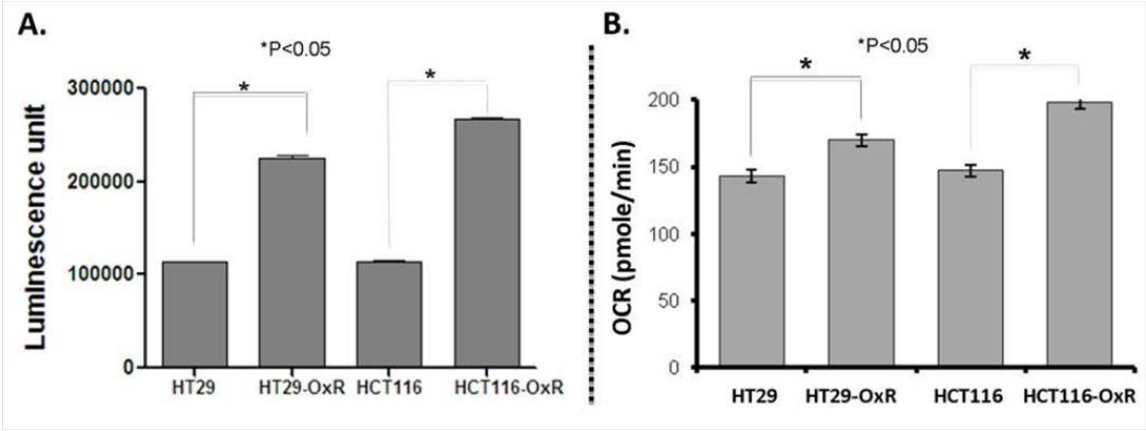
A.
*P<0.05
Luminescence unit
300000
200000
100000
0
HT29
HT29-OxR
HCT116
HCT116-OxR
B.
*P<0.05
OCR (pmole/min)
200
150
100
50
0
HT29
HT29-OxR
HCT116
HCT116-OxR

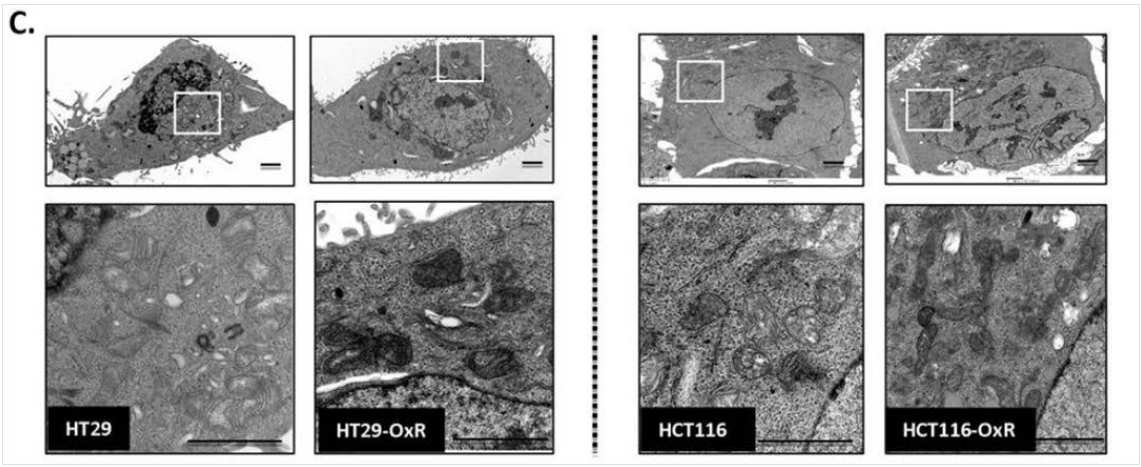
C.
HT29
HT29-OxR
HCT116
HCT116-OxR

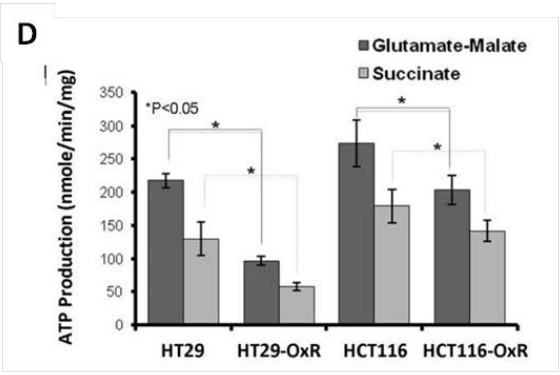
D
Glutamate-Malate
Succinate
*P<0.05
ATP Production (nmole/min/mg)
350
300
250
200
150
100
50
0
HT29
HT29-OxR
HCT116
HCT116-OxR

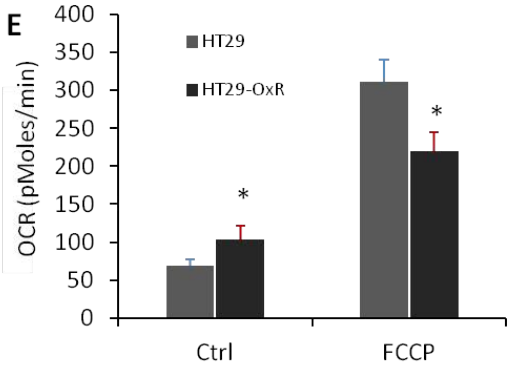
E
HT29
HT29-OxR
OCR (pMoles/min)
400
350
300
250
200
150
100
50
0
Ctrl
FCCP

**Figure 4.2.2 Measurement of intracellular ATP and mitochondrial activity**

**(A)** HT29-OxR and HCT116-OxR cells displayed more than a 2-fold increase in intracellular ATP levels compared with their parental cells. **(B)** HT29-OxR and HCT116-OxR cells consumed oxygen at a significantly higher rate than their parental cells as indicated by oxygen consumption rate (OCR, pmole/min). **(C)** HT29-OxR and HCT116-OxR cells displayed morphologic changes as examined by TEM. Bar: 2 μm. At least 20 individual cells were analyzed for each cell type. Representative images are shown. **(D)** Purified mitochondria from HT29-OxR and HCT116-OxR showed decreased substrate ATP production ability from both complex I (glutamate/malate as substrates) and complex II (succinate as a substrate) compared with that of their parental cells. (E) HT29-OxR cells exhibit less mitochondrial oxygen consumption reserve than HT29 cells when treated with the mitochondrial uncoupler FCCP. All experiments were repeated at least three times. Representative data are shown.

### 4.2.3 Elevated glycolysis of chemoresistant cells

To test whether the cross-chemoresistant cells also have altered aerobic glycolysis, we measured several key glycolytic parameters, including glucose consumption, lactate production, and expression levels of glycolytic enzymes in the resistant cells. As shown in Figure. 4.2.3a A, both HT29-OxR and HCT116-OxR cells consumed more glucose than their parental cells. Accordingly, the resistant cells released more lactate into the media (Figure. 4.2.3a B). In addition, the protein expression of glucose transporter (Glut-1) and hexokinase (HK2) were all significantly up-regulated in HT29-OxR and HCT116-OxR cells (Figure. 4.2.3b C).

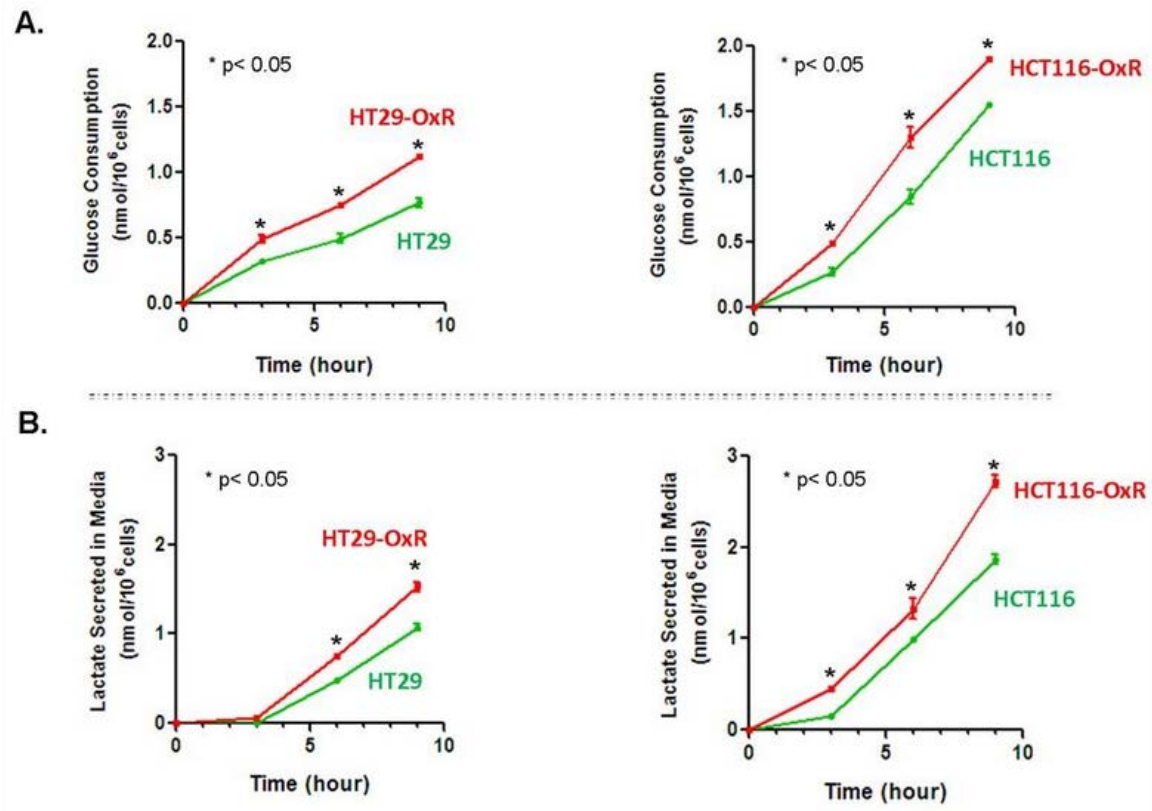


**Figure 4.2.3a Drug-resistant cells exhibited higher glycolytic activity.** **(A)** HT29-OxR and HCT116-OxR cells consumed glucose at a higher rate than their parental cells. **(B)** HT29-OxR and HCT116-OxR cells produced lactate at a higher rate than their parental cells.

A master regulator of glycolysis is HIF-1α (Semenza 2007), which is regulated by oxygen-dependent and -independent mechanisms (Yee Koh, Spivak-Kroizman et al. 2008). We next examined HIF-1α expression and found that HIF-1α was up-regulated in both HT29-OxR and HCT116-OxR cells under normoxic conditions. To further prove a functional role of HIF-1α in the resistant cells, we examined the expression of vascular endothelial growth factor A (VEGF-A), a known downstream gene of HIF-1α. We found several isoforms of VEGFA were increased in the HT29-OxR and HCT116-OxR conditioned media including the $VEGFA_{165}$ (Figure. 4.2.3b B&C). Consistently, the mRNA levels of VEGFA were significantly up-regulated in both resistant cell lines (Figure. 4.2.3b B), suggesting a functional HIF-1α pathway was elevated in the OxR cells.

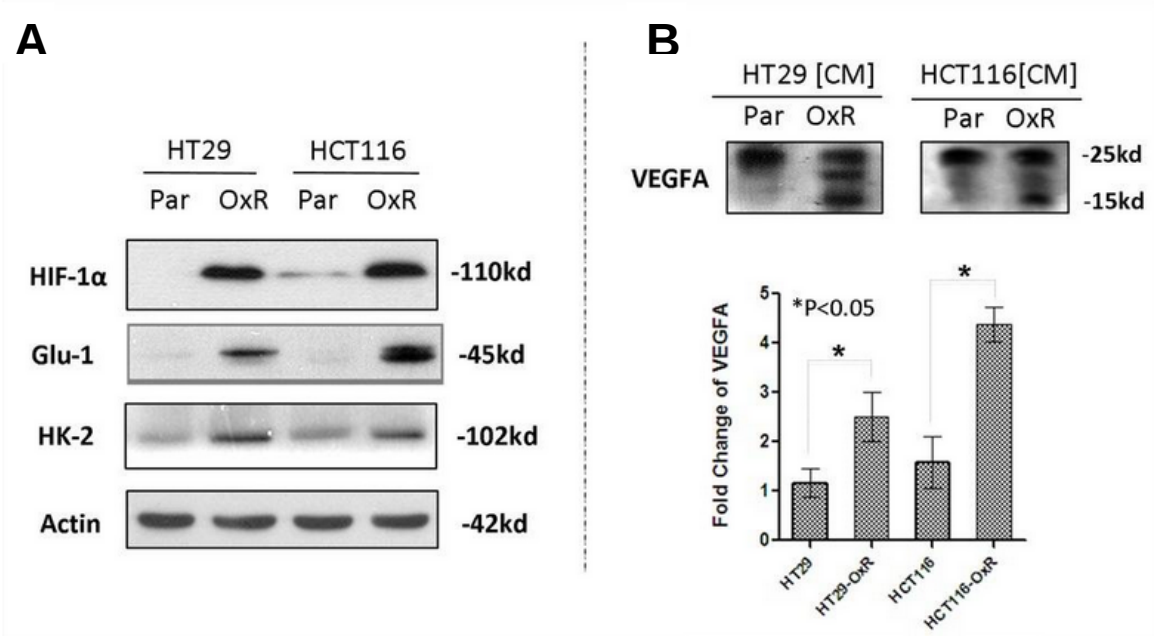
A
HT29
HCT116
Par
OxR
Par
OxR
HIF-1α
-110kd
Glu-1
-45kd
HK-2
-102kd
Actin
-42kd
B
HT29 [CM]
HCT116[CM]
Par
OxR
Par
OxR
VEGFA
-25kd
-15kd
*P<0.05
Fold Change of VEGFA
HT29
HT29-OxR
HCT116
HCT116-OxR

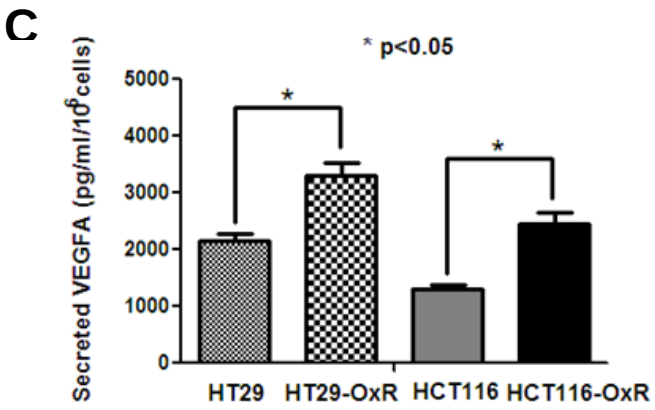
C
* p<0.05
Secreted VEGFA (pg/ml/10^6 cells)
HT29
HT29-OxR
HCT116
HCT116-OxR

**Figure 4.2.3b Drug-resistant cells exhibited enhanced HIF-1α activity.** **(A)** Key glycolytic enzymes GLUT1, HK2, LDHA, and HIF-1α were up-regulated in HT29-OxR and HCT116-OxR cells compared with their parental (Par) cells, as shown by Western blot. **(B)** HT29-OxR and HCT116-OxR produced more VEGFA into cell culture medium than their parental cells (top panel), which correlated with VEGFA mRNA level by qPCR (bottom panel). **(C)** VEGF-A level is elevated in the OxR cells conditioned media as shown by ELISA assay. All experiments were repeated at least three times. Representative data are shown.

### 4.2.4 Intracellular ATP regulates HIF-1α and induces drug-resistant phenotype

The higher intracellular ATP level and defective mitochondrial ATP production in the chemoresistant cells as compared to the parental cells indicated that the resistant cells might need more ATP to survive under genotoxic stress. It is likely that the drug-resistant cells may turn to glycolysis for more rapid ATP generation. It is known that the ADP/AMP ratio determines the glycolytic rate through stereotypic regulation of the key glycolytic enzyme phosphofructose kinase (PFK) and drives glycolysis (Gevers and Krebs 1966). Therefore we measured the levels of intracellular ADP and AMP using high-performance liquid chromatography coupled mass spectrum (HPLC-MS). As shown in Fig. 4.2.4a A, the ratio of ADP/AMP was much lower in HT29-OxR and HCT116-OxR cells than in their parental controls. We further measured the enzyme activity of PFK by a well-established in vitro biochemical assay (Kamemoto and Mansour 1986) over a time course of 5-20 minutes using extracted cell lysates. In consistent with the decreased ADP/AMP ratio, the PFK enzyme activity was elevated in HT29-OxR cells and to a much higher level in HCT116-OxR cells as compared with their parental cells (Figure.4.2. 4a B).

The activity of aerobic glycolysis, level of metabolic regulator HIF-1α, and cellular ATP level were higher in the resistant cells, which suggest that ATP has a protective role for cancer cells under genotoxic stress. To test this possibility, we artificially delivered ATP packaged in liposomal vehicles to the parental HT29

and HCT116 cells by transient transfection and examined the drug treatment effect on these cells. As shown in Figure. 4.2.4a C, exogenous ATP supplementation partially blocked the cytotoxic effect of oxaliplatin in both cell lines, indicating the role of intracellular ATP level in mediating the drug-resistant phenotype.

We further hypothesized that the resistant cells are in need of more ATP; thus, a faster ATP production mechanism, namely aerobic glycolysis, is elevated, which in turn demands a higher level of HIF-1α to enhance/sustain aerobic glycolysis (Figure. 4.2.3b A). To test whether exogenous ATP delivery could affect HIF-1α level and glycolysis, we treated the resistant cells with ATP liposomes and examined the expression levels of HIF-1α and glycolytic enzymes. Consistent with our hypothesis, ATP treatment decreased HIF-1α rapidly in both HT29-OxR and HCT116-OxR cells, and reversed the glycolytic phenotype, as evidenced by a concordant decrease in hexokinase II expression in both resistant cell lines (Figure**.** 4.2.4a D). Interestingly, the level of Glut-1 was not significantly altered at 2h ATP treatment, which is probably due to the protein turnover kinetics of Glut-1 is different from that of hexokinase II.

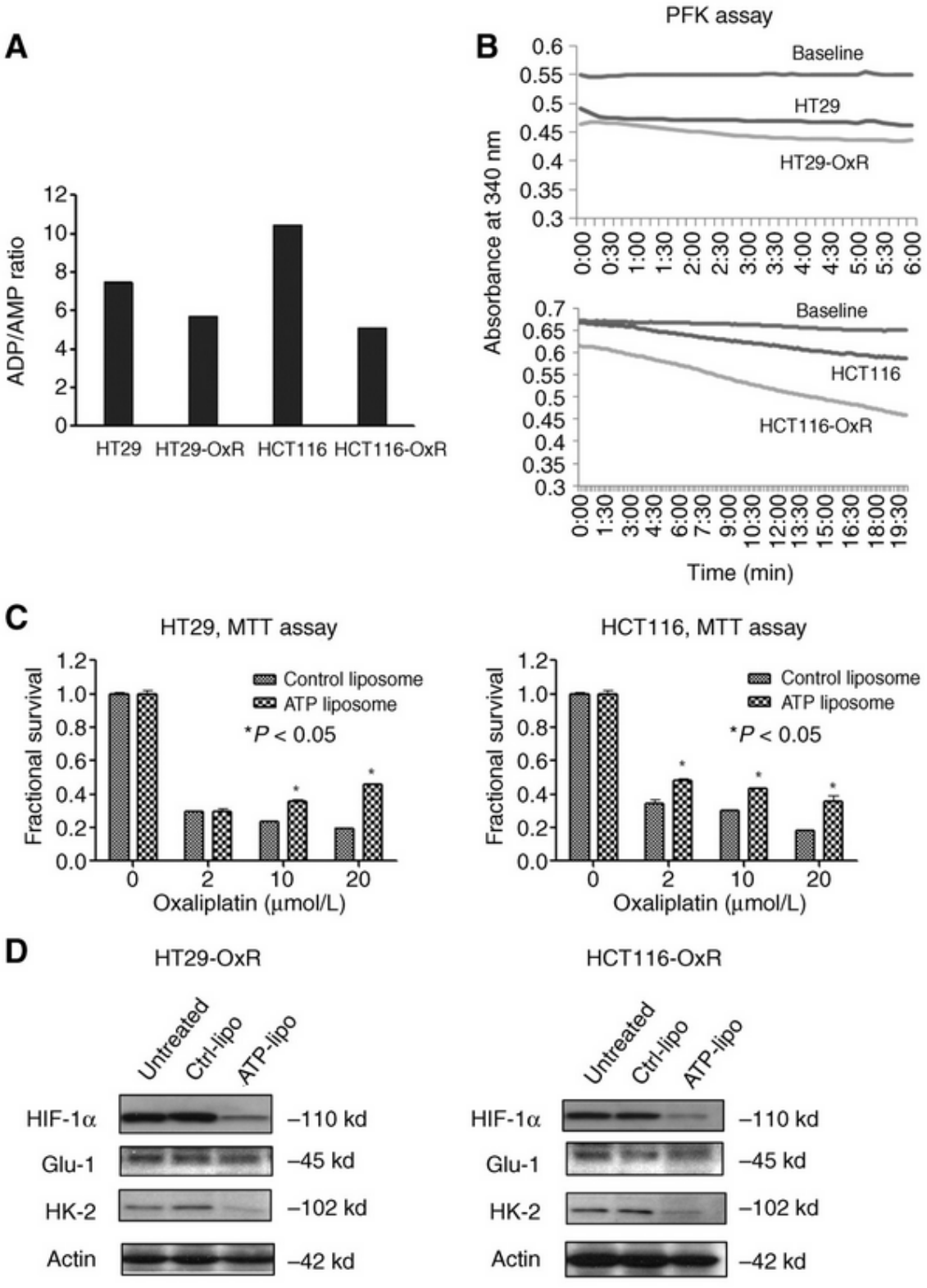
A
ADP/AMP ratio
12
10
8
6
4
2
0
HT29
HT29-OxR
HCT116
HCT116-OxR
B
PFK assay
Absorbance at 340 nm
Baseline
HT29
HT29-OxR
0.6
0.55
0.5
0.45
0.4
0.35
0.3
0:00
0:30
1:00
1:30
2:00
2:30
3:00
3:30
4:00
4:30
5:00
5:30
6:00
Baseline
HCT116
HCT116-OxR
0.7
0.65
0.6
0.55
0.5
0.45
0.4
0.35
0.3
0:00
1:30
3:00
4:30
6:00
7:30
9:00
10:30
12:00
13:30
15:00
16:30
18:00
19:30
Time (min)
C
HT29, MTT assay
Fractional survival
Control liposome
ATP liposome
*P < 0.05
1.2
1.0
0.8
0.6
0.4
0.2
0.0
0
2
10
20
Oxaliplatin (μmol/L)
HCT116, MTT assay
Fractional survival
Control liposome
ATP liposome
*P < 0.05
1.2
1.0
0.8
0.6
0.4
0.2
0.0
0
2
10
20
Oxaliplatin (μmol/L)
D
HT29-OxR
Untreated
Ctrl-lipo
ATP-lipo
HIF-1α
Glu-1
HK-2
Actin
–110 kd
–45 kd
–102 kd
–42 kd
HCT116-OxR
Untreated
Ctrl-lipo
ATP-lipo
HIF-1α
Glu-1
HK-2
Actin
–110 kd
–45 kd
–102 kd
–42 kd

**Figure 4.2.4a ATP regulates HIF-1α expression and induces a drug-resistant phenotype (**A) Ratio between absolute cellular ADP and AMP amount decreased in HT29-OxR and HCT116-OxR cells, as shown by HPLC-MS measurement. (B) PFK enzyme activity is elevated in HT29-OxR and HCT116-OxR cells compared with parental cells. The enzyme activity is reflected by the decrease of absorbance at 340nm (the Y-axis, unit) over the indicated time course (the X-axis, minute). (Baseline, blank control). (C) ATP liposomal delivery to parental HT29 and HCT116 cells induced resistance to oxaliplatin under 72h treatment, as shown by MTT assay. (D) ATP liposomal delivery to HT29-OxR and HCT116-OxR cells decreased HIF-1α expression and reverted glycolytic enzyme HK2 expression. All experiments were repeated at least three times. Representative data is shown.

If the intracellular ATP level plays a central role in sustaining the survival of cross-chemoresistant cells, depletion of ATP should sensitize these cells to chemotherapeutic agents. As shown in Fig. 4.2.4b A, 3-bromopyruvate (3-BrPA), a widely used ATP-depleting agent (Ganapathy-Kanniappan, Vali et al. 2010), depleted cellular ATP in HT29-OxR and HCT116-OxR cells in a dose-dependent manner. We pre-treated the resistant cells with a moderate does of 3-BrPA (30 μM) for 24h, then tested their sensitivity to oxaliplatin and 5-FU. As shown in Fig. 4.2.4b B-C, ATP depletion partially reversed the drug-resistant phenotype and re-sensitized both resistant cell lines to oxaliplatin and 5-FU treatment. The $IC_{50}$ values of oxaliplatin and 5-FU in the OxR cells before and after ATP

depletion by 3-BrPA treatment were calculated. There was a 2-3 fold decrease in the $IC_{50}$ in both OxR cell lines after ATP depletion (Table 7). Taken together, our data suggest that intracellular ATP plays a central role in regulation of drug-resistant phenotype of colon cancer cells.

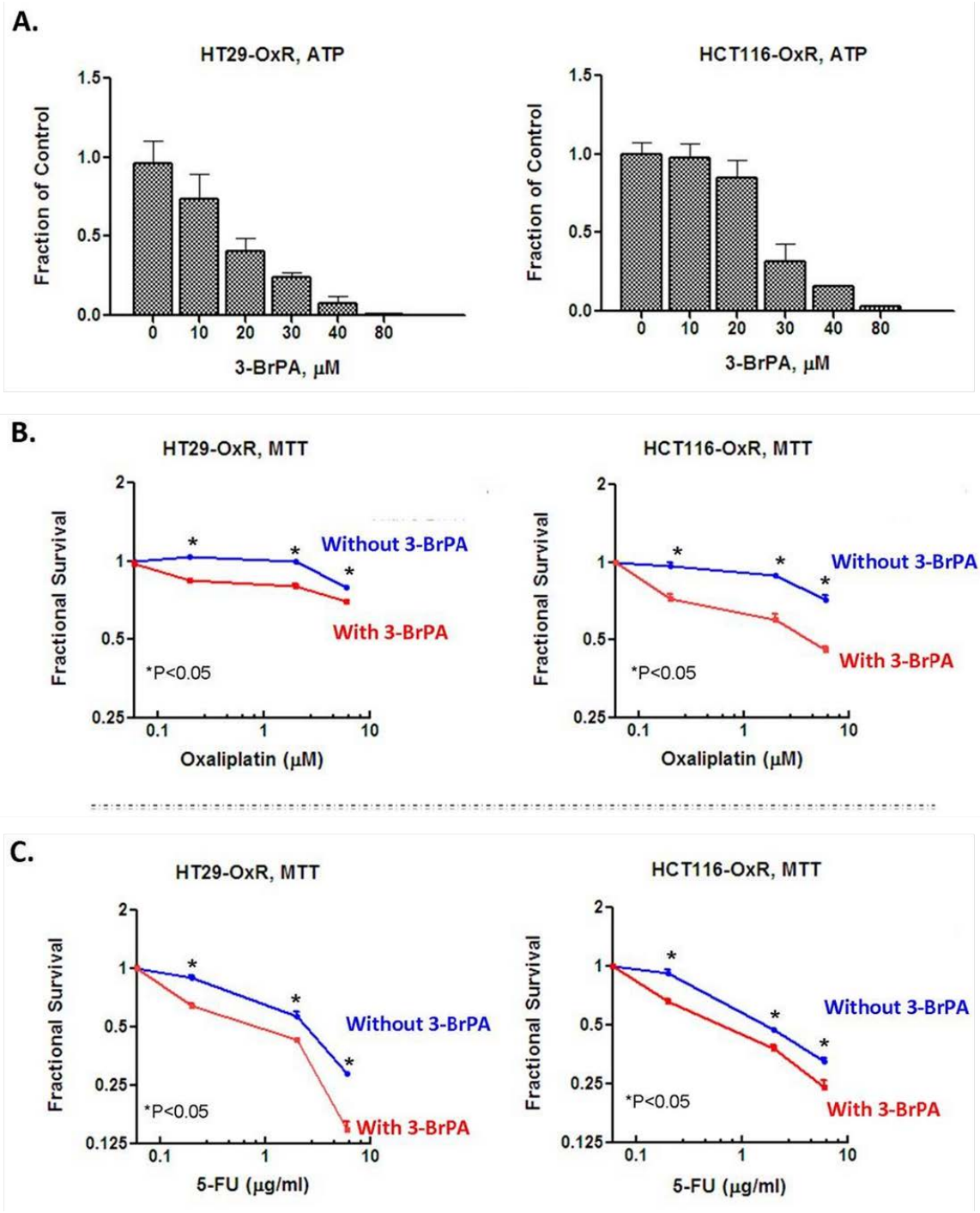
A.
HT29-OxR, ATP
Fraction of Control
1.5
1.0
0.5
0.0
0
10
20
30
40
80
3-BrPA, μM
HCT116-OxR, ATP
Fraction of Control
1.5
1.0
0.5
0.0
0
10
20
30
40
80
3-BrPA, μM
B.
HT29-OxR, MTT
Fractional Survival
2
1
0.5
0.25
*P<0.05
Without 3-BrPA
With 3-BrPA
0.1
1
10
Oxaliplatin (μM)
HCT116-OxR, MTT
Fractional Survival
2
1
0.5
0.25
*P<0.05
Without 3-BrPA
With 3-BrPA
0.1
1
10
Oxaliplatin (μM)
C.
HT29-OxR, MTT
Fractional Survival
2
1
0.5
0.25
0.125
*P<0.05
Without 3-BrPA
With 3-BrPA
0.1
1
10
5-FU (μg/ml)
HCT116-OxR, MTT
Fractional Survival
2
1
0.5
0.25
0.125
*P<0.05
Without 3-BrPA
With 3-BrPA
0.1
1
10
5-FU (μg/ml)

**Figure 4.2.4b ATP depletion sensitizes drug-resistant cells to chemoreagent.** **(A)** 3-Bromopyruvate (3-BrPA) depleted cellular ATP level in HT29-OxR and HCT116-OxR cells after 24h of treatment, as measured by ATP luminescent activity. **(B)** Pre-treatment of 3-BrPA (30μM) for 24h sensitized HT29-OxR and HCT116-OxR cells to oxaliplatin, as shown in 72h MTT assays. **(C)** Pre-treatment of 3-BrPA (30μM) for 24h sensitized HT29-OxR and HCT116-OxR cells to 5-FU, as shown in 72h MTT assays. All experiments were repeated at least three times. Representative data are shown.

**Table 7 $IC_{50}$ value of drug-resistant cells after treatment of 3-bromopyruvate**

| $IC_{50}$ | HT29-OxR | | | HCT116-OxR | | |
|---|---|---|---|---|---|---|
| | Before | After | B/A | Before | After | B/A |
| Oxal: | >20 µM | 10 µM | > 2 | 9 µM | 3 µM | 3 |
| 5-FU: | 3 µg/ml | 1 µg/ml | 3 | 2 µg/ml | 0.6 µg/ml | 3 |

B, before 3-BP treatment. A, after 3-BP treatment
B/A, ratio of IC50 values before and after 3BP treatment.

## 4.3 Discussion

ATP, the energy currency of the cell, is produced from carbon fuels at two levels of metabolism, glycolysis in the cytosol and oxidative phosphorylation in the mitochondria. Glycolysis, besides producing pyruvate for oxidative phosphorylation under non-stressful conditions, generates two moles of ATP from one mole of glucose. In normal cells undergoing stress, for example, due to a sudden drop of intracellular ATP and hypoxia, cells will accelerate glycolysis to produce ATP in order to meet the immediate energy need; accelerated glycolysis leads to increased production of lactate from pyruvate (De Feo, Di Loreto et al. 2003, Wells, Selvadurai et al. 2009). Although the efficiency of ATP production via glycolysis is lower than that of oxidative phosphorylation, the ATP generation rate of glycolysis is nearly 100 times faster than that of oxidative phosphorylation. In tumors, elevated aerobic glycolysis differentiates malignant tumors from benign tumors and non-tumor cells, a phenomenon that was identified by Otto

Warburg (Warburg, 1923) and has been repeatedly confirmed. One possible driver of the aerobic glycolysis of malignant tumor cells could be a higher ATP demand for the purposes of survival and growth as compared to demand in non-malignant or normal cells (DeBerardinis, Lum et al. 2008). Our data support the hypothesis that metabolic shift driven by higher ATP demand is also applicable to the progression of acquired chemoresistance of cancer cells.

To cope with constant chemotherapeutic stress, chemoresistant cancer cells are known to do at least one of the following: increase drug efflux, enhance drug inactivation, enhance DNA damage repair, mutate survival-related genes, deregulate growth factor signaling pathways, increase expression of anti-apoptotic genes, and/or activate intracellular survival signaling (Longley and Johnston 2005, Wilson, Longley et al. 2006). All of these activities consume ATP. Our data showing elevated aerobic glycolysis in the chemoresistant cells and sensitization of the chemoresistant cells by inhibition of glycolysis further argue that enhanced aerobic glycolysis of cancer cells occurs to provide the extra amount of ATP needed for chemoresistant cells to survive under stress. It is worth noting that the chemoresistant cells consume more oxygen while their mitochondrial ATP production is defective (Fig. 4.2.2a D-E). Oxygen consumption has often been used as an indicator of mitochondrial ATP productivity. Our data support the argument that oxygen consumption is not a reliable index for mitochondrial ATP productivity (Seyfried and Shelton 2010).

The role of enhanced oxygen consumption by chemoresistant cells warrants further investigation.

Extracellular ATP can be taken up by cells via adenosine transporters (Thorn and Jarvis 1996); however, because of signaling effects triggered by adenosine receptors (Trincavelli, Daniele et al. 2010), treating cells with naked ATP results in a complex of signaling responses besides an increase in the intracellular ATP level. Liposome-encapsulated ATP has been used to deliver ATP into cells in vivo (Liang, Levchenko et al. 2004, Liang, Levchenko et al. 2004, Hartner, Verma et al. 2009, Dvoriantchikova, Barakat et al. 2010), which allows us to avoid interfering with the signaling mediated by adenosine receptors. The comprehensive effects of delivering ATP directly into cells, reverting the aerobic glycolytic activity and HIF-1α level of cross-chemoresistant cells, and converting chemosensitive cells to resistant cells, further indicate that the chemoresistant cells are in need of more ATP.

In tumor tissues, up-regulation of HIF-1α cannot be fully attributed to hypoxia. Increased expression of HIF-1α is often found in cancer cells of tissues in which oxygen supply is sufficient (Zhong, Semenza et al. 2004, Tanaka, Yamamoto et al. 2006, Greijer, Delis-van Diemen et al. 2008), and HIF-1α is up-regulated only in the malignant tumor cells and not the benign tumor cells with the same tissue origin (Elbers, Rijksen et al. 1990, Bos, Zhong et al. 2001, Okada, Osaki et al. 2005, Mayer, Hockel et al. 2008). For example, glucose deprivation induces HIF-1α expression in the presence of an ample amount of

oxygen (Vordermark, Kraft et al. 2005, Fang, Shen et al. 2010). Our finding of the oxygen-independent degradation of HIF-1α induced by the increase of intracellular ATP is novel. While the molecular mechanism is currently under investigation, it bears important implications for cancer biology. The data suggest the possibility that insufficiency of intracellular ATP might be a driving force of oxygen-independent HIF-1α signaling in cancer cells, which in turn elevates aerobic glycolysis to produce ATP more efficiently to meet the increased demand of cancer cells. This possibility is supported by a recent finding that malignant tumor cells consume a higher amount of ATP via the endoplasmic reticulum enzyme UDPase ENTPD5, that, in turn enhances aerobic glycolysis (Fang, Shen et al. 2010).

Based on the contradiction between a higher amount of ATP, HIF-1α, and glycolysis in chemoresistant cells and downregulation of HIF-1α and glycolysis by exogenous ATP delivery, and the chemoresistant effect of ATP on chemosensitive cells, we propose the concept of “ATP debt”. ATP debt is the extra amount of ATP needed to maintain survival homeostatic pathways in cancer cells, which is equal to ATP needed for survival minus ATP produced. The decreased ADP/AMP ratio and increased PFK activity in the drug-resistant cells as compared with the parental cells indicates a higher ATP consumption rate in the drug-resistant cells. Thus the drug-resistant cells demand a faster ATP generating mechanism to maintain survival, which is met by aerobic glycolysis/fermentation. Under these conditions, HIF-1α, as a key glycolysis

regulator, is up-regulated independent of oxygen levels. The steady-state higher level of HIF-1α in the drug-resistant cells and its down-regulation by increased ATP levels suggests that more ATP is needed to cope with chemotherapeutic stress, i.e. the drug-resistant cells have higher “ATP debt”. The level of HIF-1α under normoxic conditions might be an indicator of ATP debt. Understanding the molecular mechanisms that cancer cells utilize to reduce their ATP debt may provide the foundation for the development of novel therapeutic strategies.

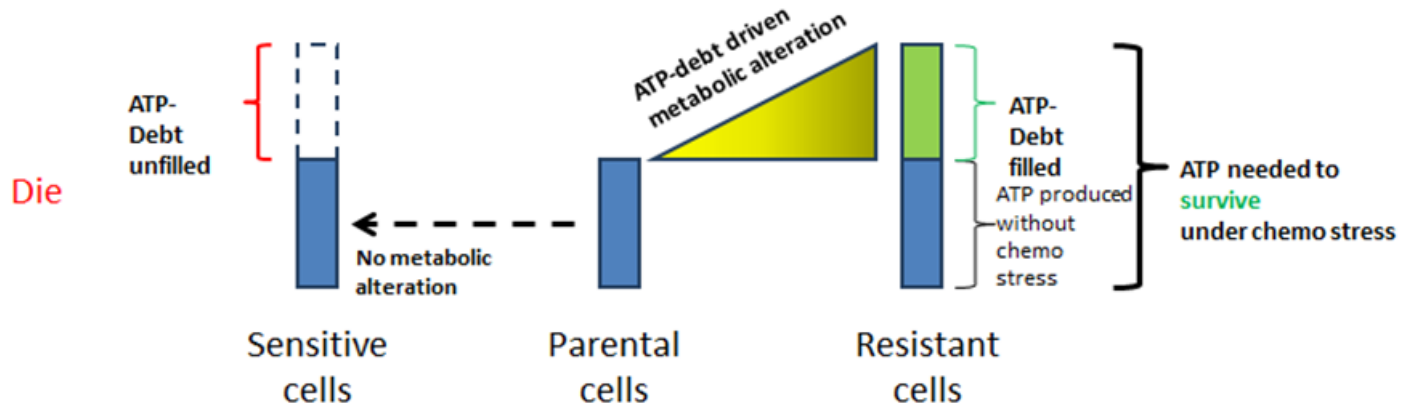




**Figure 4.3 Illustration of "ATP debt" and "ATP debt" driven metabolic shift model.** Parental cells have certain level of intracellular ATP to maintain homeostasis, yet drug-resistant cells contain higher level of intracellular ATP to maintain homeostasis under drug treatment. The gap of intracellular ATP mount in green bar is the "ATP debt" which needed for the drug-resistant cells to survive under chemo stress, and this "ATP debt" drives metabolic alteration like elevated aerobic glycolysis during development of drug resistance. Cells without metabolic alteration are unable to fulfill the "ATP debt" and thus die under chemo stress.

# CHAPTER 5 GENERAL DISCUSSION AND PERSPECTIVES

The central theme of my study is to investigate the roles of altered glucose metabolism of cancer cells in the development of metastasis and drug resistance. This central theme was developed from a set of preliminary studies designed to explore alternative explanations to the oxygen level independent glycolysis phenotype of cancer cells. One of the critical turning points during pilot phase of this study was when we revisited the literature regarding the changes of intracellular ATP level and oxygen level in skeletal muscle cells during exercise, and we realized that, in fact, a drop in intracellular ATP level precedes the drop of oxygen level in muscle tissues at the time exercise starts (Gleim, 1993; Burton, 2004). This observation leads us to speculate that intracellular ATP insufficiency may contribute to switching on up-regulation of HIF-1α and glycolysis. With this thought in mind, we continued to revisit literature pertaining to the expression of HIF-1α and oxygen or hypoxic status of cancer tissues and cancer cells. Although, not at the main stream of literature, there are many publications that have indicated that up-regulation of HIF-1α in cancer tissues and cultured cancer cells cannot be explained by hypoxia. Up-regulation of HIF-1α has been commonly observed in tumors at early stages (Okada, Osaki et al. 2005, Kimbro and Simons 2006, Simiantonaki, Taxeidis et al. 2008, Wu, Qian et al. 2011), where oxygen supply is as sufficient as the normal regions of the same tissue. HIF-1α is up-regulated in hepatic cancers induced by chemical carcinogens,

however, the oxygen level of tumor regions is the same as that of the normal tissue regions (Tanaka, Yamamoto et al. 2006). HIF-1α signaling is only up-regulated in uterine leiomyosarcoma (malignant) cells (Elbers, van Unnik et al. 1990) but not in the cells of leiomyoma (benign) of uterus (Mayer, Hockel et al. 2008), although these two types of tumors originate from the same type of cells, the smooth muscle cells. Most cancer cells cultured in vitro under normoxic conditions still express measurable level of HIF-1α, although hypoxia is often effective to further elevate it. Defective Von Hippel-Lindau (VHL) protein mediated HIF-1α degradation pathways is common in renal cancers but not in other types of cancers (Kim and Kaelin 2004). Enhanced growth factor signalings are involved in the non-hypoxia-induced HIF-1α functions in cancer cells. In general, growth factor signaling and HIF-1α signaling are mutually enhancive; however, a causative role of enhanced growth factor signaling in initiating HIF-1α up-regulation has not been established (Bardos and Ashcroft 2004, Dimova, Michiels et al. 2009). The earlier findings encouraged us to test the hypothesis that **insufficient intracellular ATP level is a driving force to upregulate HIF-1α and glycolysis in cancer cells.** Our data not only support this hypothesis but also lead us to propose a new concept, the ATP-debt. For intact cancer cells, ATP-debt refers to the extra amount of ATP needed to reverse cancerous glycolysis back to non-glycolytic status; for drug-resistant cancer cells, ATP-Debt refers to the extra amount of ATP needed to maintain survival homeostatic pathways under genotoxic stress.

The major approach of proving that there is an ATP-Debt in cancer cells was to deliver ATP into cells via ATP-liposomes, which allowed us to observe reversions of glycolysis and HIF-1α expression in both intact cancer cells and drug-resistant cancer cells. However, it is acknowledged that, at this stage, we do not know the exact level of the "ATP-Debt" is, which cannot be precisely answered by the liposome carried ATP delivery, because treating cultured cells with ATP-liposomes cannot deliver ATP into all cells evenly and the outcomes in changes of glycolysis and HIF-1α expression are from millions of cultured cells. To precisely measure the ATP-Debt in cancer cells, a single cell based system to measure of ATP and HIF-1α levels is needed.

The other question regarding the effect of ATP increase on cancer cells is: what is the mechanism by which increase of intracellular ATP level down-regulates HIF-1α? In fact, we have conducted a set of pilot studies to address this question. At this stage, we found that, the down-regulation of HIF-1α occurred at posttranslational level; the oxygen dependent degradation (ODD) domain of HIF-1α and the proteasome degradation pathway were not involved in ATP induced HIF-1α down-regulation; increasing level of intracellular ADP opposed ATP induced HIF-1α down-regulation; the N-terminus (1-410 AA) of HIF-1α, but not the C-terminus (402-826 AA), responded to ATP induced down-regulation. We are actively performing experiments aiming to identify the proteolytic pathway that mediates the ATP-induced down-regulation of HIF-1α.

The other critical turning point during pilot phase of this study was when we observed that the brain metastatic breast cancer cells were less glycolytic than their parental cells, which forced us to consider the impact of tissue microenvironment on cancer cell metabolism. Again, we were able to approach the survival mechanism of these brain metastatic cells by referring the normal physiology of glucose metabolism, i.e. what will the body do when glucose is deprived? To produce glucose from other sources of carbohydrates, gluconeogenesis, is one of the answers. Indeed, the brain metastatic cells have gained the ability of gluconeogenesis. Of course, this finding so far has brought up more questions that it has answered, such as is the metabolic shift in brain metastatic cells an outcome of selection or adaptation? Are there genetic or epigenetic changes that support the growth and survival of these brain metastatic cells? At which step during the process of metastasizing to the brain is the gluconeogenic feature is required? Is the gluconeogenic feature also applicable to brain metastasis of other types of cancers, such as lung and melanoma? Are there more altered metabolisms in the brain metastatic cancer cells compared to cancer cells at the primary sites? Do cancer cells metastasized to different organs display different metabolic alterations? Further studies are needed to address these immediate questions.

# REFERENCES


Bangsbo, J., et al. (2000). "Muscle oxygen kinetics at onset of intense dynamic exercise in humans." Am J Physiol Regul Integr Comp Physiol **279**(3): R899-906.

Bardos, J. I. and M. Ashcroft (2004). "Hypoxia-inducible factor-1 and oncogenic signalling." Bioessays **26**(3): 262-269.

Bensaad, K., et al. (2006). "TIGAR, a p53-inducible regulator of glycolysis and apoptosis." Cell **126**(1): 107-120.

Berwick, D. C., et al. (2002). "The identification of ATP-citrate lyase as a protein kinase B (Akt) substrate in primary adipocytes." J Biol Chem **277**(37): 33895-33900.

Bos, P. D., et al. (2009). "Genes that mediate breast cancer metastasis to the brain." Nature **459**(7249): 1005-1009.

Bos, R., et al. (2001). "Levels of hypoxia-inducible factor-1 alpha during breast carcinogenesis." J Natl Cancer Inst **93**(4): 309-314.

Bricker, D. K., et al. (2012). "A mitochondrial pyruvate carrier required for pyruvate uptake in yeast, Drosophila, and humans." Science **337**(6090): 96-100.

Buzzai, M., et al. (2005). "The glucose dependence of Akt-transformed cells can be reversed by pharmacologic activation of fatty acid beta-oxidation." Oncogene **24**(26): 4165-4173.

Cantor, J. R. and D. M. Sabatini (2012). "Cancer cell metabolism: one hallmark, many faces." Cancer Discov **2**(10): 881-898.

Chaffer, C. L. and R. A. Weinberg (2011). "A perspective on cancer cell metastasis." Science **331**(6024): 1559-1564.

Chen, E. I., et al. (2007). "Adaptation of energy metabolism in breast cancer brain metastases." Cancer Res **67**(4): 1472-1486.

Daikhin, Y. and M. Yudkoff (2000). "Compartmentation of brain glutamate metabolism in neurons and glia." J Nutr **130**(4S Suppl): 1026S-1031S.

Dang, C. V., et al. (2006). "The c-Myc target gene network." Semin Cancer Biol **16**(4): 253-264.

De Feo, P., et al. (2003). "Metabolic response to exercise." J Endocrinol Invest **26**(9): 851-854.

DeBerardinis, R. J., et al. (2008). "The biology of cancer: metabolic reprogramming fuels cell growth and proliferation." Cell Metab **7**(1): 11-20.

del Amo, E. M., et al. (2008). "Pharmacokinetic role of L-type amino acid transporters LAT1 and LAT2." Eur J Pharm Sci **35**(3): 161-174.

Deprez, J., et al. (1997). "Phosphorylation and activation of heart 6-phosphofructo-2-kinase by protein kinase B and other protein kinases of the insulin signaling cascades." J Biol Chem **272**(28): 17269-17275.

Dimova, E. Y., et al. (2009). "Kinases as upstream regulators of the HIF system: their emerging potential as anti-cancer drug targets." Curr Pharm Des **15**(33): 3867-3877.

Divakaruni, A. S., et al. (2013). "Thiazolidinediones are acute, specific inhibitors of the mitochondrial pyruvate carrier." Proc Natl Acad Sci U S A **110**(14): 5422-5427.

Dominguez-Sola, D., et al. (2007). "Non-transcriptional control of DNA replication by c-Myc." Nature **448**(7152): 445-451.

Dvoriantchikova, G., et al. (2010). "Liposome-delivered ATP effectively protects the retina against ischemia-reperfusion injury." Mol Vis **16**: 2882-2890.

Elbers, J. R., et al. (1990). "Activity of glycolytic enzymes and glucose-6-phosphate dehydrogenase in smooth muscle proliferation." Tumour Biol **11**(4): 210-219.

Elbers, J. R., et al. (1990). "Activity of glycolytic enzymes and glucose-6-phosphate dehydrogenase in lipoblastic and neurogenic proliferations." Tumour Biol **11**(5): 262-273.

Elstrom, R. L., et al. (2004). "Akt stimulates aerobic glycolysis in cancer cells." Cancer Res **64**(11): 3892-3899.

Erickson, J. W. and R. A. Cerione (2010). "Glutaminase: a hot spot for regulation of cancer cell metabolism?" Oncotarget **1**(8): 734-740.

Fang, M., et al. (2010). "The ER UDPase ENTPD5 promotes protein N-glycosylation, the Warburg effect, and proliferation in the PTEN pathway." Cell **143**(5): 711-724.

Fellows, L. K., et al. (1992). "Extracellular brain glucose levels reflect local neuronal activity: a microdialysis study in awake, freely moving rats." J Neurochem **59**(6): 2141-2147.

Ferreira, L. M. (2010). "Cancer metabolism: the Warburg effect today." Exp Mol Pathol **89**(3): 372-380.

Fidler, I. J. (2003). "The pathogenesis of cancer metastasis: the 'seed and soil' hypothesis revisited." Nat Rev Cancer **3**(6): 453-458.

Fisher, R., et al. (2013). "Cancer heterogeneity: implications for targeted therapeutics." Br J Cancer **108**(3): 479-485.

Fisslthaler, B. and I. Fleming (2009). "Activation and signaling by the AMP-activated protein kinase in endothelial cells." Circ Res **105**(2): 114-127.

Fritz, V. and L. Fajas (2010). "Metabolism and proliferation share common regulatory pathways in cancer cells." Oncogene **29**(31): 4369-4377.

Ganapathy-Kanniappan, S., et al. (2010). "3-bromopyruvate: a new targeted antiglycolytic agent and a promise for cancer therapy." Curr Pharm Biotechnol **11**(5): 510-517.

Gevers, W. and H. A. Krebs (1966). "The effects of adenine nucleotides on carbohydrate metabolism in pigeon-liver homogenates." Biochem J **98**(3): 720-735.

Greijer, A. E., et al. (2008). "Presence of HIF-1 and related genes in normal mucosa, adenomas and carcinomas of the colorectum." Virchows Arch **452**(5): 535-544.

Guindi, M. (1999). "Role of Helicobacter pylori in the pathogenesis of gastric carcinoma and progression of lymphoid nodules to lymphoma." Can J Gastroenterol **13**(3): 224-227.

Hanahan, D. and R. A. Weinberg (2011). "Hallmarks of cancer: the next generation." Cell **144**(5): 646-674.

Hartner, W. C., et al. (2009). "ATP-loaded liposomes for treatment of myocardial ischemia." Wiley Interdiscip Rev Nanomed Nanobiotechnol **1**(5): 530-539.

Hatzivassiliou, G., et al. (2005). "ATP citrate lyase inhibition can suppress tumor cell growth." Cancer Cell **8**(4): 311-321.

Hu, Y. and G. S. Wilson (1997). "Rapid changes in local extracellular rat brain glucose observed with an in vivo glucose sensor." J Neurochem **68**(4): 1745-1752.

Ishiwata, K., et al. (1993). "Re-evaluation of amino acid PET studies: can the protein synthesis rates in brain and tumor tissues be measured in vivo?" J Nucl Med **34**(11): 1936-1943.

Ishiwata, K., et al. (1993). "Brain tumor accumulation and plasma pharmacokinetic parameters of 2'-deoxy-5-18F-fluorouridine." Ann Nucl Med **7**(3): 199-205.

Jiang, P., et al. (2011). "p53 regulates biosynthesis through direct inactivation of glucose-6-phosphate dehydrogenase." Nat Cell Biol **13**(3): 310-316.

Jones, R. G. and C. B. Thompson (2009). "Tumor suppressors and cell metabolism: a recipe for cancer growth." Genes Dev **23**(5): 537-548.

Kaelin, W. G., Jr. and C. B. Thompson (2010). "Q&A: Cancer: clues from cell metabolism." Nature **465**(7298): 562-564.

Kamemoto, E. S. and T. E. Mansour (1986). "Phosphofructokinase in the liver fluke Fasciola hepatica. Purification and kinetic changes by phosphorylation." J Biol Chem **261**(9): 4346-4351.

Kelly, A. D., et al. (2011). "Metabolomic profiling from formalin-fixed, paraffin-embedded tumor tissue using targeted LC/MS/MS: application in sarcoma." PLoS One **6**(10): e25357.

Khakh, B. S. and R. A. North (2006). "P2X receptors as cell-surface ATP sensors in health and disease." Nature **442**(7102): 527-532.

Kim, J. W. and C. V. Dang (2006). "Cancer's molecular sweet tooth and the Warburg effect." Cancer Res **66**(18): 8927-8930.

Kim, J. W., et al. (2004). "Evaluation of myc E-box phylogenetic footprints in glycolytic genes by chromatin immunoprecipitation assays." Mol Cell Biol **24**(13): 5923-5936.

Kim, L. S., et al. (2004). "Vascular endothelial growth factor expression promotes the growth of breast cancer brain metastases in nude mice." Clin Exp Metastasis **21**(2): 107-118.

Kim, S. J., et al. (2011). "Astrocytes upregulate survival genes in tumor cells and induce protection from chemotherapy." Neoplasia **13**(3): 286-298.

Kim, W. Y. and W. G. Kaelin (2004). "Role of VHL gene mutation in human cancer." J Clin Oncol **22**(24): 4991-5004.

Kimbro, K. S. and J. W. Simons (2006). "Hypoxia-inducible factor-1 in human breast and prostate cancer." Endocr Relat Cancer **13**(3): 739-749.

Kirikae, M., et al. (1989). "Quantitative measurements of regional glucose utilization and rate of valine incorporation into proteins by double-tracer autoradiography in the rat brain tumor model." J Cereb Blood Flow Metab **9**(1): 87-95.

Kohn, A. D., et al. (1996). "Expression of a constitutively active Akt Ser/Thr kinase in 3T3-L1 adipocytes stimulates glucose uptake and glucose transporter 4 translocation." J Biol Chem **271**(49): 31372-31378.

Koppenol, W. H., et al. (2011). "Otto Warburg's contributions to current concepts of cancer metabolism." Nat Rev Cancer **11**(5): 325-337.

Kovacevic, Z. and J. D. McGivan (1983). "Mitochondrial metabolism of glutamine and glutamate and its physiological significance." Physiol Rev **63**(2): 547-605.

Langley, R. R. and I. J. Fidler (2011). "The seed and soil hypothesis revisited--the role of tumor-stroma interactions in metastasis to different organs." Int J Cancer **128**(11): 2527-2535.

Laplante, M. and D. M. Sabatini (2012). "mTOR signaling in growth control and disease." Cell **149**(2): 274-293.

Lemasters, J. J., et al. (2002). "Role of mitochondrial inner membrane permeabilization in necrotic cell death, apoptosis, and autophagy." Antioxid Redox Signal **4**(5): 769-781.

Liang, W., et al. (2004). "ATP-containing immunoliposomes specific for cardiac myosin." Curr Drug Deliv **1**(1): 1-7.

Liang, W., et al. (2004). "Encapsulation of ATP into liposomes by different methods: optimization of the procedure." J Microencapsul **21**(3): 251-261.

Locasale, J. W. and L. C. Cantley (2011). "Metabolic flux and the regulation of mammalian cell growth." Cell Metab **14**(4): 443-451.

Locasale, J. W., et al. (2012). "Metabolomics of Human Cerebrospinal Fluid Identifies Signatures of Malignant Glioma." Mol Cell Proteomics.

Longley, D. B. and P. G. Johnston (2005). "Molecular mechanisms of drug resistance." J Pathol **205**(2): 275-292.

Lu, G., et al. (2009). "Protein phosphatase 2Cm is a critical regulator of branched-chain amino acid catabolism in mice and cultured cells." J Clin Invest **119**(6): 1678-1687.

Martin, D. S., et al. (2000). "ATP depletion + pyrimidine depletion can markedly enhance cancer therapy: fresh insight for a new approach." Cancer Res **60**(24): 6776-6783.

Mayer, A., et al. (2008). "Lack of hypoxic response in uterine leiomyomas despite severe tissue hypoxia." Cancer Res **68**(12): 4719-4726.

Menendez, J. A. and R. Lupu (2007). "Fatty acid synthase and the lipogenic phenotype in cancer pathogenesis." Nat Rev Cancer **7**(10): 763-777.

Moreno-Sanchez, R., et al. (2007). "Energy metabolism in tumor cells." FEBS J **274**(6): 1393-1418.

Moreno-Sanchez, R., et al. (2009). "The bioenergetics of cancer: is glycolysis the main ATP supplier in all tumor cells?" Biofactors **35**(2): 209-225.

Murphy, S. L. (2000). "Deaths: final data for 1998." Natl Vital Stat Rep **48**(11): 1-105.

Nogaki, M. and H. Ichihashi (1988). "[A new chemosensitivity test for cancer cells by measuring intracellular ATP content]." Nihon Geka Gakkai Zasshi **89**(12): 1950-1956.

Nyberg, M., et al. (2010). "Low blood flow at onset of moderate-intensity exercise does not limit muscle oxygen uptake." Am J Physiol Regul Integr Comp Physiol **298**(3): R843-848.

Okada, K., et al. (2005). "Expression of hypoxia-inducible factor (HIF-1alpha), VEGF-C and VEGF-D in non-invasive and invasive breast ductal carcinomas." Anticancer Res **25**(4): 3003-3009.

Ota, S., et al. (2013). "Ultrasound-guided direct delivery of 3-bromopyruvate blocks tumor progression in an orthotopic mouse model of human pancreatic cancer." Target Oncol.

Pandey, P. R., et al. (2012). "Anti-cancer drugs targeting fatty acid synthase (FAS)." Recent Pat Anticancer Drug Discov **7**(2): 185-197.

Patiar, S. and A. L. Harris (2006). "Role of hypoxia-inducible factor-1alpha as a cancer therapy target." Endocr Relat Cancer **13 Suppl 1**: S61-75.

Pellerin, L. (2008). "Brain energetics (thought needs food)." Curr Opin Clin Nutr Metab Care **11**(6): 701-705.

Pittas, A. G., et al. (2005). "Interstitial glucose level is a significant predictor of energy intake in free-living women with healthy body weight." J Nutr **135**(5): 1070-1074.

Previs, S. F., et al. (2009). "Is there glucose production outside of the liver and kidney?" Annu Rev Nutr **29**: 43-57.

Previs, S. F. and H. Brunengraber (1998). "Methods for measuring gluconeogenesis in vivo." Curr Opin Clin Nutr Metab Care **1**(5): 461-465.

Qian, W. and B. Van Houten (2010). "Alterations in bioenergetics due to changes in mitochondrial DNA copy number." Methods **51**(4): 452-457.

Rathmell, J. C., et al. (2003). "Akt-directed glucose metabolism can prevent Bax conformation change and promote growth factor-independent survival." Mol Cell Biol **23**(20): 7315-7328.

Read, R., et al. (2009). "Ectonucleoside triphosphate diphosphohydrolase type 5 (Entpd5)-deficient mice develop progressive hepatopathy, hepatocellular tumors, and spermatogenic arrest." Vet Pathol **46**(3): 491-504.

Robey, I. F., et al. (2005). "Hypoxia-inducible factor-1alpha and the glycolytic phenotype in tumors." Neoplasia **7**(4): 324-330.

Schwartzenberg-Bar-Yoseph, F., et al. (2004). "The tumor suppressor p53 down-regulates glucose transporters GLUT1 and GLUT4 gene expression." Cancer Res **64**(7): 2627-2633.

Semenza, G. L. (2003). "Targeting HIF-1 for cancer therapy." Nat Rev Cancer **3**(10): 721-732.

Semenza, G. L. (2007). "HIF-1 mediates the Warburg effect in clear cell renal carcinoma." J Bioenerg Biomembr **39**(3): 231-234.

Seyfried, T. N. and L. M. Shelton (2010). "Cancer as a metabolic disease." Nutr Metab (Lond) **7**: 7.

Shinano, T., et al. (2001). "Differences in nitrogen economy of temperate trees." Tree Physiol **21**(9): 617-624.

Simiantonaki, N., et al. (2008). "Hypoxia-inducible factor 1 alpha expression increases during colorectal carcinogenesis and tumor progression." BMC Cancer **8**: 320.

Skulachev, V. P. (2006). "Bioenergetic aspects of apoptosis, necrosis and mitoptosis." Apoptosis **11**(4): 473-485.

Stapleton, D., et al. (1996). "Mammalian AMP-activated protein kinase subfamily." J Biol Chem **271**(2): 611-614.

Talks, K. L., et al. (2000). "The expression and distribution of the hypoxia-inducible factors HIF-1alpha and HIF-2alpha in normal human tissues, cancers, and tumor-associated macrophages." Am J Pathol **157**(2): 411-421.

Tanaka, H., et al. (2006). "Hypoxia-independent overexpression of hypoxia-inducible factor 1alpha as an early change in mouse hepatocarcinogenesis." Cancer Res **66**(23): 11263-11270.

Tang, J., et al. (2013). "Key structure of brij for overcoming multidrug resistance in cancer." Biomacromolecules **14**(2): 424-430.

Tatsumi, T., et al. (2003). "Intracellular ATP is required for mitochondrial apoptotic pathways in isolated hypoxic rat cardiac myocytes." Cardiovasc Res **59**(2): 428-440.

Tennant, D. A., et al. (2010). "Targeting metabolic transformation for cancer therapy." Nat Rev Cancer **10**(4): 267-277.

Thorn, J. A. and S. M. Jarvis (1996). "Adenosine transporters." Gen Pharmacol **27**(4): 613-620.

Trincavelli, M. L., et al. (2010). "Adenosine receptors: what we know and what we are learning." Curr Top Med Chem **10**(9): 860-877.

Vander Heiden, M. G., et al. (2009). "Understanding the Warburg effect: the metabolic requirements of cell proliferation." Science **324**(5930): 1029-1033.

Vanlangenakker, N., et al. (2008). "Molecular mechanisms and pathophysiology of necrotic cell death." Curr Mol Med **8**(3): 207-220.

Verrax, J., et al. (2011). "Intracellular ATP levels determine cell death fate of cancer cells exposed to both standard and redox chemotherapeutic agents." Biochem Pharmacol **82**(11): 1540-1548.

Vordermark, D., et al. (2005). "Glucose requirement for hypoxic accumulation of hypoxia-inducible factor-1alpha (HIF-1alpha)." Cancer Lett **230**(1): 122-133.

Vousden, K. H. and K. M. Ryan (2009). "p53 and metabolism." Nat Rev Cancer **9**(10): 691-700.

Ward, P. S. and C. B. Thompson (2012). "Metabolic reprogramming: a cancer hallmark even warburg did not anticipate." Cancer Cell **21**(3): 297-308.

Weinberg, R. A. (2007). The biology of cancer. New York, Garland Science.

Wells, G. D., et al. (2009). "Bioenergetic provision of energy for muscular activity." Paediatr Respir Rev **10**(3): 83-90.

Wilson, T. R., et al. (2006). "Chemoresistance in solid tumours." Ann Oncol **17 Suppl 10**: x315-324.

Winder, W. W. (2001). "Energy-sensing and signaling by AMP-activated protein kinase in skeletal muscle." J Appl Physiol **91**(3): 1017-1028.

Wise, D. R. and C. B. Thompson (2010). "Glutamine addiction: a new therapeutic target in cancer." Trends Biochem Sci **35**(8): 427-433.

Wu, X. H., et al. (2011). "Correlations of hypoxia-inducible factor-1alpha/hypoxia-inducible factor-2alpha expression with angiogenesis factors expression and prognosis in non-small cell lung cancer." Chin Med J (Engl) **124**(1): 11-18.

Yee Koh, M., et al. (2008). "HIF-1 regulation: not so easy come, easy go." Trends Biochem Sci **33**(11): 526-534.

Yuan, M., et al. (2012). "A positive/negative ion-switching, targeted mass spectrometry-based metabolomics platform for bodily fluids, cells, and fresh and fixed tissue." Nat Protoc **7**(5): 872-881.

Yudkoff, M. (1997). "Brain metabolism of branched-chain amino acids." Glia **21**(1): 92-98.

Yudkoff, M., et al. (1993). "Brain glutamate metabolism: neuronal-astroglial relationships." Dev Neurosci **15**(3-5): 343-350.

Zadra, G., et al. (2010). "New strategies in prostate cancer: targeting lipogenic pathways and the energy sensor AMPK." Clin Cancer Res **16**(13): 3322-3328.

Zadran, S., et al. (2012). "ENTPD5-mediated modulation of ATP results in altered metabolism and decreased survival in gliomablastoma multiforme." Tumour Biol **33**(6): 2411-2421.

Zhang, F. and G. Du (2012). "Dysregulated lipid metabolism in cancer." World J Biol Chem **3**(8): 167-174.

Zhang, R. D., et al. (1991). "Relative malignant potential of human breast carcinoma cell lines established from pleural effusions and a brain metastasis." Invasion Metastasis **11**(4): 204-215.

Zhong, H., et al. (1999). "Overexpression of hypoxia-inducible factor 1alpha in common human cancers and their metastases." Cancer Res **59**(22): 5830-5835.

Zhong, H., et al. (2004). "Up-regulation of hypoxia-inducible factor 1alpha is an early event in prostate carcinogenesis." Cancer Detect Prev **28**(2): 88-93.

Zhou, Y., et al. (2012). "Intracellular ATP levels are a pivotal determinant of chemoresistance in colon cancer cells." Cancer Res **72**(1): 304-314.